STRUCTURAL EVOLUTION OF THE DEEPWATER WEST NIGER DELTA PASSIVE MARGIN

SEPRIBO EUGENE BRIGGS

Submitted in partial fulfilment of the requirements for the degree of Ph.D.

Cardiff University

October, 2007

UMI Number: U585138

Dissertation Publishing

This thesis is dedicated in memory of my late father,

Eugene Dikio Briggs and to my mother Daba Briggs

SUMMARY

A detailed investigation of the structural evolution of the deepwater west Niger Delta was undertaken from the combination of industry 2D and 3D seismic reflection datasets. The study has been focused on three themes: crustal architecture, thrusting in oceanic crust and the role of multiple detachments in developing the structural style in the area. Detailed analysis and mapping of the basement structures, crustal thickness and distribution, identification and analysis of thrust-fault pattern and its relationships to detachment levels have provided a completely new understanding of the structural evolution of the deepwater west Niger Delta.

The study shows that the area is underlain by oceanic crust that is characterised by a thickness of 5-7 km and by internal reflectivity consisting of both dipping and sub-horizontal reflectors. Inclined reflections can be traced up to the top of the crust where they offset it across a series of minor to major SW-NE striking basement thrusts in the SE of the study. The crust is thinnest around a major transform structure, the Chain Fracture Zone possibly related to the local geometry of the spreading fabrics with no significant variation the crustal thickness across the transform zone.

Detachments are located within the 'Dahomey unit', and the transition between the Agbada and Akata Formations (Top Akata). Quantitative measurements of fault displacements show that the utilisation of different detachments results in contrasting styles of thrust propagation and fold growth. Two geographical zones are defined. In zone A, (NW sector of the study area), the stratigraphically shallowest Dahomey detachment is dominant and is associated with *thrust truncated folds* while in zone B, (SE sector of the study area) a stratigraphically lower detachment approximately at the Agbada-Akata Formation boundary is associated with *thrust propagation folds*.

AUTHOR'S NOTE

Chapters Three, Four and **Five** of the present Thesis have been submitted as papers to three different international publications. The present status of these publications are summarised as follows:

- **Chapter Three** has been submitted to Marine and Petroleum Geology as: *Crustal structure of the Deepwater West Niger Delta Passive Margin from the interpretation of seismic reflection data.* Sepribo E. Briggs, Joe Cartwright & Richard J. Davies.

- **Chapter Four** has been submitted as: *Thrusting in oceanic crust during continental drift offshoreNiger Delta, Equatorial Africa.* Sepribo Eugene Briggs[*1], Richard J Davies, Joe Cartwright & Richard Morgan

- **Chapter Five** has been published in Basin Research as: *Multiple detachment levels and their control on fold styles in the compressional domain of the deepwater west Niger Delta.* Sepribo .E. Briggs, Richard J. Davies, Joe A. Cartwright & Richard Morgan.

ACKNOWLEDGEMENTS

TABLE OF CONTENTS

CHAPTER ONE

CHAPTER TWO

CHAPTER THREE

CHAPTER FOUR

CHAPTER FIVE

CHAPTER SIX

CHAPTER SEVEN

List of figures

Chapter One: Introduction

Chapter Two: Regional Geology and Tectonic Evolution of the Deepwater West Niger Delta Margin

	and minor dextral strike-slip motion within the Salado and Colorado Basins since approximately 150 Ma (Tithonian). (Redrawn from Nurnberg and Muller, 1991).	
2.3	Chron M4 (126.5 Ma, Hauterivian). The further northward propagation of South Atlantic rifting between 130 Ma (Hauterive) and Chron M4 (126.5 Ma) induced rifting combined with strike-slip motion along the Parana/Chacos Basin deformation zone in South America. At Chron M4, seafloor spreading has propagated up to 28° S. Rifting and strike-slip motion in the Salado and Colorado basins ceased at about Chron M4 (126.5 Ma) having generated 20-25 km and 40-45 km of crustal extension in the Salado Basin and Colorado Basin, respectively and 20 to 30 km of dextral strike-slip in both basins. For figure captions see Figure 2.1.	2-7
2.4	Between Chrons M4 and M0, rifting propagated northwards into the Benue trough. The Benue Trough/Niger Rift system constitutes a large Cretaceous rift/ sinistral strike-slip system that were active until 80 Ma before present (Fairhead and Okereke, 1987). At Chron M0 movement along the Parana/Chacos Basin deformation zone ceased, having generated 60 to 70 km of crustal extension and 20 to 30 km of dextral shear. It is believed that Africa was still rigidly attached to South America in the Equatorial Atlantic, since there is no evidence for sediments older than Aptian (Jones, 1987). For the legend see figure 2.1. (Redrawn from Nurnberg and Muller, 1991)	2-8
2.5	The separation of South America from Africa at 100 Ma (Albian). After Chron M0, the Equatorial Atlantic began to open, connecting the South and Central Atlantic. Subsequently, South America behaved as a rigid plate, while intracontinental deformation in Africa was active until approximately 80 Ma (Late Cretaceous). Also see figure 2.1 for the legend. (Redrawn from Nurnberg and Muller, 1991).	2-9
2.6	The separation of South America from Africa at 84 Ma (Campanian). Intracontinental movement ceased within Africa at approximately Chron 34 (84 Ma). Nurnberg and, Muller, 1987 in agreement with Fairhead and Okereke, 1987 proposed 50-60 km of rifting combined with 40-50 km of sinistral strike-slip motion in the Benue Trough. After Chron 34, the South Atlantic is assumed to have opened as two plate system. (Redrawn from Nurnberg and Muller, 1991).	2-13
2.7	The South Atlantic evolution during Chron 27 (63 Ma). The subsequent opening of the South Atlantic since Chron 34 (84 Ma) has been characterised by simple divergence of two continental plates. At approximately Chron 27 (63 ma), seafloor spreading rates reached a minimum during a period of slow spreading between Chron 30 (66.7 Ma) and Chron 20 (44.7 Ma), resulting in the creation of many new fracture zones. (Redrawn from Nurnberg and Muller, 1991)	2-14
2.8	The South Atlantic evolution during Chron 16 (38.1 Ma). After Chron 20 (44.7 Ma), South Atlantic spreading rates accelerated, resulting in a decreasing number of fracture zones. A subtle S-shaped curve of the fracture zone throughout the Atlantic indicates a change in the spreading direction during Eocene time at approximately Chron 16 (38.1 Ma). (Redrawn from Nurnberg and Muller, 1991)	2-15
2.9	Satellite derived gravity map of the present day Central, Equatorial and South Atlantic showing evidence of the complex phase of its evolution from initial extension in the Cretaceous to the present day (after Sandwell	2-17

Chapter Three: Crustal Structure of the Deepwater West Niger Delta Passive Margin from the interpretation of seismic reflection data.

Chapter Five: Multiple detachment levels and their control on fold styles in the compressional domain of the deepwater west Niger Delta

Figure No.	Figure Caption	Page No.
5.1	(a) Map of the Niger Delta showing the different structural domains (modified after Damuth, 1994). Note IFTB, DFB and OFTB are equivalent to the inner fold and thrust belt, detachment fold belt and outer fold and thrust belt respectively (b) Regional dip line extending across the onshore into the deepwater west Niger delta. Modified after Haack et al., (2000). Vertical exaggeration = 2.0.	5-4
5.2	Chronostratigraphic diagram showing the regional variability in stratigraphy along a NW-SE transect across the deepwater west Niger Delta.. 2D seismic line showing the abrupt change in stratigraphy between units 1a, 1b and unit 2. Note that BSM, PASW, Unit 2, Unit 1a and unit 1b corresponds to the basement (Ajakaiye & Bally, 2002), pre-Akata sediment wedge (see Morgan, 2003, 2004), Akata Formation (Avbovbo, 1978; Knox & Omatsola, 1989), Dahomey wedge (Morgan, 2003; 2004) and Agbada Formation (Short & Stauble, 1967; Avbovbo, 1978) respectively.	5-7
5.3	Non-interpreted and Interpreted seismic lines from (a) the 2D dataset (b) the 3D dataset, showing the major stratigraphic subdivisions of the deepwater west Niger delta. The major reflectors defined in this section are the BSM, the PASW, unit 2 corresponding to the Akata Formation, unit 1A which is the Dahomey detachment unit, and unit 1b which defines the Agbada Formation. Note the sinusoidal geometry of the Dahomey unit that thins towards the SW direction here and in the SE direction on Fig. 2 but becomes relatively thicker towards the NE. The compressional faults tip out from the thick units marked DW. Older inactive fold features are observed buried without seafloor expression.	5-11
5.4	Location map of the study area showing the 2D and 3D seismic database, the approximate demarcation of zones A and B and the location of faults F1 – F8 described in this study. It also shows the approximate extent of the Dahomey wedge.	5-12
5.5	Time structural map of Miocene (10.3 Ma) showing the parallelism between fold axes and the strike of the thrust faults. The figure is dominated by dip-slip regime. The measurements of the fault displacements were made on profiles that are generally parallel to the likely transport direction.	5-14
5.6	Uninterpreted (a) and interpreted (b) representative seismic section from zone A showing a typical fault (F1) detaching within the Dahomey wedge. (c) An enlarged section of the sole segment where the fault plane reflection terminates within a bedding parallel layer marked as BPR.	5-16
5.7	Uninterpreted (a) and interpreted (b) representative seismic section from zone A showing a typical fault (F2) detaching in the Dahomey wedge.	5-17
5.8	Representative (a) Uninterpreted and (b) interpreted seismic section from zone B showing fault F3. Note how the thrust ramps up forming a thrust wedge. Also observed is the amount of displacement between the footwall and hanging walls. The upper tip is invisible within a trishear zone (c) A	5-18

Chapter Six: Tectono-stratigraphic Evolution of Cretaceous to Recent Deepwater West Niger Delta

	compressional belt within the region (From Morgan, 2004).	

List of Tables

Enclosures

Published papers:

Briggs, S.E., Davies, R.J., Cartwright, J. and Morgan, R. 2006. Multiple detachment levels and their control on fold styles in the compressional domain of the deepwater west Niger Delta. *Basin Research* 18, pp. 435-450.

Chapter One: Introduction

1.1 Rationale

A good understanding of the structure and mode of evolution of the continental margin of the Niger Delta is crucial for many reasons. In terms of hydrocarbon exploration, the area is of high economic importance as demonstrated by the high level of hydrocarbon exploration activities, interest and investments that have been maintained in the area for the past five decades. The deepwater Niger Delta slope area has become one of the world's exploration hotspots over the last few years (1995 to present). Previously, the advance of exploration off the shelf and onto the slope area of the Niger Delta produced a succession of large significant discoveries -Bonga, Agbami/Ekoli/ Ikija, Bosi/Erha, Ukot, Akpo/Egina/Preowei/Kuro, Nnwa/Doro, Chota to name a few and hopes have been high for a continuation of this success further downslope.

The existing information on the evolution and structure of the margin are largely due to the results of surveys of a regional nature carried out by several international organisations. The most useful of these are the reports of Mascle et al. 1973; Emery et al. 1975 and that of Lehner and De Ruiter, 1977. Petroleum exploration activities in the region, particularly in the Niger Delta have also led to the acquisition of a vast amount of data in order to study the structure of the delta (Short and Stauble, 1967; Hospers, 1971, Evamy et al. 1978). Nevertheless, the results from the studies carried out by oil and gas exploration companies are always placed in an archive, and as such there has not been much published works on the deepwater part of the Niger Delta.

Despite the plethora of studies on the subaerial delta and on the adjacent inner continental shelf, the continental slope and rise seaward of the shelf break off the Niger Delta remains one of the least surveyed and studied

continental margin of the world. At a time when most continental margins throughout the world are being increasingly subjected to sophisticated geophysical surveys, studies on the structure and tectonic evolution of the deepwater Niger Delta are limited and are based largely on widely spaced reconnaissance seismic lines on the West African margin (Burke, 1972; Mascle et al. 1973; Delteil et al. 1974; Emery et al. 1975; Mascle, 1976; Lehner and De Ruiter, 1977; Gorini, 1981). Many of these studies have focused on mapping the trends of fracture zones and other basement structures in order to reconstruct the plate tectonic history of the Equatorial Atlantic. As petroleum exploration activity is rapidly advancing into the deep and ultra-deepwater Niger Delta, an understanding of its structural and tectonic evolution is now imperative and necessary for the successful and economic hydrocarbon exploration.

Understanding of the crustal structure is a major challenge for regional basin analysis and petroleum exploration in frontier regions such as deepwater Niger Delta. However, many questions remain relating to: (1) the crustal architecture and a better definition of the position and nature of the Continent-Ocean Boundary (COB), (2) the causes of the intraplate compressional deformation within the deepwater west Niger Delta, and (3) the causes of the variability in fold styles across the deepwater and their structural evolution. Many of these questions are unresolved simply because of the inadequacy of the widely spaced data, their limited scale and the general lack of well bore calibration of stratigraphy within the area. This is now possible with recently acquired 2D and 3D seismic reflection data and well information.

This PhD project uses this available and recently acquired commercial 2D and 3D seismic reflection data to study the structural evolution of the deepwater west Niger Delta and to improve our current understanding of the basement and cover structures that formed the delta.

In this chapter a list of the principal aims of this PhD research project is provided. Subsequently, a concise overview of the location and geological setting of the study area, the data and the methods used, and an account of the history of hydrocarbon exploration in the Niger Delta are presented. The chapter concludes with the layout of the thesis. More detailed background to the geological setting of the study area; the datasets and methodologies employed throughout this research, and a review of the previous literature are provided in subsequent chapters.

1.2 Aims of the study

This thesis has a broad range of aims, the majority of which are related to improving the current understanding of the structural evolution of the deepwater West Niger Delta. However, because this research is focused on an area that is currently housing world class hydrocarbon discoveries and at the moment undergoing increased and aggressive exploration efforts, a series of resultant aims are to recognise how these results could aid hydrocarbon exploration in the Niger Delta margins.
The aims of this thesis are:

- To determine the crustal architecture and evolution of the crust under the deepwater west Niger Delta basin.

- Address the spatial and temporal variability in crustal type, structure and thickness under the toe region of the delta.

- To describe the anomalous crustal features inherent in the oceanic crust.

- To document the causes of the regional structural variability within the fold and thrust belts of the deepwater west Niger Delta.

- To investigate the role of multiple detachments in the deepwater west Niger Delta folds and thrust belt. This particular theme has the aim of answering questions which includes

  - Are multiple detachments responsible for the development of different sets of structures in the west Niger Delta fold and thrust belt? Can these structures easily be distinguished by their geometry and wavelength?

  - In what way does the presence of multiple detachments influence the spatial-temporal evolution of the deepwater west Niger Delta compressional belt?

To address these issues, extensive interpretation of the regional 2D seismic reflection data complimented with detailed interpretation of 3D seismic reflection data in the deepwater west Niger Delta provided by Veritas DGC, was undertaken.

1.3 Significance of the study

This study is one of the first to explore the application of large coverage and high quality 2D and 3D seismic reflection data to the study of basement structures and as such has important value for further development in this direction. It is expected that the ability to image basement structure available through the application of 2D and 3D seismic reflection data will provide the much needed insight that will further advance our understanding of the plate tectonic history of the Equatorial Atlantic.

The advancement of our understanding of the structural evolution has a number of implications for plate tectonic reconstruction, hydrocarbon exploration, basin modelling and this study is, therefore, of general interest beyond the field of structural geology and seismic interpretation.

1.4 Location and geological setting

The Niger Delta (Figs. 1.1 and 1.2) is located in the Gulf of Guinea and regarded as one of the most prolific hydrocarbon provinces in the world. It is typically a wave and tide dominated delta that is located on the Atlantic coast of Africa and fed by the Niger River (Doust and Omatsola, 1990). It is characterised by a thick succession of deltaic sediments that have prograded over the passive margin and overlie a ductile substrate of overpressured shales reaching a maximum thickness of 10-12 km (Doust and Omatsola, 1990; Cohen and McClay, 1996). It is characterised by large regional and counter-regional extensional growth faults that have mainly formed on the delta top together with a belt of imbricate thrusts and folds at the delta toe (Fig. 1.2). It is generally accepted that the delta top growth fault systems form as a result of differential progradation and loading of the ductile substrate of overpressured pro-delta shales and that the extensional growth faults are mechanically linked to the contractional fold/thrust system at the delta toe (Morley and Guerin, 1996; McClay et al. 1998).

The compressional domain of the deepwater Niger Delta is divided into three (3) subdomains which have been termed the inner fold and thrust belt, the transitional inter-thrust and the outer fold and thrust subdomains (Fig. 1.2) (Connors et al. 1988; Corredor et al. 2005a; Briggs et al. 2006).

> (1) The inner fold and thrust subdomain is a highly shortened and imbricate fold and thrust belt while the outer fold and thrust belt is a more classic toe thrust zone with thrust-cored anticlines that are typically separated from one another by several kilometres (Corredor et al. 2005a).
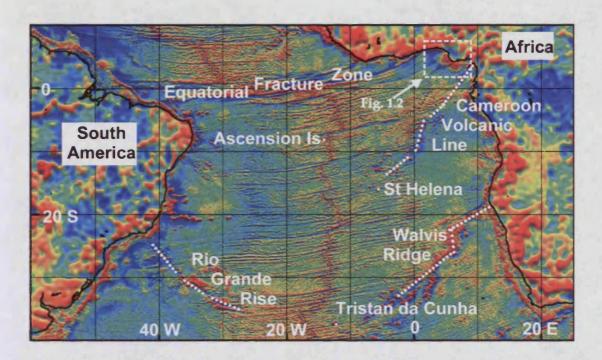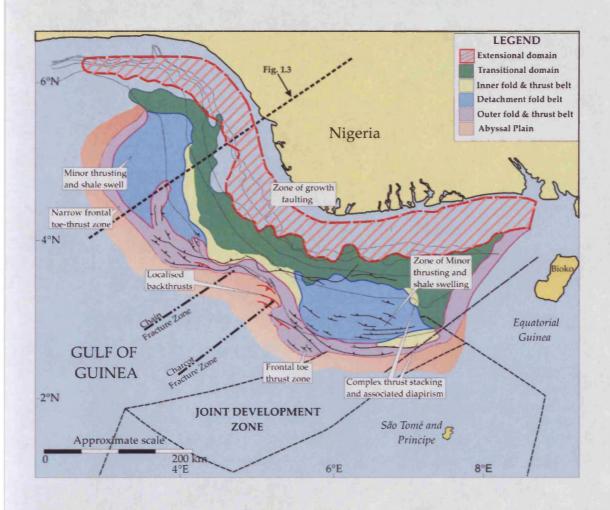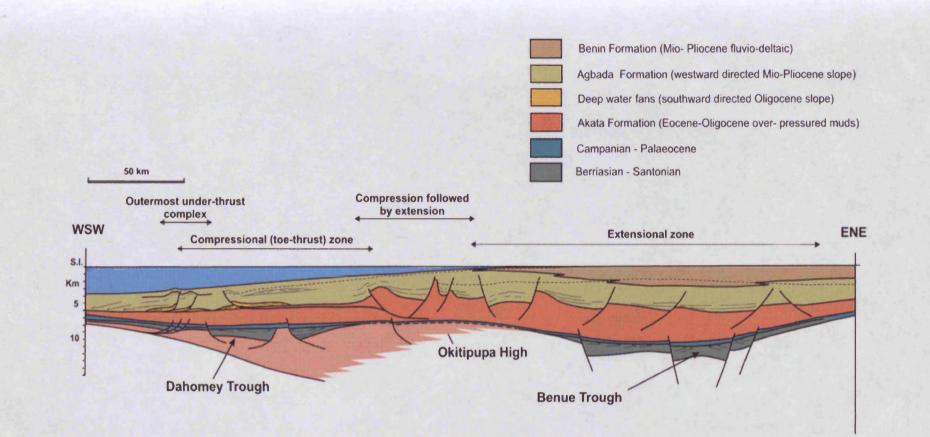
Figure 1.1.Satellite-derived free air gravity map of the present day configuration of the South Atlantic Ocean showing the major tectonic features (Modified after Sandwell and Smith, 1997). Warm colours depict gravity highs and cool colours indicate gravity lows. Inset in box (fig.1.2) is the location of the study.

Figure 1.2. Structural map of the Deepwater Niger Delta showing the different structural domains and their associated sub-domains (Redrawn and modified from JDZ Licensing Round, 2004).

Benin Formation (Mio- Pliocene fluvio-deltaic)

Agbada Formation (westward directed Mio-Pliocene slope)

Deep water fans (southward directed Oligocene slope)

Akata Formation (Eocene-Oligocene over- pressured muds)

Campanian - Palaeocene

Berriasian - Santonian

50 km

Outermost under-thrust complex

Compression followed by extension

WSW

Compressional (toe-thrust) zone

Extensional zone

ENE

S.I.

Km

5

10

Okitipupa High

Dahomey Trough

Benue Trough

Figure 1.3. A regional scale cross section showing the structural and stratigraphic subdivision of the Niger Delta. In terms of the structure it shows the variations in structural styles from the extensional to the compressional zones. The litho-stratigraphic distributions of the different formations are clearly observed. Note that the topmost Benin Formation disappears downslope. Overpressure in the Akata Formation has rendered the Akata structurally weak and the entire sediment cone has collapsed on intra-Akata detachment faults creating extensional, faulted-diapiric and compressional belt within the region (From Morgan, 2004).

(2) The inter-thrust subdomain is a transitional subdomain between the inner and outer fold and thrust subdomains and characterised by regions of little or no deformation interspersed with broad detachment anticlines that accommodates relatively small amount of shortening (Bilotti and Shaw, 2005).

(3) The outer fold and thrust belt is comprised of local depocentres and both basinward and hinterland verging thrusts. This domain is situated further downdip, with channelised turbidite sands trapped in broad wavelength anticlines above incipient thrust propagation zones.

1.5 History of hydrocarbon exploration in Nigeria

The Nigeria National Petroleum Corporation (NNPC) upstream operations are in joint partnership with major oil companies. These multinational companies are operating predominantly in the on-shore Niger Delta, coastal offshore areas and lately in the deepwater. As with many other developing countries, the multinationals have been operating under what is called a concession system, with NNPC being the concessionaire, while the companies are the operators. The NNPC also is responsible for the management of the exploration bidding round for oil and gas until lately when it was transferred to the DPR (Department of Petroleum Resources) in the Federal Ministry of Petroleum Resources now called Ministry of Energy. The multinational oil companies operate in partnership with NNPC under a Joint Operating Agreements (JOA`s) or Production Sharing Contracts (PSC`s). Others, especially the indigenous oil companies, operate in partnership with international companies under sole risk or as independents.

The Niger Delta has been an area of immense oil and gas exploration since 1908 when the German Nigeria Bitumen Corporation commenced

exploration activities and drilled the first well (total of 14 until the end of 1914) in the vicinity of the tar seep deposit of Araromi area, west of Nigeria in the northern part of the delta (Frost, 1997). These pioneering efforts ended abruptly with the outbreak of the First World War in 1914. Oil prospecting efforts resumed in 1937, when Shell D`Arcy (the forerunner of Shell Petroleum Development Company of Nigeria) was awarded the sole concessionary right covering the whole territory of Nigeria. Their activity was also interrupted by the Second World War, but resumed in 1947. However, significant oil shows were not found in the Tertiary rock until 1956 when Shell-British Petroleum brought the first commercially viable discovery well at Oloibiri on stream with a modest production rate of 5,100 barrels per day.

This discovery opened the oil industry in 1961, bringing Gulf, Agip, Safrap (now Elf/Total), Tenneco and then Amoseas (ChevronTexaco) to join the exploration efforts both in the onshore and shallow offshore areas of Nigeria. Subsequently, the quantity doubled the following year in 1962 and progressively as more players came onto the oil scene, the production rose to 2.0 million barrels per day in 1972 and reached a peak at 2.4 million barrels per day in 1979. Nigeria thereafter, attained the status of a major oil producer, ranking 7th in the world in 1972, and has since grown to become the sixth largest oil producing country in the world. The country's reserves of crude oil currently stand at 36.220 billion barrels with a natural gas reserves total of 181.900 trillion standard cubic feet (scf) (Radler, 2006).

From the very beginning of oil exploration in Nigeria in 1937 by Shell-D`Arcy till early 1993, virtually all exploration and production activities were restricted to land and swamps. Where prospecting ventured offshore, it was in areas not greater than 200 m water depth. The year 1991 herald the entry of more new players like BP, Statoil, Amoco, Esso, Conoco, Total and other indigenous companies. This development was enhanced by the extension of the concessionary rights previously a monopoly of Shell. But in 1993, the

federal government opened up a new frontier in oil and gas exploration, heralding the bright prospects of a promising future, by allocating some deepwater acreage in water depths reaching 2500 m. Though these deepwater operations are technically challenging and massively capital intensive, experienced multinational companies have been awarded some deep offshore blocks and even ultra deep concessions. By the end of 1998, the deepwater operators in Nigeria have archived the following:

(a) Acquisition of 21, 000 sq. km 2D Seismic Lines

(b) Acquisition of 21, 500 km 3D Seismic Lines

(c) Drilling of 33 exploration/appraisal wells in a depth range between 300 and 1460 m.

The technical challenges of deep and ultra-deepwater depths meant a number of less than 20 wells drilled worldwide in water depths greater than 1000 m. Expectedly, since most of the deep water activity in Niger Delta is in, so called, "virgin" territory and lacking infrastructural support and services, the cost of prospecting is extremely high. This is however ameliorated and set off against the PSC (Production Sharing Contract) with the Federal Government of Nigeria under the auspices of the NNPC.

1.6 Database and Methodology

2D and 3D seismic reflection datasets represent the main primary source of information used in this study. This deep seismic reflection data consists of recently acquired high resolution 120 fold 2D seismic reflection data acquired in 1998, with 6 km cable length and 12 second recording interval, processed using the Kirchhoff bent ray pre-stack time migration. The 3D seismic reflection data were acquired in 1999 and imaged deep levels to approximately 12 seconds (s) two-way travel time (TWT). The 2D seismic

reflection data consists of 2 strike lines of about 320 km combined length which are oriented in a WNW-ESE direction with spacing of 20 km between them. The rest of the 2D seismic reflection data is made up of 8 strike lines of 1648 km oriented in a NW-SE direction and 33 dip lines of 4089 km with a SW-NE orientation (Fig. 1.4). They cover an area of 3057 km^2 acquired from 6 km offset length and 12 s record interval, with line spacing of 25 m and has a similar processing sequence to the rest of the data. These dataset were acquired from an area where the water depth is between 1500- 4000 m. The specifics of the seismic data acquisition allowed for the imaging of deep reflections from the crust below the Niger Delta. The quality of the data is excellent due to the application of pre-stack time migration (PSTM). The data are displayed with a reverse polarity (European convention) so that an increase in acoustic impedance is represented by a trough and is black on the seismic data in all figures presented here. The data are displayed in seconds two-way-travel time marked TWT.

The dominant frequency of the seismic data varies with depth, but it is approximately 10 Hz at the level of interest. When calculating the resolution, realistic seismic interval velocity of 6000 m/s was assumed within the crust. This velocity is estimated from studies on other areas in the South Atlantic (Sage et al. 2000; Wilson et al. 2003). Vertical resolution ($\lambda/4$) is estimated to be about 150 m for the studied crustal interval.

This study is also supported by satellite derived gravity data from the world database compiled by Sandwell and Smith (1997) which images the Chain and Charcot fracture zones (Fig. 1.2). It covers the Gulf of Guinea region of the Equatorial Africa from about latitude 9° 00` N to 2° 00` S and longitude 1° 00` E to 12° 00` E (Fig. 1.1).
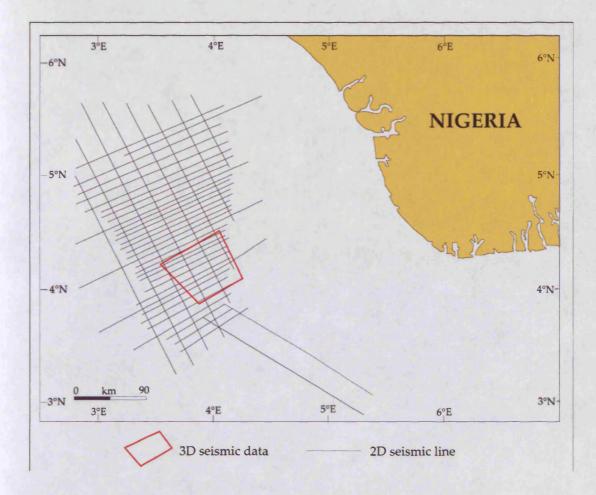
Figure 1.4 Location map of the study area showing the full extent of the 2D and 3D seismic surveys.

The interpretation of 2D and 3D seismic data represents the core method used in this PhD research project. In the past, seismic interpretations have been used for studying the evolution of the Niger Delta. However, previous works on this field have been limited to the analysis of widely spread 2D seismic data. The present research project represents the first comprehensive work on the structural evolution using the combination of 2D and 3D seismic data. This has allowed an excellent coverage of the basinal distribution of the crust and revealed anomalous structures in the region and promoted the investigation for the causes of the variation in structural styles within the fold belts. Each of the main composite chapters (3, 4 and 5) contains a description of the methods used for the study.

1.7 Thesis layout

The core of this thesis consists of three paper-style chapters (**Chapter 3, 4 and 5**). These have been structured according to the guidelines for authors as specified for Marine and Petroleum Geology (**Chapter 3**); the journal "Tectonics" (**Chapter 4**) and Basin Research (**Chapter 5**). There are elements of repetition in the introductory and review sections of these chapters. Also, there are unavoidable overlaps between discussion topics and conclusions in the chapters due to the location of the study and the data set used. The duplication however has been kept to a minimum. The three core chapters (**3, 4 and 5**) are put in between two introductory, scene setting chapters (**1 and 2**), and two summative and concluding chapters (**6 and 7**).

- **Chapter 2** reviews the existing literature on regional geology and the plate tectonic evolution of the deepwater west Niger Delta.

- **Chapter 3** examines the structure of the deepwater west Niger Delta, looking at the crustal thickness and type, internal structural elements and other inherent features of the crust.

- **Chapter 4** deals with some of the novel features of thrust systems that have been observed in **Chapter 3**. It is focused on looking at the evolution of thrusting in oceanic crust within the study. These thrusts are anomalous features that are very important to the general evolution of the Niger Delta.

- **Chapter 5** examines the role of multiple detachments in the variability in structural styles within the compressional domain of the study area. It uses various methods to characterise the different structural areas and differentiate them from the others.

- **Chapter 6** is an extended and detailed discussion of the topics that were introduced in chapters **1 and 2** and which form the main body of the thesis (**Chapters 3, 4 and 5**). These are the crustal structure and architecture, evolution of the thrusting within the Charcot fracture zone, and the significance of multiple detachment levels on the evolution of fold and thrust belts in the delta. This chapter has been developed as the tectono-stratigraphic evolution of the Deepwater West Niger Delta.

- **Chapter 7** concludes the thesis by drawing together the various strands of discussion that have emerged from the entire study and arrives at a series of conclusions.

Chapter Two: Regional Geology and Tectonic Evolution of the Deepwater West Niger Delta Margin

2.1 Introduction

This chapter aims to lay the foundation for the three investigative chapters that follow, and begins with a synthesis of the regional geology and evolution of the Niger Delta margin. This involves a review of the relevant literature, which is interwoven with and complemented by observations drawn from the regional mapping components in this study. It is aimed at chronologically describing the evolution and the regional geological context of the deepwater west Niger Delta. The ensuing section will covers some introductory material on the plate tectonic origin of the Equatorial Atlantic, and aims to arrive at an understanding of the place of the Niger Delta margin within a global plate tectonic context. This is followed by a review of the general structural geology of the deepwater Niger Delta without isolating the west from the east/south lobes of the delta and then rounded up with an insight to the stratigraphy in the area.

      The Niger Delta is situated in the Gulf of Guinea and is one of the largest deltaic systems in the world (Doust and Omatsola, 1990). The subaerial part of the delta covers about 75, 000 km², extending for more than 300 km from the apex to the mouth. The regressive delta and adjacent margins comprise a wedge of clastic sediments of about 12 km thick formed by series of offlap cycles (Evamy et al. 1978; Doust and Omatsola, 1990).

2.2 Geodynamic evolution of West African margin

2.2.1 Permo-Triassic rifting episode related to break up of Gondwana

This stage is associated with the break up of the Gondwana which started in the Middle Jurassic with the opening of the Central Atlantic (Klitgord and Schouten, 1986). There was no associated major intra-continental basin development in North West Africa that is coincident with this phase of opening, probably due to the location of the stable West African cratonic block. By the Mid-Jurassic, the Indian Ocean had started to open with the drift of Madagascar, India and Antarctica away from Africa. This break up was preceded by a significant phase of intra-continental rifting and sedimentation within the extensive Karoo basin of East and Southern Africa. The Karoo basin started developing in the Permo-Triassic (Lambiase, 1989) utilizing the weak zones of the Pan-African mobile belts surrounding the cratonic blocks of southern Africa.

2.2.2 The initial opening of the South Atlantic

Numberg and Muller (1991) suggested a stepwise, northward-propagating rift for the South Atlantic (Figs. 2.1-2.4). The first rift phase is tentatively dated as 150 Ma (Tithonian) to about 130 Ma (Hauterivian) from Nurnberg and Muller, (1991). This rift propagated from the southernmost tip of the South Atlantic to about 38° S in the vicinity of the Salado Basin. This rifting phase caused continental stretching and minor dextral strike-slip motion within the Colorado and Salado Basins. The post upper Jurassic sediment fill as well as the inception of faulting between Middle and Upper Jurassic lines (Urien and Zambrano, 1973) supports this assumption. At about 130 Ma, rifting combined with dextral strike-slip motion is assumed to have started along the Parana/Chacos Basin deformation zone. It has been recognized that this strike-slip motion was related to further northward propagation of rifting in the South Atlantic up to 28°S. North of this rift, Africa and South America are assumed to have been rigidly attached until Chron M4 (126.5 Ma) (Fig.2.3).

Between Chron M4 (126.5 Ma) (fig.2.3) and Chron MO (118.7 Ma) (Fig.2.4) rifting propagated northward into the Benue Trough. There is no evidence for opening in the equatorial Atlantic before Aptian time (118.7 Ma) (Jones, 1987; Castro, 1987; Mascle et al. 1988). The extension south of the equatorial Atlantic was taken up by continental stretching and sinistral strike slip motions in the Benue Trough/Niger rift system in accordance with Fairhead and Okereke (1987) and Fairhead (1988). No evidence of compressional phase in the equatorial Atlantic is evident during this stage (Castro, 1987; Mascle et al. 1988) as was proposed by Rabinowitz and LaBrecque (1979). At Chron MO (118.7 Ma) movements along the Parana/Chacos Basin deformation zone ceased, having generated 60 to 70 km of crustal extension and between 20 and 30 km of dextral shear.

After Chron MO (118.7 Ma) (fig. 2.4), the equatorial Atlantic began to open. According to Mascle et al. (1988), continental rifting in the equatorial Atlantic resulted in the creation of small divergent basins in the Aptian times characterised by thinned continental crust. Not until Late Albian to Early Cenomanian time (ca. 100 Ma) (fig. 2.5), small oceanic basins were created establishing the final breach between the continental crusts of Brazil and Africa (Mascle et al. 1988: Popoff et al. 1989). Paleo-current interconnection between Central and South Atlantic was established around Upper Albian times documented from the presence of Atlantic and Tethyan faunas (Wiedmann, 1978).

While intracontinental movements within Africa continued until about Chron 34 (84 Ma) (fig. 2.6) (Fairhead and Okereke, 1987; Castro, 1987), rifting in the Salado and Colorado basins is assumed to have ceased about chron M4 (126.5 Ma), having generated 20-25 km and 40-45 km of crustal extension in the Salado Basin and Colorado Basin, respectively, and 20 to 30 km of dextral strike-slip in both basins. Since Chron 34 (84 Ma) (fig. 2.6), the South Atlantic has opened as a two plate system. The strike-slip/rift zones present during

various times at the northernmost end of the propagating rift can be regarded

as stress buffers that prevented the translation of compression into the region

north of the rotation pole.

2.2.3 Neocomian-Early Aptian rifting episode
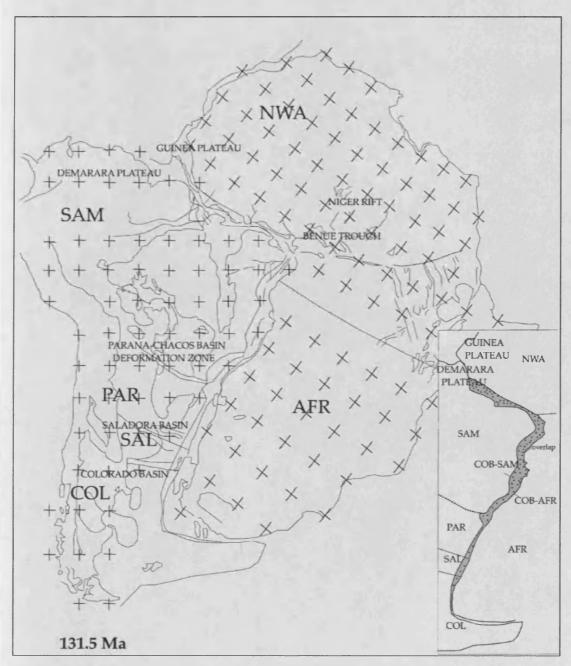
From Late Juraissic –Early Cretaceous onwards, rifting took place along the

lines of the proto-South Atlantic, as South America commenced its separation

from Africa (fig. 2.1). This is coincident with the second phase of intra-

continental rifting which led to the development of the west and central

Africa rift systems (Burke et al. 1971; Genik, 1992; Guiraud and Maurin, 1992).

This continental separation has been defined by the emplacement of oceanic

crustal material dated at ~130 Ma for the Cape Basin area (Rabinowitz and

LaBrecque, 1979) becoming younger northwards, so that the Equatorial region

had only just began separation by ~119 Ma (fig. 2.4) (Mascle et al. 1986). Prior

to the opening of the Equatorial Atlantic, the Central and South Atlantic

oceans were opening independently from one another resulting in

considerable stress building up in the Equatorial region (Fairhead and Binks,

1991). This stress was dissipated into the Caribbean (Pindell and Dewey,

1982), West and Central Africa (Fairhead, 1988, Fairhead and Binks, 1991),

northeast Brazil (Chang et al. 1992).

Voluminous tholeiitic flood basaltic volcanism in Brazil and Southern

Africa between 120-130 Ma (Parana province, Brazil; Etendeka province,

Namibia) has been related to the activity of a deep mantle plume (Tristan da

Cunha hotspot) beneath the newly developing plate boundary (White and

McKenzie, 1989; O`Connor and Duncan, 1990; Davison, 1999). This suggests

that at least for the opening of the South Atlantic, there is an intimate

relationship between hotspot activity and continental rifting.
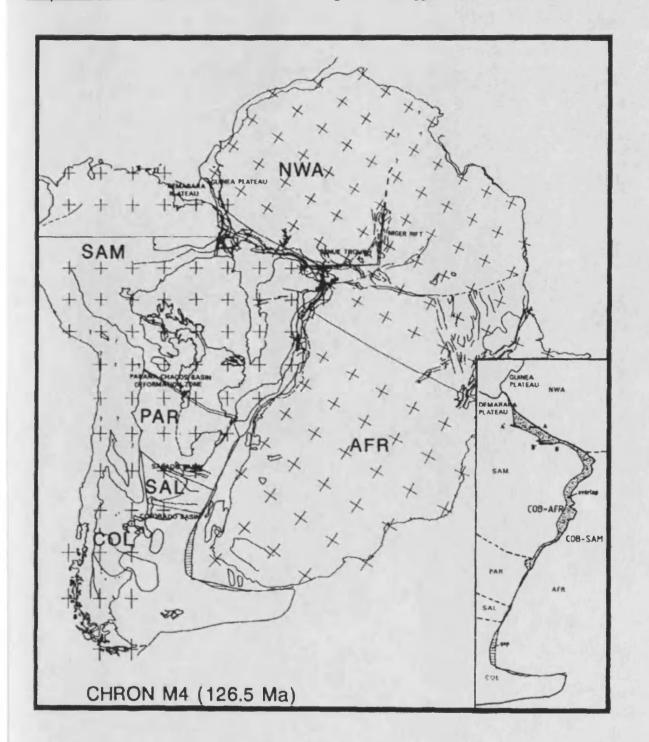
Figure 2.1. A pre-drift reconstruction of the South Atlantic at 150 Ma (Tithonian) without significant gaps between the continental margins of Africa and South America. The figure shows rift propagation in several steps giving rise to intracontinental deformation at the northernmost rift extensions. The intracontinental deformation is assumed to have taken place within the South American marginal Salado and Colorado basins and along the South American Parana/Chacos Basin deformation zone. In Africa, rifting and strike-slip motion in the Benue Trough and Niger Rift are assumed to have been active since the early opening of the South Atlantic until approximately 80 Ma. The amount of continental stretching along the deformation zone is shown by overlaps of hypothetical subplate-boundaries (stippled areas in insets). Plate identification numbers: AFR=Southern Africa, NWA=northwestern Africa, SAM=South America, PAR= Parana Plate, SAL=Salado Plate, COL=Colorado Plate. (Redrawn from Nurnberg and Muller, 1991)
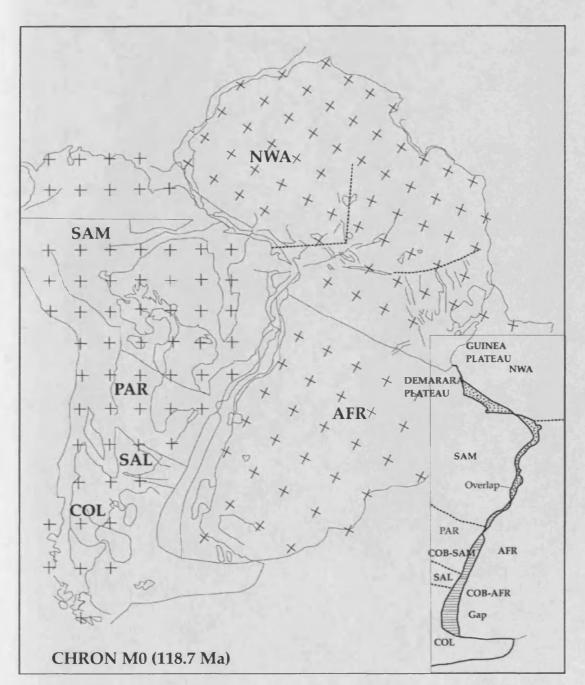
Figure 2.2. The separation of South America from Africa at approximately 130 Ma (Hauterivian). The South Atlantic rift propagated in the vicinity of the Salado basin to about 38°S. The rifting stage caused continental stretching and minor dextral strike-slip motion within the Salado and Colorado Basins since approximately 150 Ma (Tithonian). (Redrawn from Nurnberg and Muller, 1991).
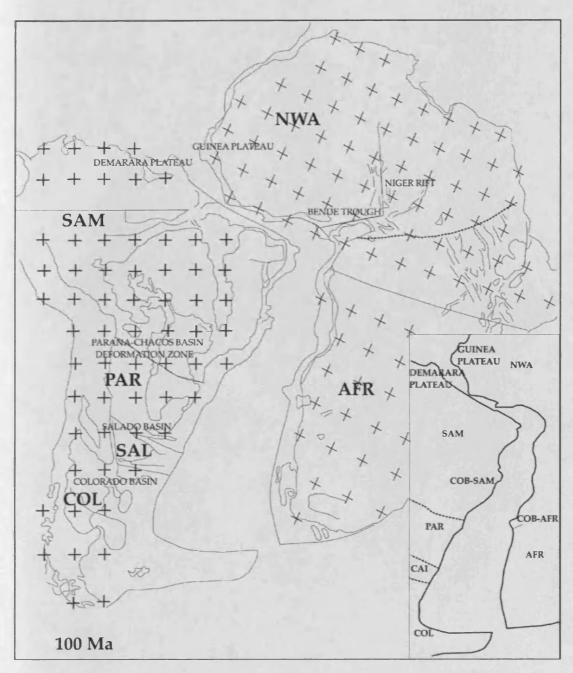
Figure 2.3. Chron M4 (126.5 Ma, Hauterivian). The further northward propagation of South Atlantic rifting between 130 Ma (Hauterive) and Chron M4 (126.5 Ma) induced rifting combined with strike-slip motion along the Parana/Chacos Basin deformation zone in South America. At Chron M4, seafloor spreading has propagated up to 28° S. Rifting and strike-slip motion in the Salado and Colorado basins ceased at about Chron M4 (126.5 Ma) having generated 20-25 km and 40-45 km of crustal extension in the Salado Basin and Colorado Basin, respectively and 20 to 30 km of dextral strike-slip in both basins. For figure captions see Figure 2.1.

Figure 2.4. Between Chrons M4 and M0, rifting propagated northwards into the Benue trough. The Benue Trough/Niger Rift system constitutes a large Cretaceous rift/ sinistral strike-slip system that were active until 80 Ma before present (Fairhead and Okereke, 1987). At Chron M0 movement along the Parana/Chacos Basin deformation zone ceased, having generated 60 to 70 km of crustal extension and 20 to 30 km of dextral shear. It is believed that Africa was still rigidly attached to South America in the Equatorial Atlantic, since there is no evidence for sediments older than Aptian (Jones, 1987). For the legend see figure 2.1. (Redrawn from Nurnberg and Muller, 1991)

Figure 2.5. The separation of South America from Africa at 100 Ma (Albian). After Chron M0, the Equatorial Atlantic began to open, connecting the South and Central Atlantic. Subsequently, South America behaved as a rigid plate, while intracontinental deformation in Africa was active until approximately 80 Ma (Late Cretaceous). Also see figure 2.1 for the legend. (Redrawn from Nurnberg and Muller, 1991).

2.2.4 Aptian-Albian rifting episode

The final separation of the African and South American continents occurred between approximately 100-105 Ma (Mascle et al. 1986; Nurnberg and Muller, 1991) but subsidence within some of the rift basins continued until the Santonian (fig. 2.6) when there was a major phase of regional deformation (Benkhelil et al. 1988) possibly related to N-S compression between the African and the European plates (Guiraud et al. 1987). Following this Santonian event at ca. 85+/-5 Ma (Genik, 1992), localised rifting continued into the Lower Eocene (Guiraud et al. 1992) with little associated magmatic activity.

One consequence of the pronounced history of the African continental extension is that plate scale compressional events have received relatively little attention in the geological literature, though they were noted by early workers (e.g. Burke et al. 1971). This is partly because these events were short-lived and because in some cases evidence for their existence is only present within the surface sections of pre-existing rift basins. Amongst these compressive events are those of the Late Santonian (ca. 83-85 Ma) (Guiraud and Bosworth, 1997) which corresponds to a major change in the pole of opening for the Atlantic Ocean (Binks and Fairhead, 1992; Guiraud et al. 1992), and the Maastrichtian compressive event. This particular event is described in more detail below. Another problem has been the general lack of detailed chronostratigraphic data due to the abundance of terrigenous continental series which have hindered the correlation of events across the large areas that have been involved.

2.2.5 South Atlantic seafloor spreading since Chron 34

The subsequent opening of the South Atlantic since Chron 34 is characterized
by simple divergence of two plates (Fig. 2.6-2.8). This simple spreading
history is complicated by minor ridge jumps, fracture zone jumps as well as
variations in seafloor spreading rate and direction. These reorganizations are
reflected in the present day satellite gravity map (Fig. 2.9). Fluctuations of half
spreading rates indicate considerable variations in seafloor spreading during
the South Atlantic opening. Between Chron M4 (126.5 Ma) (Fig. 2.3) and
Chron 34 (84 Ma) (Fig. 2.6) spreading half rates increased to a maximum of 28-
38 mm/yr at Chron 34 (Nurnberg and Muller, 1991). From this time, half rates
gradually decreased, reaching a minimum of about 14-16 mm/yr (Chron 27 to
25) in the early Cenozoic. This period of slow spreading lasted from about
Chron 30 (66.7 Ma) to Chron 21 (48.3 Ma), coincident with slow convergence
between the Nazca and the South American plates (Pardo-Casas and Molnar,
1987) and resulting in the creation of many new fracture zones.

An increase of spreading half-rates to 25-29 mm/yr at Chron 20 (44.7 Ma)
resulting in a decreasing number of fracture zones is followed by fine scale
fluctuations until present day (Figs. 2.9) which, in general, show a decreasing
trend. In general, the magnetic anomaly pattern of the South Atlantic
indicates asymmetrical spreading. According to Cande et al. (1988), spreading
rates have been about 7% faster on the west flank of the South Atlantic than
on the east flank since Chron 34 (Figs. 2.6). Although this asymmetry in
spreading rate cannot be regarded as spatially or temporally uniform (Cande
et al. 1988).

2.2.6 The Santonian (80-85 Ma) compressive event

Many African basins contain stratigraphic records of intra-Santonian hiatus,
whereby Campanian sediments unconformably overly Coniacian strata or
occasionally older folded strata. This hiatus can be related to a regional
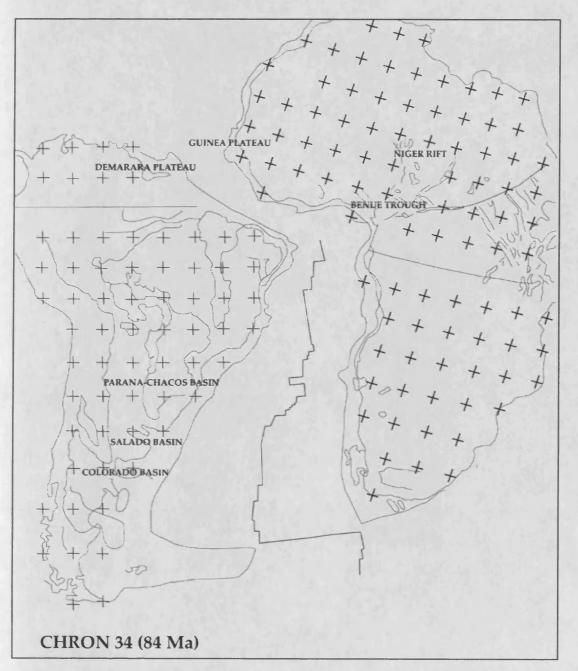
compressional episode referred to as the "the Santonian event" which affected much of the West and Central Atlantic rift systems from the Lower Benue trough to the Chad-Sudan border (Avbovbo et al. 1986; Benkhelil et al. 1983). This event is associated with folding, conjugate strike-slip faulting, reverse faulting often generating transpressional flower structures, development of local schistocity (Abakaliki anticlinorium) and inversion of some of the deepest Early to Middle Cretaceous basins (Genik, 1992; Bosworth, 1992; Guiraud and Maurin, 1993; Guiraud and Bellion, 1995; Guiraud, 1997).
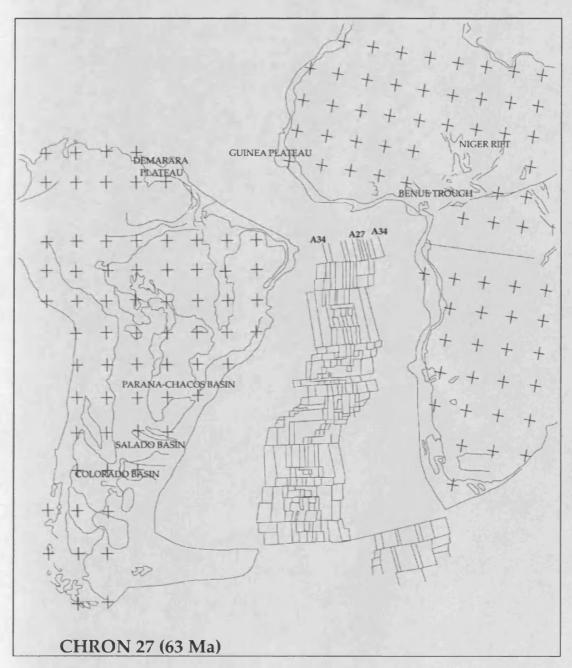
This event is synchronous with a rapid change in the direction of the African plate motion that is well established by kinematic studies of the Atlantic opening (Klitgord and Schouten, 1986; Fairhead and Binks, 1991; Binks and Fairhead, 1992). This rapid change in the African plate motion entails the onset of its collisional interaction with the European plate (Ziegler, 1988). At the same time, differences in spreading rates between the Central and South Atlantic spreading ridges were taken up in Africa along the broad WSW-ENE striking zone of deformation (Guiraud et al. 1992). This zone extends from the Equatorial Atlantic across Africa, with deformation focused in the rift zones located along pre-existing zones of lithospheric weakness. The Santonian compressive event marked a change in the intra-plate stress regime of Africa which led to distinct changes in fault geometries in many of the intracontinental basins (Genik, 1992).

2.2.7 Summary of the tectonic evolution
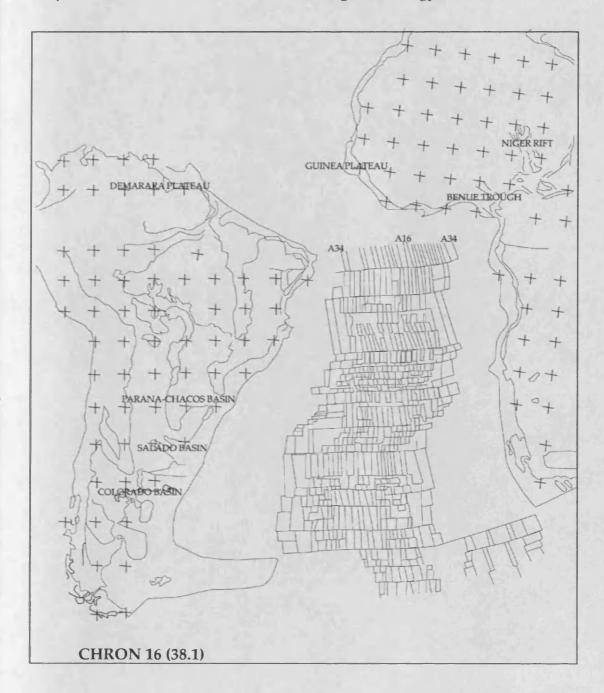
The Niger Delta continental margin is a passive margin system formed in the Equatorial part of the African plate (Fig. 2.8) and has undergone a complex phase of evolution from initial extension in the Cretaceous to the present day passive margin. The Central and South Atlantic basins developed independently of each other during the early stages of their evolution.

CHRON 34 (84 Ma)

Figure 2.6. The separation of South America from Africa at 84 Ma (Campanian). Intracontinental movement ceased within Africa at approximately Chron 34 (84 Ma). Nurnberg and, Muller, 1987 in agreement with Fairhead and Okereke, 1987 proposed 50-60 km of rifting combined with 40-50 km of sinistral strike-slip motion in the Benue Trough. After Chron 34, the South Atlantic is assumed to have opened as two plate system. (Redrawn from Nurnberg and Muller, 1991).

CHRON 27 (63 Ma)

Figure 2.7. The South Atlantic evolution during Chron 27 (63 Ma). The subsequent opening of the South Atlantic since Chron 34 (84 Ma) has been characterised by simple divergence of two continental plates. At approximately Chron 27 (63 ma), seafloor spreading rates reached a minimum during a period of slow spreading between Chron 30 (66.7 Ma) and Chron 20 (44.7 Ma), resulting in the creation of many new fracture zones. (Redrawn from Nurnberg and Muller, 1991)

CHRON 16 (38.1)

Figure 2.8. The South Atlantic evolution during Chron 16 (38.1 Ma). After Chron 20 (44.7 Ma), South Atlantic spreading rates accelerated, resulting in a decreasing number of fracture zones. A subtle S-shaped curve of the fracture zone throughout the Atlantic indicates a change in the spreading direction during Eocene time at approximately Chron 16 (38.1 Ma). (Redrawn from Nurnberg and Muller, 1991)
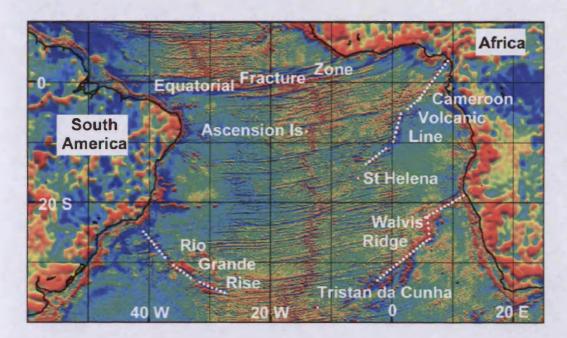
Initial seafloor spreading in the Central and South Atlantic occurred

during the Bathonian (165 Ma) and Barremian (130 Ma), respectively

(Rabinowitz and LaBrecque, 1979; Klitgord and Schouten, 1986; Nurnberg

and Muller, 1991) (with absolute age based on the time scale of Harland et al.

(1990). Seafloor spreading in the Equatorial Atlantic began during the Aptian

(118 Ma), with shearing along the Equatorial fracture zones and rifting in the

Benue trough (see fig. 2.10). The South and Central Atlantic Ocean continued

to open independently until the Early Santonian (84 Ma), when continental

Africa and South America were no longer in contact. This time coincided with

a change in the poles of rotation and the Atlantic Ocean began to open as a

two plate system (Nurnberg and Muller, 1991).

Plate tectonic reconstructions suggest that sea-floor spreading began in

the Equatorial Atlantic at half-spreading rates of between 9 and 28 mm/yr

concurrently with the Cretaceous constant polarity interval (anomalies M0 to

34, 124-83 Ma) (Le Pichon and Hayes, 1971; Nurnberg and Muller, 1991). Thus

the spreading rate in the Gulf of Guinea during most of the Cretaceous cannot

be verified from sea-floor spreading magnetic anomalies.

2.3. Regional Geology of the deepwater west Niger Delta

2.3.1 General gravity tectonics of passive margins

Most passive margins are usually typified by distinctive zones of linked

extensional, transitional and contractional deformation, where post rift cover

sediments are driven by downslope gravitational failure of the margin

towards the abyssal plains (Evamy et al. 1978; Doust and Omatsola, 1990;

Cobbold et al. 1995; Letouzey et al. 1995; Peel et al. 1995; Spathopoulos,
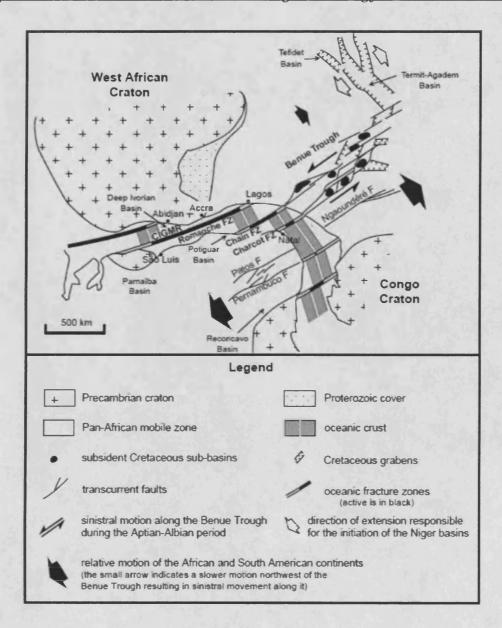
Figure 2.9. Satellite derived gravity map of the present day Central, Equatorial and South Atlantic showing evidence of the complex phase of its evolution from initial extension in the Cretaceous to the present day (after Sandwell and Smith, 1987).

Figure 2.10. General reconstruction of the Gulf of Guinea area during the Albian showing the Benue Trough (From Benkhelil et al. 1998).
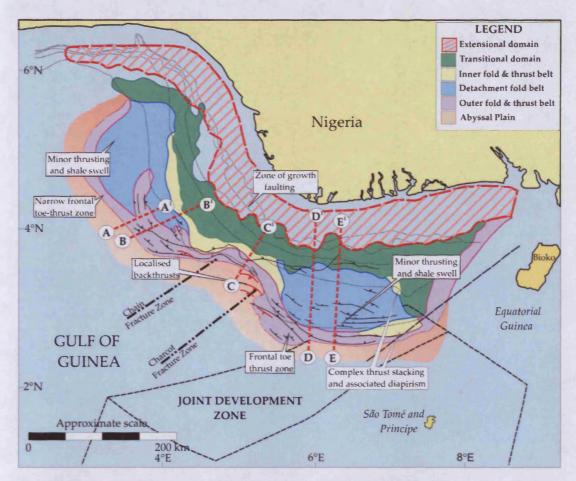
1996; Morley and Guerin, 1996; McClay et al. 1998; Marton et al. 2000; McClay et al. 2000; Cramez and Jackson, 2000; Rowan et al. 2000; Wu and Bally, 2000; Morley, 2003; Van Rensbergen and Morley, 2003; Rowan et al. 2004). This gravitational failure is compensated by a linked system of updip extension and downdip contraction.
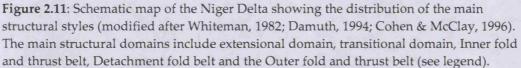
Deltaic systems developed in post-rift cover sequences of passive margins also exhibit gravity driven deformation with linked thin-skinned upslope extensional faults and downslope contractional fold and thrust systems above single or multiple ductile detachment levels (Evamy et al. 1978; Wu et al. 1990; Doust and Omatsola, 1990; Morley and Guerin, 1996; Poblet and McClay, 1996; McClay et al. 1998; McClay et al. 2000, 2003; Wu and Bally, 2000; Morley, 2003; Van Rensbergen and Morley, 2003; Cobbold et al. 2004; Rowan et al. 2004; Briggs et al. 2006).
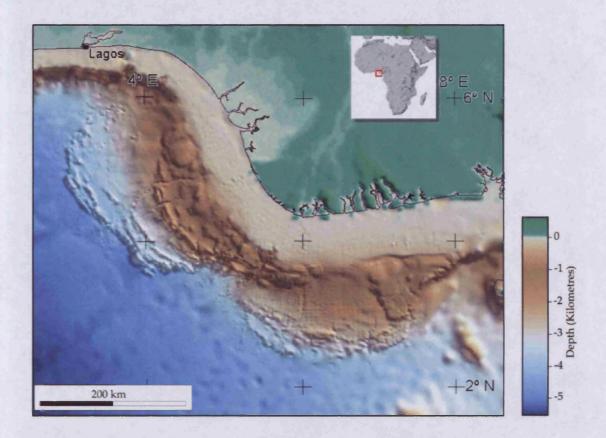
Some fold and thrust belts found in deepwater passive margins detach on overpressured and undercompacted shales due to rapid burial as, for example, in the fold belts of the Western Gulf of Mexico (Trudgill et al. 1999; Vazquez-Meneses and McClay, 2003), Sergipe-Alagoas and Para-Maranhao basins of Brazil (Zalan, 1999), Niger Delta (Evamy et al, 1978, Doust and Omatsola, 1990; Morley and Guerin, 1996; Connors et al. 1998; Wu and Bailly, 2000). Others detach on either post-rift or syn-rift salt and associated evaporites, as for example, the Mississippi fan (Atwater) and Perdido fold belt of the Northern Gulf of Mexico (Wu et al. 1990, Weimer and Buffler, 1992; Peel et al. 1995, Trudgill et al. 1995; Rowan et al. 2000 ; Wu and Bally, 2000); fold belts in the Campos, Santos and Espirito Santo Basins of Brazil (Demercian et al. 1993; Cobbold et al. 1995; Mohriak et al. 1995), and the Benguela Kwanza, Congo, Gabon and Rio Muni Basins of West Africa (Lundin, 1992; Duval et al. 1992; Spathopoulous, 1996; Morley and Guerin, 1996; Marton et al. 2000; Cramez and Jackson, 2000).

In the following section of this chapter, a review of the regional geology of the deepwater west Niger Delta is made that describes the characteristics of the gravity-driven tectonic system.

2.3.2 Regional Structure of the Niger Delta

The Niger Delta has been described structurally in terms of three linked gravity systems of updip extension dominated by extensional growth faults and a downdip thrust related fold dominated compressional systems with a transitional shale diapir controlled system intermediate between them (see Fig. 2.11). A major detachment zone within the Akata Formation that will be described later in this chapter, links the extensional province across the mud-diapir zone to the contractional fold-thrust belts in the lower slope. (Evamy et al. 1978; Doust and Omatsola, 1990; Damuth, 1994; Cohen and McClay, 1996; Morley and Guerin, 1996; Jubril et al. 1998; Connors et al. 1998; Hooper et al. 2002; Corredor et al. 2005a; Briggs et al. 2006). These three tier systems are further subdivided into five (5) major structural provinces or zones based on structural styles imaged on seismic data and high resolution bathymetry. These structural zones (figs. 2.11 and 2.12) include (1) an extensional province (2) a mud diapir zone (3) the inner fold and thrust belts (4) a transitional detachment fold zone, and (5) an outer fold and thrust belt zone. The deformation across these structural provinces is active today, resulting in the pronounced bathymetric expression of structures that are not buried by recent sediments as illustrated on figure 2.12. To illustrate the deformation styles in the Niger Delta, cross sections (figs. 2.13-2.17) are used to describe the structural style. The positions of these regional structural cross sections are presented on figure 2.11. The ensuing sub-sections will deal with the detailed description of these structural styles.

Figure 2.11: Schematic map of the Niger Delta showing the distribution of the main structural styles (modified after Whiteman, 1982; Damuth, 1994; Cohen & McClay, 1996). The main structural domains include extensional domain, transitional domain, Inner fold and thrust belt, Detachment fold belt and the Outer fold and thrust belt (see legend).

Figure 2.12. High resolution bathymetric map of the Niger Delta showing the main structural domains. (Inset is the map of Africa showing the approximate position of the study area marked in red box (from Corredor et al. 2005b).
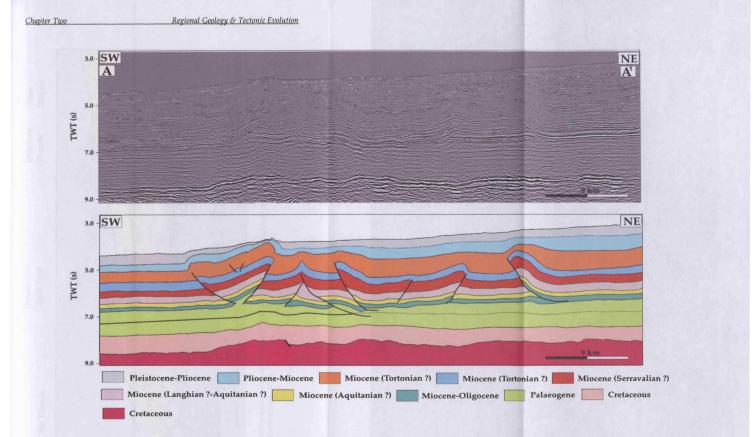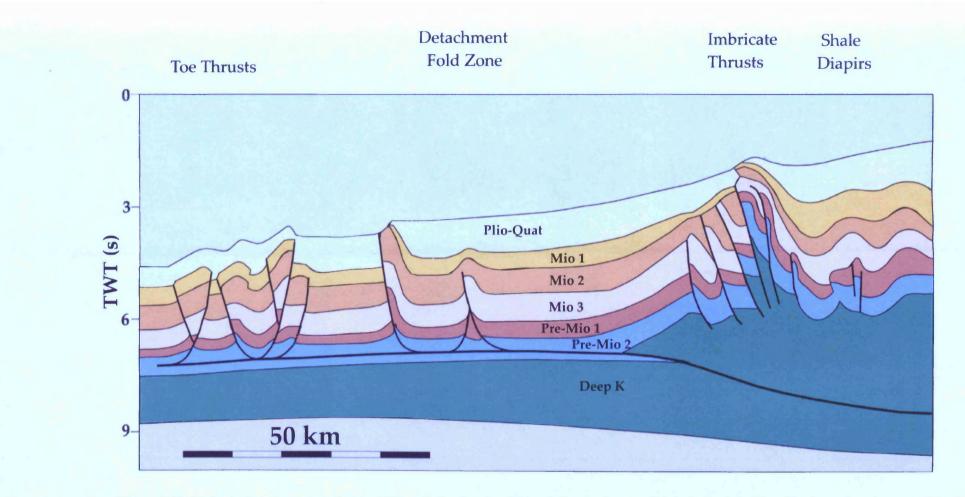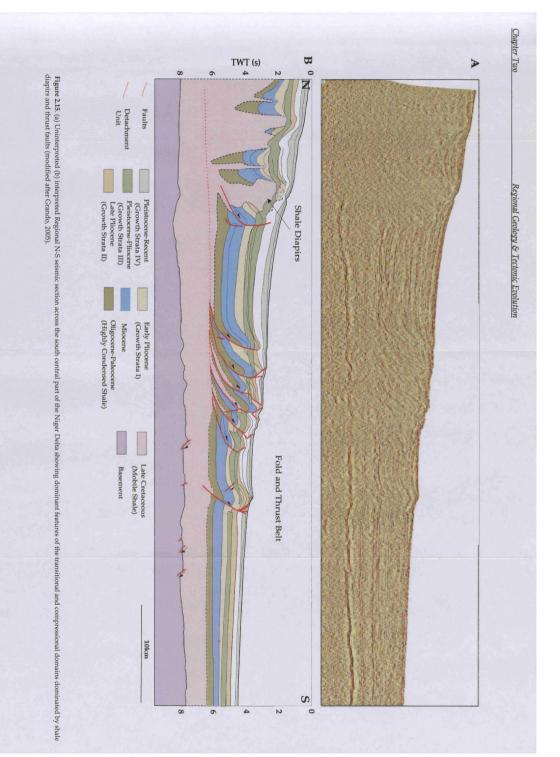
Figure. 2.13. A dip line from the 3D seismic reflection dataset showing the possible age of some major reflectors in the study area. The possible age markers were based on correlation with nearby wells where the stratigraphy has been defined. Note that the Akata Formation which is defined by the Palaeogene section is generally devoid of any internal reflections except for a high amplitude reflection that is present almost at the middle of the formation.

Figure 2.14. Geological section across the west Niger Delta showing the variation in structural style in the transitional and compression zones (modified after Krueger, 2006).

TWT (s)

A

B 0 N

Shale Diapirs

Fold and Thrust Belt

S

Faults

Detachment Unit

Pleistocene-Recent (Growth Strata IV)

Pleistocene-Pliocene (Growth Strata III)

Late Pliocene (Growth Strata II)

Early Pliocene (Growth Strata I)

Miocene

Oligocene-Paleocene (Highly Condensed Shale)

Late Cretaceous (Mobile Shale)

Basement

10km

Figure 2.15. (a) Uninterpreted (b) interpreted Regional N-S seismic section across the south central part of the Niger Delta showing dominant features of the transitional and compressional domains dominated by shale diapirs and thrust faults (modified after Grando, 2005).

Figure 2.16. Interpretation of a SW-NE regional 2D seismic line across the Niger Delta showing the structural characteristics of gravity driven thin-skinned tectonics related with an overpressure shale detachment layer. The position of this line is indicated of figure 2.11 (figs. 2.16A and 2.16B were modified from Hooper et al. 2002 and Saugy & Eyer, 2003 respectively).

Figure 2.17. A regional cross section from the East/South Niger Delta showing the structural variations (modified after Krueger, 2006). Note that the IFTB signifies Inner fold and thrust belt. The thickness of the Pliocene-Quaternary sediments could be observed to reduce towards the Abyssal Plain.

2.3.2.1. Extensional growth fault zone

The extensional domain is located beneath the outer continental shelf and uppermost slope and is characterised by extensive listric and seaward dipping growth faults. These faults are formed in response to the rapid seaward progradation and loading of the delta sediment (Bruce, 1973; Evamy et al. 1978; Knox and Omatsola, 1990; Damuth, 1994). Sediment accumulations of up to several kilometres thick, often with well developed rollover structures occur on the downthrown sides of these faults. Deformed shale structures and diapirs associated with these faults are generally deeply buried. Large landward-dipping antithetic or counter-regional faults also develop back to back with some of the listric faults over the buried shale ridges (see figs. 2.17AB) (Knox and Omatsola, 1989; Damuth, 1994; Morley and Guerin, 1996).

On the north side of the section (see figs.2.16AB), both basinward-dipping and counter-regional growth normal faults are present in the extensional province beneath the continental shelf. Counter-regional normal fault systems consist of upper Miocene to lower Pliocene prograding sequences, whereas down-to-basin growth fault systems contain upper Pliocene and Pleistocene distal prograding units with shingled toe turbidites (Mitchum et al. 2000).

2.3.2.2 Transitional Mud diapir zone

The zone is so termed because it lies between the extension fault-dominated zone and the fold-and-thrust belt (Figs. 2.11 & 2.16B). This intermediate, transitional zone is characterised by shale diapirs and ridges of variable size, shape, distribution, orientation and depth of burial beneath the upper

continental slope and upper rise. This shale diapir zone is characterized by passive, active, and reactive mud diapirs (Morley and Guerin, 1996), including shale ridges and massifs, shale overhangs, vertical mud diapirs that form mud volcanoes at the seafloor (Graue, 2000), and inter-diapir depocentres. In many instances such as in figure 2.15, growth and upward movements have folded the overlying strata and occasionally deforming or eroding the seafloor. Most of the diapiric structures show tremendous subsurface relief and may extend hundreds of metres above the surrounding seafloor. Deep intraslope basin, partially to completely fill with relatively undisturbed and ponded sediment up to several kilometres thick occurs between these diapirs (see fig. 2.15) (Damuth, 1994; Morley and Guerin, 1996).

The mobile shale detachment sequence of the Akata Formation underlies all the structural zones and dominates deformation in the shale diapir zone. Morley and Guerin (1996) described the shale diapirs as elongate both sub-parallel and sub-perpendicular to the delta front. Some shale diapirs are round in plan view and hence show no strong orientation. Some of the sub-perpendicular trends can be attributed to pre-existing basement fabrics (probably tilted fault blocks). Morley and Guerin (1996) further noted that the faults associated with the shale diapirs are generally smaller in size and displacement, than the major faults in the extensional growth fault depobelt.

2.3.2.3 Compressional thrust related fold system

The deformation within the contractional toe of the Niger delta is driven by updip and gravitational collapse of shelf sediments. Basinward motion of these shelf sediments are accommodated by normal faults that sole to detachments with the prodelta marine shales that overlie the Cretaceous basement. Slip on the detachment is transmitted to the deepwater, where it is

diverted onto thrust ramps and consumed by contractional folds in the deepwater fold and thrust belts.

The deepwater compressional fold and thrust belts form two arcuate regions that die out laterally at the western and eastern/southern margins of the Niger delta system (Evamy et al. 1978; Doust and Omatsola, 1990) (Figs. 2.11 and 2.12). The highly developed portion of the zones can be up to 70 km wide and contains numerous imbricates. The lower compressional zone is characterised by widespread imbricate thrusts and fault-related fold structure beneath the lower continental slope and uppermost rise (Lehner and De Ruiter, 1977; Doust & Omatsola, 1990; Damuth, 1994; Cohen & McClay, 1996; Morley & Guerin, 1996; Wu & Bally, 2000; Corredor et al. 2005b). These compressional structures are in the toe-of-slope setting outboard of both the zone of shale structure and in the more distal transitional zone comprising relatively undeformed strata. The contractional portion of the delta can be divided based on structural styles as seen on seismic data and from high resolution bathymetry into an inner thrust belt (figs. 2.14 and 2.16A) and an outer toe thrust belt (figs. 2.13-2.15, 2.16A and 2.17) which are commonly separated by large transitional detachment fold belt (figs. 2.14 and 2.17) Connors et al. (1998) and Corredor et al. (2005a). The inner and outer fold and thrust belts are most evident in the bathymetry (fig. 2.12), where ridges represent the crests of fault-related folds, and low regions correspond to piggyback basins formed above the backlimbs of fault imbricates. Highly imbricated thrust sheets containing Tertiary to Holocene delta-front to deep-marine sediments form the inner and outer fold and thrust belts (Corredor et al. 2005a).

The inner fold and thrust belt extends in an arcuate path across the centre of the offshore delta, whereas the outer fold and thrust belt consists of northern and southern sections that define two outboard lobes of the delta (figs. 2.11 and 2.12). These two lobes, and their associated fold belts, are

separated by a major rise in the basement topography that corresponds to the

northern culmination of the Charcot fracture zone (Figs. 2.16B). The break

between the northern and southern sections of the outer fold and thrust belt

results from thrust sheets being stacked in a narrow zone above and behind

this major basement uplift (Connors et al. 1998; Wu and Bally, 2000).

2.3.2.3.1 Inner fold and thrust belt

This zone is characterised by basinward-verging thrust faults (typically

imbricated) and its associated folds. This zone is also typified by higher

structural dip with average distance between the imbricate thrust sheets of

between 1 and 2 km with occasional piggy-back basins (Corredor et al. 2005a).

2.3.2.3.2 Transitional detachment fold belt

This zone is situated beneath the lower continental slope that is characterized

by large areas of little or no deformation interspersed with large, broad

detachment anticlines that accommodate relatively small amount of

shortening (Bilotti et al. 2005; Briggs et al. 2006). The detachment fold belt is a

transitional zone between the inner and outer fold and thrust belts. The along

transport thrust sheet dimensions range from between 2 and 5 km. Within this

transitional fold belt zone, the deformation is dominated by localized

detachment folds and/or buckles above duplexes within the thin detachment

layers. The boundary between the translational zone and the outer toe thrust

belt is loosely defined by where the detached deformation breaks to the

surface.

2.3.2.3.3 Outer toe thrust belt

The outer toe thrust belt (figs. 2.13-2.15, 2.16A and 2.17) is characterized by both basinward and hinterland-verging thrust faults and its associated folds. This zone could be described as a more classic toe-thrust zone with thrust-cored anticlines that are typically separated from one another by several kilometres (Corredor et al. 2005a). This zone is situated further downdip, with channelised turbidite sands trapped in broad wavelength anticlines above incipient thrust propagation zones.

The outer toe thrust belt typically consists of an in-sequence set of 10 to 20 fault-fold structures. While the majority of the structures are forward verging, there are local domains dominated by backthrusting and a frontal wedge. The structures are predominantly fault-propagation folds, often initiated by thrusting out of early low-relief buckles. Detailed reconstructions (Krueger et al. 2006) of the western fold belt suggest that the timing of progressive initiation of motion on the basal detachment is strongly linked to the onset of elevated fluid pressures within the detachment shale due to disequilibrium under-compaction in response to rapid burial by the advancing delta. The basal detachment of the outer toe thrust belt differs dramatically from that farther updip. The basal shear inboard of the inner thrust belt is characterised by diffuse slip across a thick Cretaceous mobile shale sequence. The advance of the deformation front was initiated when some of the distributed shear within the Cretaceous mobile shale sequence began to transfer into more discrete detachments in Upper Cretaceous and Palaeogene shales beneath the abyssal fan, rather than simply breaching to the surface.

Broad regional anticlines developed where this slip transfer involved a climb in the stratigraphic level, resulting in complex fault-bend folds above the ramp. The downslope transition from thick mobile shale to more discrete detachments has led to complicated imbrication of the deep section even where no obvious ramp is observed.

The sediments involved in the deformation of the outer toe thrust belt are unconsolidated to weakly consolidated muds, silts and sands that behave in a very ductile manner. Folds tend to develop very rounded forms, and the faults show only minor bending after ramping up from the detachment. Only minimal structural topography can develop because the surface sediment is unconsolidated, and downslope failure quickly removes the crest of the growing structures. As a result, breaching thrusts are quickly truncated and rarely roll over onto the seafloor.

Detailed analysis of the growth history of several fault-propagation folds (Krueger et al. 2006) suggests that once initiated they propagate rapidly to near their ultimate length. Subsequent deformation increases the fault slip and structural relief without significant increase in length. Later deformation along an individual structure frequently retreats to localized deformation near the structural crest, while the extremities are successively abandoned. It is proposed by Krueger (2006) that this localization of deformation is being driven by the effective weakening of the shales at the crest of the fold due to elevated fluid pressures being transported from the back syncline along interbedded sands.

Most thrust faults in these systems, with exceptions in the northern and central parts of the delta, verge toward the deep ocean and sole to detachment levels located within the Akata Formation (Briggs et al. 2006).

2.3.2 Regional Stratigraphy of the Niger Delta

2.3.2.1 Stratigraphic Setting

The Niger Delta basin consists of Cretaceous to Holocene marine clastic strata that overlie oceanic and fragments of continental crust (Fig. 2.18). In this basin, Cretaceous marine clastics consist mainly of Albian–Maastrichtian shallow marine clastic deposits. The precise distribution and nature of

correlative Cretaceous deposits beneath the offshore Niger Delta is unknown. From the Campanian to the Paleocene, both tide-dominated and river-dominated deltaic sediments were deposited during transgressive and regressive cycles, respectively. In the Paleocene, a major transgression initiated deposition of the Imo shale in the Anambra basin and the Akata shale in the Niger Delta basin. During the Eocene, the sedimentation changed to being wave dominated. At this time, deposition of paralic sediments began in the Niger Delta basin, and as the sediments prograded south, the coastline became progressively more convex seaward. Today, delta sedimentation remains wave dominated (Corredor et al. 2005a).

The stratigraphic subdivision of the Tertiary sedimentary sequence of the Niger Delta has been studied and documented by most petroleum exploration companies; however the results of the studies only reside in the files of these companies as proprietary information. Nevertheless large volumes of published literature also exist that describes the stratigraphic subdivision of the Tertiary Niger Delta strata (Short and Stauble, 1967; Avbovbo, 1978; Evamy et al. 1978; Whiteman, 1982; Knox and Omatsola, 1989; Doust and Omatsola. 1990, Kulke, 1995).

Generally, the stratigraphy of the delta has been divided into three (3) major litho-stratigraphic units representing major regressive offlap cycles of Eocene to Recent age that can be distinguished based on their sand-shale ratio into the Akata, Agbada and Benin Formations. The type sections of these formations have been described by Short and Stauble (1965), subsequently other authors have also described these formations i.e. Avbovbo, (1978); Evamy et al. (1978); Whiteman (1982); Doust and Omatsola (1989); Knox and Omatsola (1989) and Kulke, (1995) as an overall regressive mega-sequence broken up into a series of offlap cycles. A generalised cross section of stratigraphic section of the Niger delta highlighting all the formations is presented on Figure 2.18 and would be described in more detail below.

2.3.3.1.1 Akata Formation

The Akata Formation which is the base of the Cenozoic delta complex is composed mainly of marine shales deposited as the high energy delta advanced into deep water. This formation has a thickness range of 2000 m at the most distal part of the delta and reaching about 7000 m beneath the continental shelf (Doust and Omatsola, 1990). The type section of this formation is the Akata-1 well which has been described by Short and Stauble, (1967). They are characterised by uniform shale development evident from gamma-ray and spontaneous potential logs responses and are rich in benthonic foraminifera. These prodelta shales are medium to dark grey, medium hard, in places soft and sandy or silty. The shales are under-compacted and may contain lenses of abnormally high pressured siltstones or fine-grained sandstones.
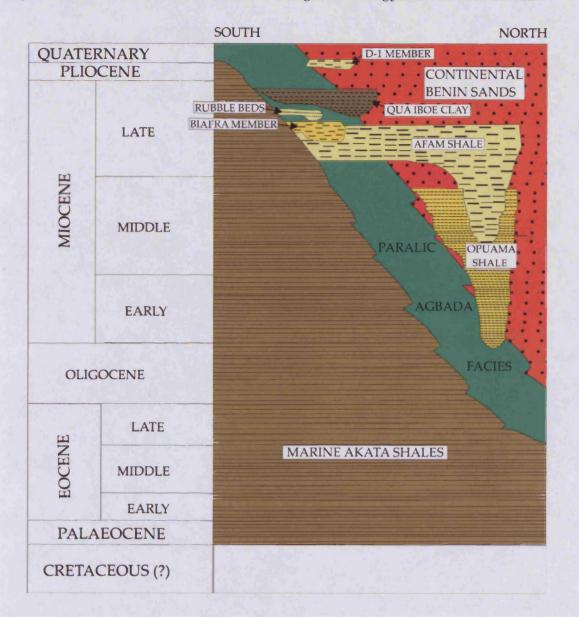
In the fold and thrust belts areas of the Niger delta, this formation is up to 5000 m thick due to structural replication by thrust ramps as described in Corredor et al. 2005a and in the core of large detachment folds (Bilotti et al. 2005). The formation is composed of shale sequences that are believed to contain the source rocks and may also possibly contain some turbidite sands which are potential reservoirs targets in the deepwater environments and minor amounts of clay and silt. The turbidites are thought to be deposited by turbidity currents during the development of the delta. This formation is generally of a low reflectivity, lacking any internal reflection apart from a single strong, high amplitude reflection that is locally present at the middle of the formation. This mid-Akata reflection serves as an important structural marker for the definition of a detachment levels (Corredor et al. 2005a; Briggs et al. 2006). This formation is characterised by an abnormal P-wave velocity of ~2000 m/s that may reflect regional fluid overpressures (Bilotti and Shaw,

2001). It could also present the detachment horizon for large growth faults that define depobelts in the updip part of the delta (Knox and Omatsola 1989). The Akata and Agbada Formation in the deep and ultra-deepwater areas appear to be divided by a major regional sequence boundary which marks the abrupt change in the depositional environment with the appearance of deepwater fans. In the main study area, the base of the probable Akata Formation can be seen to onlap an older progradational package. This formation is thought to range from Palaeocene to Holocene in age (Doust and Omatsola 1990). Conceptually deepwater Palaeocene Imo Shale and even the Late Cretaceous Nkporo shales are of the Akata facies (Short and Stauble 1967; Whiteman, 1982).

2.3.3.1.2 Agbada Formation

The type section for the Agbada Formation has also been described by Short and Stauble, (1967) from the Agbada-2 well. This formation overlies the Akata Formation, is the main hydrocarbon bearing sequence in the Niger Delta (Doust and Omatsola, 1990) and is composed of alternating sequence of sandstones and shales of deltaic front, distributory channel and deltaic plain origin. This formation has been shown by Weber, (1971) from electric logs patterns, well cores and dipmeter data to be cyclic sequence. However, there are problems inherent with the definition of the top and bottom of the Agbada Formation. The top is usually defined as the base of fresh-water invasion, whereas the base is often placed at the onset of overpressure during drilling. The contacts are difficult to determine lithologically due to local argillaceous intercalations of considerable thickness in sands of the overlying Benin Formation, and also to turbidite sand units well below the top of the

Figure 2.18. A Generalised stratigraphic column showing the three formations of the Niger Delta (modified after Doust and Omatsola, 1990; Jubril et al. 1998).

Akata Formation. This formation has been dated as Eocene to Recent (Reijers et al. 1997).

2.3.3.1.3 Benin Formation

The Benin Formation which is the uppermost unit of the delta complex has been described from the Elele-1 well by Short and Stauble (1967) as composed of predominantly massive highly porous, freshwater bearing massive sandstones and gravels with local thin shale interbeds considered to be of braided stream origin. The base of this formation could be defined by the deepest freshwater-bearing sandstone exhibiting high resistivity or by the first marine Foraminifera within shales as the Benin Formation is nonmarine. The youngest dated shales underlying these continental sands are probably of early Miocene age. This formation has however not been encountered in the deepwater regions of the Niger delta (Morgan, 2003).

In addition to these three major formations, there are also several intra-formational clay members e.g. the Opuama and Afam Members (Jubril et al., 1998) (fig.2.18). These shale members are considered to have been deposited in submarine paleo-channels (Knox and Omatsola, 1989; Jubril and Amajor, 1991). The distribution of these clay-filled paleo-channels in the Miocene of the eastern Niger Delta has been reported by Weber and Daukoru (1975) while that of the Opuama canyon and its fill in the western delta has also been reported in Petters (1984). A detailed description of the Afam clay member in the eastern delta has also been undertaken by Jubril and Amajor (1991). For the purpose of simplicity in this study, the three (3) basic stratigraphic formations; the Akata, Agbada and Benin are used.

2.3.2.5 Development of the escalator regression model

The evolution of the Niger delta has been described by Doust and Omatsola (1990) in terms of a stepwise outbuilding involving the deposition of fluviomarine offlap (paralic Agbada Formation) sequence controlled by subsidence along synsedimentary faults and punctuated by rapid shifts from one depobelt to the other, each active for a relatively short time span of a few million years. The one-way, stepwise outbuilding of the delta through geological time has been termed the "*Escalator Regression*" by Knox and Omatsola, (1989). Stacher (1995) showed that the delta sequence consists of a series of discrete *depocentres* or *depobelts* which were the main belts of deposition of the paralic Agbada Formation that succeeded each other progressively as the delta shifted its loci downdip through time. The main characteristics of this regression are the rapid advancement of alluvial sands due to the cessation of subsidence in a depobelt and the continuation of sediment supply

This model was developed to explain the particular association of stratigraphy, lithofacies and structure in the Cenozoic Niger Delta. The entire sedimentary wedge in the delta was laid down sequentially in five or six major depobelts (Evamy et al. 1978; Doust and Omatsola, 1990) each 30-60 km wide that prograde southwest ward 250 km over oceanic crust into the Gulf of Guinea (Stacher, 1995) with the oldest depobelt lying furthest inland and the youngest located offshore. The important factor here is the degree of the mobility of the overpressured marine shale which moves in response to gravity loading of deltaic sediments. Decrease in the mobility caused sand/shale sedimentation to be displaced southwards by continental sand deposition under conditions of lowered subsidence rate (Evamy et al. 1978).

Chapter Three: Crustal Structure of the Deepwater West Niger Delta Passive Margin from the interpretation of seismic reflection data.

3.1 Abstract

The interpretation of 2D and 3D seismic reflection data complimented with gravity data allows the crustal architecture of the deepwater west Niger delta passive margin to be defined. The data show that the area is underlain by oceanic crust that is characterised by a thickness of 5-7 km and by internal reflectivity consisting of both dipping and sub-horizontal reflectors. Some of the dipping reflections can be traced up to the top of the basement where they offset it across a series of minor to major thrust faults. Other internal reflections are attributed to extensional shear zones and possibly due to intrusions in the lower crust. The Moho can be correlated as a discrete reflection over >70% of the study area. It is generally smooth, but localised relief of up to 1 km is observed. The southeastern part of the study area is dominated by a zone of SW-NE striking basement thrusts.

The crustal thickness in the study area is below the global average for a typical oceanic crust. Generally the crust is thinnest around a major transform structure, the Chain Fracture Zone, possibly related to the local geometry of the spreading fabrics. There is no significant variation in the thickness of the crust across this ocean-ocean transform in the area. The recognition of oceanic crust has profound implications for heat flow and thermal maturation of hydrocarbons in the Niger Delta petroleum province.

3.2 Introduction

The understanding of the crustal architecture at passive continental margins in the deepwater provinces has been a major challenge for regional basin analysis and for petroleum exploration in frontier regions such as in the hydrocarbon-rich Niger Delta. The geological interpretation of subsurface structures in the deepwater Niger delta has advanced immensely with the acquisition and processing of abundant high quality 2D and 3D seismic reflection dataset by petroleum exploration companies. These data, supported with other geophysical information, were used to investigate the nature of the deep crustal structure of the west Niger Delta. As hydrocarbon exploration extends into the deeper parts of the west Niger Delta region, it has become critical to prospectivity prediction to understand the nature of the crust beneath the toe region in this area.

Prior to this study, previous studies of the crustal structure of the continental margins off the Niger Delta have been limited and restricted to the use of widely spaced reconnaissance 2D seismic lines (e.g. Hospers, 1965, 1971; Mascle et al. 1973; Delteil et al. 1974; Emery et al. 1975; Lehner and De Ruiter, 1977). These studies mainly focused on the mapping of fracture zone trends and other basement structures in order to reconstruct the plate tectonics history of the Equatorial Atlantic. However, on these older seismic data, the deeper structure of this margin is not adequately imaged because acquisition and processing parameters were tuned to the shallow sedimentary architecture and were mostly restricted to a maximum record length of between 5 and 6 s TWT (seconds, two way travel time). Deepwater seismic surveys with processing limited to the first 6 s TWT usually lose resolution while still imaging post-breakup sedimentary layers of the basin. The seismic lines therefore fail to reveal a number of features that are presently recognised as being crucial in the understanding of basin forming
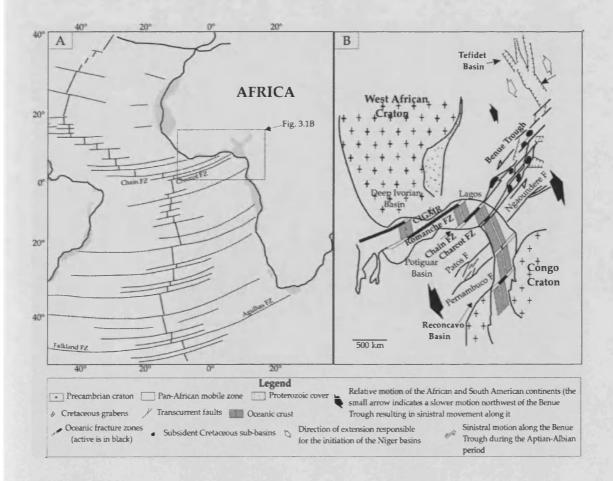
processes and the tectonic evolution of sedimentary basins. More recently, newly acquired 3D seismic reflection data was used to image the differences in crustal structure across the Chain Fracture Zone (Davies et al. 2005). This study builds on the work of Davies et al. (2005), and extends their approach to a broader context using a large modern, regional 2D seismic grid.

This chapter aims to examine the crustal architecture of the deepwater west Niger Delta offshore Equatorial West Africa (Figs 3.1A & 3.2AB) from deep-imaging of 2D and 3D seismic reflection and gravity data in order to address the spatial and temporal variability in crustal structure and thickness. The main aim is to examine whether reflection seismic data can be used to differentiate between probable oceanic and probable continental crust. In the absence of wide-angle seismic data providing first order constraints of crustal velocities, the issue is whether reflection seismic characteristics alone can build a robust case for discriminating between end member crustal types. This question has wider relevance for deepwater exploration beyond the important but parochial specifics of the deepwater Nigerian margin. Many areas of current and future exploration potential do not have a full geophysical database normally regarded as a minimum to classify crustal type, but simply have deep reflection seismic coverage and seasat-derived gravity data (Brever and Oliver, 1980). So any insights on crustal structure that can be derived from this study may assist in the interpretation of crustal type in other margins.

Despite the considerable amount of exploration and discovery of a number of oil and gas fields on the deepwater Niger Delta margin, the crust here is still relatively understudied as compared to other areas of the Equatorial Atlantic. Our key observation in this study is the identification of a single Moho reflection. By mapping this horizon and a prominent shallower reflection which is interpreted to define the top of the crust, and making use of seismic

Figure 3.1. (A) Tectonic map of the South Atlantic showing the location of tectonic flowlines and oceanic fracture zones (modified after Le Pichon and Fox, 1971). Note the location of the Falkland and Agulhas Fracture Zones. (B) Reconstruction of the Gulf of Guinea during the Albian time showing the Benue trough (modified after Benkhelil et al. 1998)

velocity information from nearby areas, the crustal thickness over an area of about 49 000 km² were mapped.

3.3 Geodynamic setting of the study area
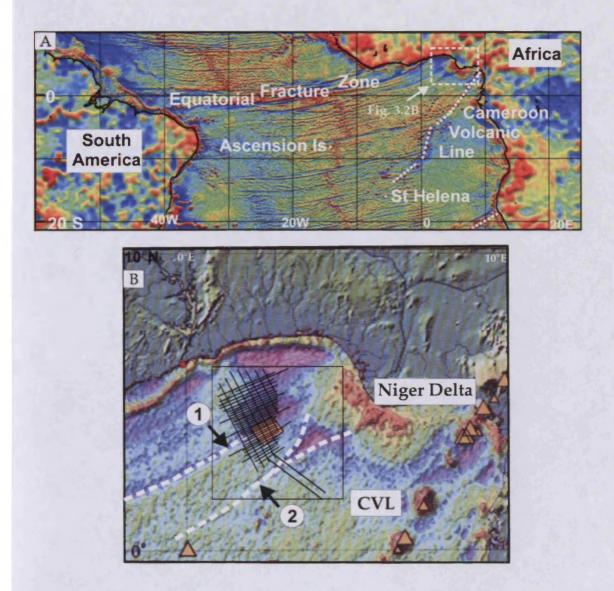
The study area is located in the Equatorial region of the South Atlantic margin (see Fig 3.1A) that developed as a continental margin during the Early Cretaceous. Rifting spread northwards from the Falkland-Agulhas fracture zone (Fig 3.1A) so that the ocean opened diachronously from south to north in a 'zipper-like' manner (Le Pichon and Hayes, 1971; Rabinowitz and LaBreque, 1979; Uchupi, 1989; Nürnberg and Muller, 1991). Nürnberg and Muller (1991) suggested that the first phase of rifting started in the Tithonian (150 Ma) and by the Aptian (118 Ma), seafloor spreading had extended into the Equatorial Atlantic and the Benue trough (Fig 3.1B). At this stage, the simple model of two plates diverging became more complicated with shearing motion along the Equatorial fracture zones, and continued opening along the South Atlantic and Benue trough arm of the essentially Ridge-Ridge-Transform fault (RRF) triple junction which is situated beneath the present day Niger Delta (Burke et al. 1971; Whiteman, 1982; Fairhead, 1988a). The Equatorial Atlantic was the locus of intersection of the Central and South Atlantic rifts, and therefore had to accommodate the differential opening of these two ocean basins. The complexity of this opening led to the development of intra-continental rifts in West Africa and Northeast Brazil (Fairhead and Binks, 1991; Matos, 2000).

Once the central and south Atlantic mid-oceanic ridges were linked through the equatorial Atlantic, the ocean basin began to open as one system (Guiraud et al. 1992). Unfortunately the onset of seafloor spreading in the Gulf of Guinea coincided with the Cretaceous magnetic quiet zone (anomaly M0 to anomaly 34, 118-83 Ma) so, lacking other information, the spreading

rate in the Gulf of Guinea during the Cretaceous is not precisely known. From plate tectonic reconstruction of the opening of the South Atlantic different authors have proposed a range of half-spreading rate from 9mm/yr (Le Pichon and Hayes, 1971) to 28mm/yr (Nürnberg and Muller, 1991). The absence of magnetic stripes means that fracture zone traces are the only major aid to plate kinematic reconstruction in this region.

A satellite-derived gravity map (Figs 3.2AB) generated from public domain data (Sandwell and Smith, 1997) shows that the seafloor of the South Atlantic is interrupted by a large number of sub-parallel crustal discontinuities identified as oceanic fracture zones, that occur symmetrically disposed on both sides of the mid-Atlantic ridge. These discontinuities represent inactive segments of transform faults associated with seafloor spreading axes that can generally be detected by steps in the bathymetry, by displacements of the magnetic anomalies in the oceanic basement and by the alignment of gravity anomalies. The area of this study is clearly crossed by the Chain and Charcot Fracture Zones (Figs 3.1AB & 3.2B). Other smaller fracture zones can be traced in the region surrounding the study area, but they are not discussed further.

3.4 Database and Methodology

The deep seismic reflection coverage of the area consists of recently acquired high resolution 120 fold 2D seismic reflection data acquired in 1998 with a 6 km cable length and 12 s recording interval, processed using the Kirchhoff bent ray pre-stack time migration (PSTM), consisting of 5640 km combined length, distributed along 33 dip lines oriented in SW-NE and scattered over approximately 3586 km, 8 NW-SE striking lines covering a distance of 1644 km and two WNW-ESE oriented strike lines of about 410 km combined length. The distribution and positioning of these data are shown on figs

Figure 3.2. (A) Gravimetric Satellite imagery map of the Central, Equatorial and South Atlantic showing the study area and the position of the major fracture zones in the area (Sandwell and Smith, 1997) but modified after Fairhead and Wilson, 2005. (B) Satellite Gravity map of the study showing the (1) Chain and (2) Charcot Fracture Zones (Sandwell and Smith, 1997) and the approximate position of the 2D and 3D seismic data utilised superimposed on it.
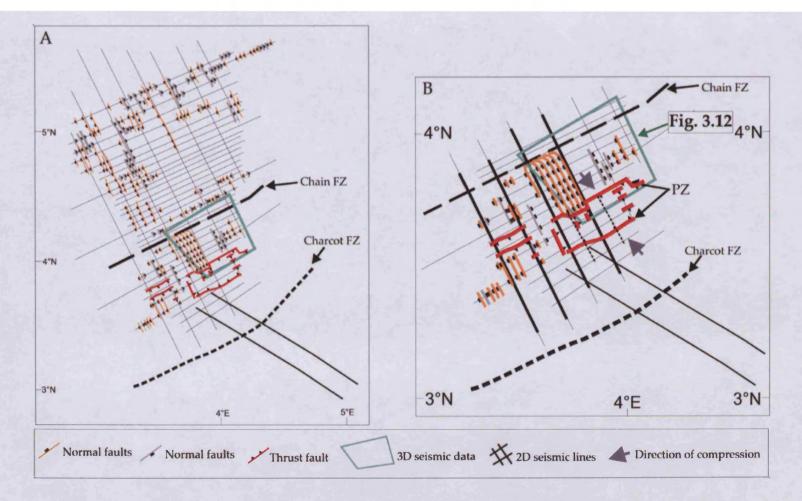
3.2B and 3.3. These data have dip and strike line spacing of 8 and 20 km

respectively. A 3D seismic reflection dataset (see Figs 3.3AB) which images

the deeper levels to approximately 12 s TWT was also made available for this

study.

The 3D seismic reflection data were acquired by Veritas DGC using a

general line spacing of 25 m, covering an area of 3057 km² obtained from 6 km

offset length and 12 s record interval with the same processing sequence as

the 2D data. These data were acquired over water depths ranging from 1.5-4

km. The general parameters used for the acquisition allowed the imaging of

the deeper crustal reflections. The data quality is regarded as good due to the

application of pre-stack time migration (PSTM). The data however lacked

independent constraints because no deep drilling or wide angle seismic study

has ever been conducted down to the studied depth in the area. Seismic

velocities used to depth convert some of the regional reflections were derived

from stacking velocities used in processing and from velocity information

from similar studies conducted in nearby regions (e.g. Sage et al. 2000; Wilson

et al. 2003). Estimated errors in average velocity and hence depth conversion

is up to 15%, but even with this large uncertainty, it is considered that the

main conclusions of the paper are not invalidated.

The dominant frequency of the seismic data varies with depth, but it is

approximately 10 Hz at the level of interest. Using a crustal seismic interval

velocity of 6.0 km/s (Sage et al. 2000; Wilson et al. 2003), the vertical resolution

($\lambda/4$) is estimated to be about 150 m for the main interval of interest in the

crystalline crust.

This study has defined two key seismic horizons that can be correlated with

high confidence throughout the study area on the 2D and 3D grid and are referred

to as Horizons **B** and **M** (Fig 3.4). These horizons are imaged consistently enough

that they can be mapped in detail with the grid spacing of 10-20km in the 2D

survey area.
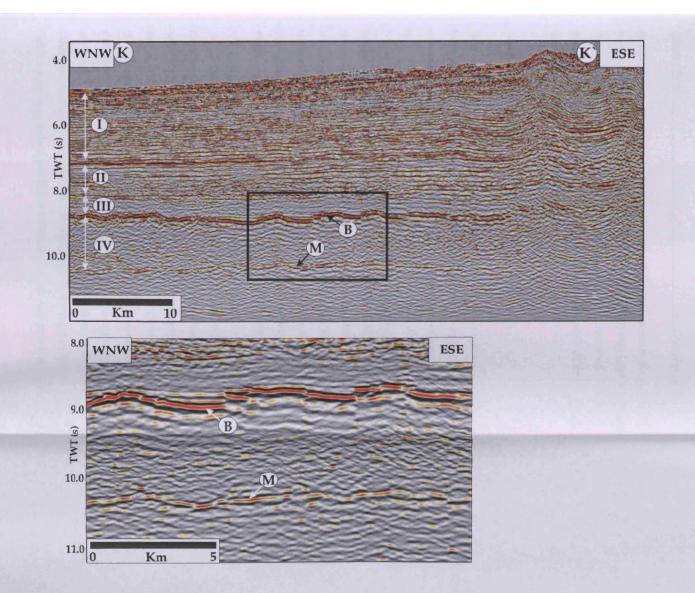
Figure 3.3. A generalised map showing the distribution of the 2D and 3D seismic reflection dataset used for the study with the structural interpretation of horizon B over it. (B) An enlarge portion of the southern portion of the study showing the spreading fabrics and also the compression events.

The free-air gravity map from Sandwell and Smith (1997) that images some of the major fracture zones in the South Atlantic (Fig 3.2A) was used for additional structural control through the Gulf of Guinea region of the Equatorial Africa from latitude 7°00` N to 0° 00` N and longitude 1° 00` E to 7° 00` E. Gravity modelling was not attempted as part of this study.

3.5 Regional seismic characteristics of Deepwater West Niger Delta

3.5.1 Geologic setting

The study area covers an area of about 49 000 km² and encompasses a large sector of the mid-lower slope region of the west Niger Delta. This region of the slope is characterised by what are interpreted to be shale-cored folds and toe thrust structures (see Damuth, 1994). The sedimentary succession in this sector consists of major prograding system of slope deposits that are of Cretaceous-Recent age (Frankl and Cordry, 1967; Short and Stauble, 1967), and consisting of hemipelagites, turbidite fan deposits and channel-levee complexes, with variable elements of interbedded mass transport complexes (Heinio and Davies, 2006). This highly reflective and dominantly clastic slope succession overlies a seismically opaque interval at depth which has been interpreted as the crystalline basement (Wu and Bally, 2000; Ajakaiye and Bally, 2002).

The Cretaceous-Recent slope sediments are relatively undeformed in the updip direction, but near the foot of the present day slope, they are thrusted and folded into a series of detachment and thrust propagation folds that propagate upwards to deform the seafloor in places (McClay et al. 2003; Corredor et al. 2005; Briggs et al. 2006). This series of folds began growing mainly from the Late Oligocene to Miocene (Roberts, 2004), but in some areas from the Mid Pliocene (Ajakaiye and Bally, 2002) and their growth continues to the present day. The level of the main detachment for the deepwater thrust and fold belt is within the Akata Formation, presumed to be highly overpressured. Hence this deformational

Figure 3.4. Representative 2D seismic reflection line showing the seismic subdivision of the deepwater west Niger Delta passive margin. Horizons M and B are contained within package IV and have been enlarged to show the internal seismic character of the crust between horizons M and B.

system is decoupled from the basement, although there are some indications that topography at the top of the crystalline basement (Horizon B) may have influenced the structural style for the fold belt (Briggs et al. 2006). The Cretaceous to Recent succession is divided into three major seismic- stratigraphic units (Units I, II and III) and described in more detail below.

3.5.1.1 Seismic Stratigraphy

Seismic unit **I** (Fig 3.4A) represents a package consisting of acoustically chaotic, hummocky or transparent seismic reflection packages which are occasionally separated by high-continuity reflection complexes with the reflection configuration typical of hemipelagic drape (*sensu* Brown and Fisher, 1977). This unit is equivalent to the Agbada Formation and consists of alternating sequence of sandstones and shale (Short and Stauble, 1967; Avbovbo, 1978) deposited by channelised turbidites, debrites and hemipelagites (Davies, 2003; Deptuck et al. 2003; Morgan, 2004; Adeogba et al. 2005; Heinio and Davies, 2005). The sands constitute the main reservoirs. The age of this unit has been interpreted by some as pre- Miocene (Chapin et al. 2002) and has been defined elsewhere as Eocene-Pleistocene (Short and Stauble, 1967; Doust and Omatsola, 1990). The base of this unit is marked by a major regional sequence boundary (Morgan, 2003).

Seismic unit **II** (Fig 3.4A) is a low reflectivity package, lacking laterally continuous internal reflections except for a single mid-level high amplitude reflection which may be related to a zone of detachment (Corredor et al. 2005; Briggs et al. 2006). This unit corresponds to the Akata Formation of Avbovbo (1978) and Knox and Omatsola (1989). It is thought to be composed of marine shales which are believed to be the source rock for hydrocarbons generated in the area, and contains some locally developed sand and silt intervals. This unit exhibits anomalous P-wave seismic velocity of (2.0 km/s) that may reflect regional fluid overpressure (Bilotti and Shaw, 2001) and conceivably provides a detachment

surface for the evolution of some of the thrust propagation folds in the area (Briggs et al. 2006). This unit both downlaps and onlaps the low reflectivity package beneath, the Late Cretaceous – Palaeocene age Pre-Akata sediment wedge succession (Morgan, 2003, 2004). Unit **III** (Fig 3.4A) is a regionally extensive and almost featureless seismic unit which is of deepwater marine origin, and probably mainly consists of pelagites and hemipelagites.

The basement, upon which we focus here is below the Cretaceous-Recent succession and is referred to as Unit **IV** (Figs 3.4AB). In the following section we provide the justification for regarding Unit IV as being composed predominantly of crystalline basement.

3.5.1.1.1 *Horizon B*

The top of the basement beneath the deepwater west Niger Delta progradational system is defined by Horizon B, representing the upper boundary of a generally unreflective interval marked as unit **IV** (Figs 3.4AB). From its context, and the lack of any significant internal reflectivity over such a large area, we consider Horizon B to form the upper boundary to the crystalline crust in this area. The seismic character of the underlying interval down to the level of Horizon M bears a striking resemblance to crystalline basement imaged by reflection seismic data from other regions of crystalline crust (see, for example, Hobbs et al. 1995). Precisely what type of crystalline crust is bounded by Horizon B is discussed in later sections.

Horizon B (Figs 3.4AB) is correlated with high confidence over (95%) of the study area as a high amplitude continuous reflection with a strong positive acoustic impedance contrast signifying a major change in density and velocity from the overlying slope mudstones of Unit III. Horizon B is disrupted by numerous faults, the vast majority of which have extensional offsets of up to a few hundreds of metres (see below). Horizon B exhibits an irregular relief related to this faulting, whose character is best constrained in the 3D seismic survey area. In some areas,

Horizon B is distorted and obscured by the seafloor multiple and occasionally by uncollapsed diffractions. In some areas, immediately below Horizon B are some less continuous moderate to high amplitude reflections.

The two-way travel time structural map of Horizon B shows that it lies between 7.50 to 9.50 s (Fig 3.5), dipping gently landwards beneath the slope (Fig 3.6) except near the Charcot fracture zone (see Figs 3.1AB and 3.2B) where it is associated with high basement relief block (Wu and Bally, 2000) and also at point marked **PZ** on Figs 3.3AB where it is shown as an uplifted structure between the Chain and the Charcot Fracture Zones. In general, the time structure map of Horizon B shows an irregular relief that varies rather smoothly, with positive structural features having relief of no more than several hundreds of metres (Fig 3.5) above regional. The contour pattern is almost certainly partly aliased by the large spacing of the 2D grid, but nonetheless reveals relief that has a wavelength of c. 20 km. Strong alignments in contours are seen in the central region, where the contours strike predominantly WSW-ESE.

Representative examples of dip and strike profiles that cross some of the main positive features on this horizon map and are presented in figures 3.6 and 3.7, respectively. The geometry of Horizon B seen on these lines varies from very smooth and flat (Fig 3.6B), to smooth but broken by normal faults (Fig 3.6A) to stepped in an almost dip slope-scarp slope topography (Figs 3.6CD). On the strike lines we observe a combination of smooth and irregular topography (Figs 3.7AB). These profiles also give a good indication of the discontinuous distribution of the internal reflectivity seen within the basement. Local sub-Horizon B reflections are clearly seen over distances of 5-10 km, for example, on fig 3.6D, and particularly on fig 3.7B. The southeastern extremities of both strike profiles show excellent examples of asymmetric folds developed at Horizon B, which are interpreted to be associated with thrust faults within the basement. This interpretation is supported by prominent fault plane reflections that can be seen extending across almost the entire interval between Horizons B and M, best seen on fig 3.7B.
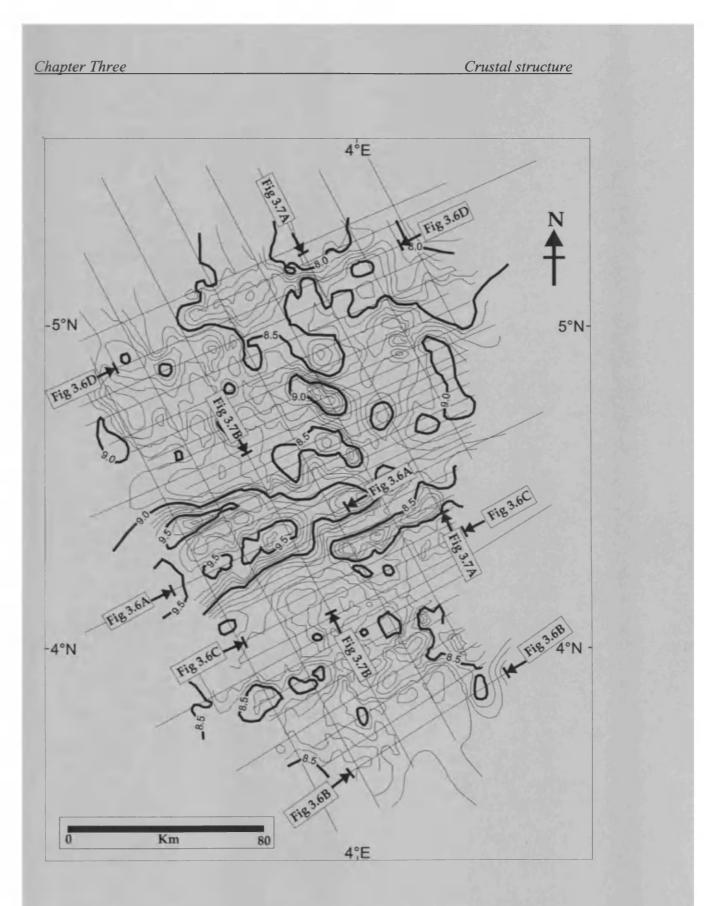
Figure 3.5. Two-way travel-time (seconds) structural map of horizon B.

3.5.1.1.2 Horizon M

Horizon M (see Fig 3.4AB) is a high amplitude coherent event which can be traced almost continuously over about 85% of the study area. It is recognisable as a discrete reflection beneath an approximately 2 seconds thick interval of opaque basement. Horizon M closely parallels Horizon B and is highly mappable in some areas while in others it is difficult to correlate. The loss of continuity in this reflection is attributed mainly to attenuation and scattering related to overburden complexities such as those related to the deepwater fold and thrust belt (Fig 3.6), rather than to genuine structural effects or differences in reflection M characteristics. The two-way travel time to this horizon ranges from about 9.60 to 11.40 s (Fig 3.8).

Based on the context and continuity of Horizon M, and its consistent depth (5 to 7 km below the oceanic basement (horizon B)), we interpret this important reflection as representing the reflection Moho. The seismic character of the Moho seen here in the study compares closely with that of Rosendahl et al. 1991, 1992; Meyers et al. 1996a, 1996b; Rosendahl and Groschel-Becker, 1999, based on their studies of crustal structure in adjacent sectors of the West African continental margin.

Moho two-way travel-times are significantly distorted by local shallow lateral velocity variations. The cover sequence is the main cause of this and in certain instances produces significant local velocity push downs (Fig 3.6A). The time structural map of Horizon M from fig 3.8 shows that this horizon varies rather smoothly with the presence of certain topographic features. These features are sometimes associated with near-surface geological structures which are not meaningful in the context of the Moho. The grid spacing of the seismic dataset
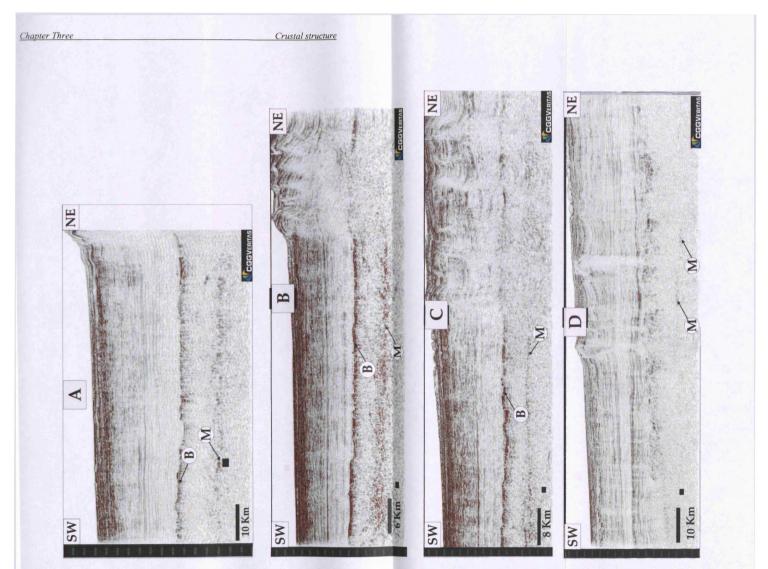
Figure 3.6. Dip line of different transect cutting the study area and showing some important structural features. M and B signifies Moho and top basement respectively.
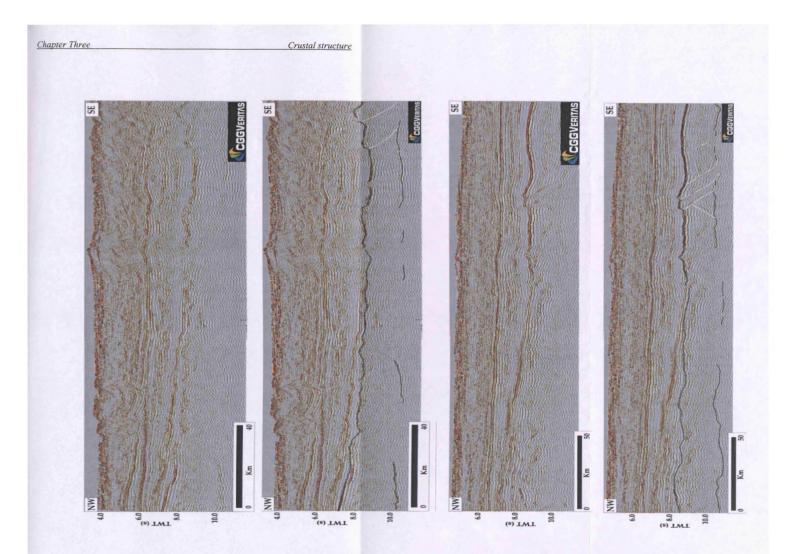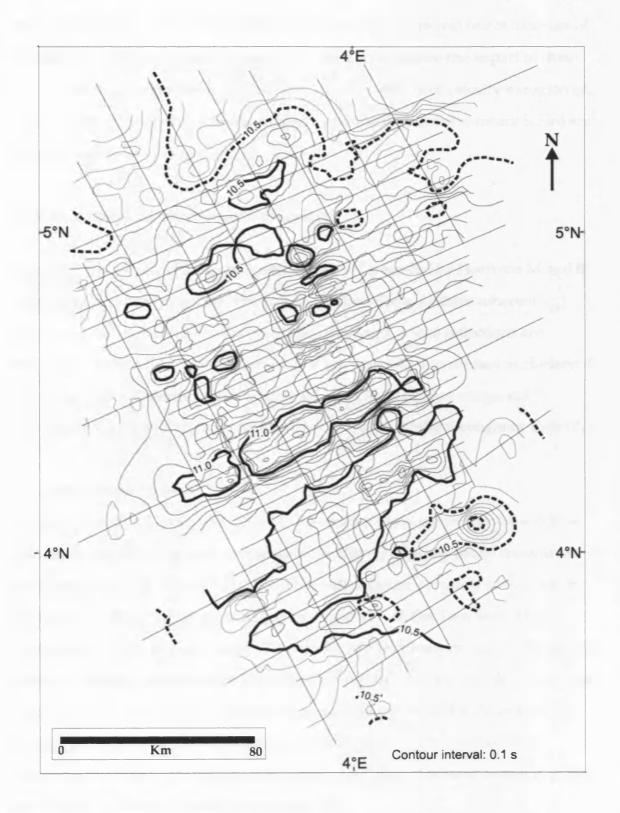
Figure 3.7 Two Strike line transect (see position on figure 3.5) showing the crustal variation in the area. The Moho can be easily picked in places while in others it is difficult to trace.

Figure 3.8. Two-way travel-time (seconds) structural map of horizon M. The contours shown in dotted lines are areas where it is difficult to pick reflections from horizon M.

does not allow for accurate mapping to ascertain if they are real or not. Because of this the two-way travel time map was smoothed to minimise the impact of these short-wavelength velocity-induced distortions. The effects of velocity variation on a more regional scale (e.g. velocity push-down beneath the sedimentary basin) are however preserved in the map.

3.5.1.1.3 Internal seismic character of Unit IV

Although the general characteristic of the interval bounded by Horizons M and B is that it is seismically opaque, there are a number of areas where coherent reflections can be identified over significant distances. These reflections are interpreted in two categories: (A) those that are generally concordant to Horizon B and occur in the uppermost part of Unit IV, and (B), those that are generally discordant to both Horizons B and M and occur sporadically throughout Unit IV.

A: concordant upper interval:

The uppermost 0.12 –0.6 s (0.4 -2 km) of the crust (between Horizons M and B) is commonly marked by a series of moderate to high amplitude, partly continuous reflections (Figs 3.4, 3.6 and 3.7). This reflection package is crudely concordant to the basement morphology represented by Horizon B. Reflections within this package are locally of much higher amplitude, and terminate abruptly. The seismic facies are strongly reminiscent of interbedded volcanic and volcanoclastic rocks as described from volcanic continental margins (Planke et al. 2000). A detailed 3D seismic description of this unit from the southeastern part of the study area interprets this package to represent the uppermost part of oceanic crust (i.e. pillow lava flows) (Davies et al. 2005) (see section 3.6).

B: discordant reflections:

Two main types of discordant reflections have been interpreted within Unit IV. Firstly we identify a series of planar reflections whose dip ranges between 20 and 50°. These dips were calculated assuming an average velocity of 6000 m/s for Unit IV. This value of interval velocity was based on averaging the stacking velocities and applying the conversion from stacking to interval velocities using the Dix equation (see Yilmaz, 2001). They are seen equally on both dip and strike lines, but with limited lateral continuity such that their strike cannot be measured confidently over lateral distances of more than 5 km (Fig 3.10). These planar reflections can be traced from Horizon B downwards (see Fig 3.4), terminating just above the level of Horizon M. The majority of these reflections exhibit apparent dip towards the southwest and are nearly regularly spaced when seen in groups on any individual line. They are typically of positive polarity, and laterally uniform in character. They are strongly reminiscent of reflections that have been ascribed to intra-crustal shear zones (Collier et al. 1997).

A second group of more moderately discordant reflections within Unit IV are also observed (e.g. labelled as H on Fig 3.10). This group of reflections are generally of high amplitude and discontinuous and have been mapped over an area of 2200 km^2 within the southwestern area of the study area. They are seen in the middle of Unit IV, generally between 2 and 3 km below Horizon B (Fig 3.10). Their geometry is in places almost subhorizontal, and together with their mixed polarity suggests that they may represent a complex lithological boundary within the crust, or possibly sheet-like intrusions (sills). A strike line perpendicular to fig 3.10 (Fig 3.11) also shows that these subhorizontal reflections are offset by some compressional faults in the area indicating that they have not acted as a mechanical detachment for these faults (see next section).
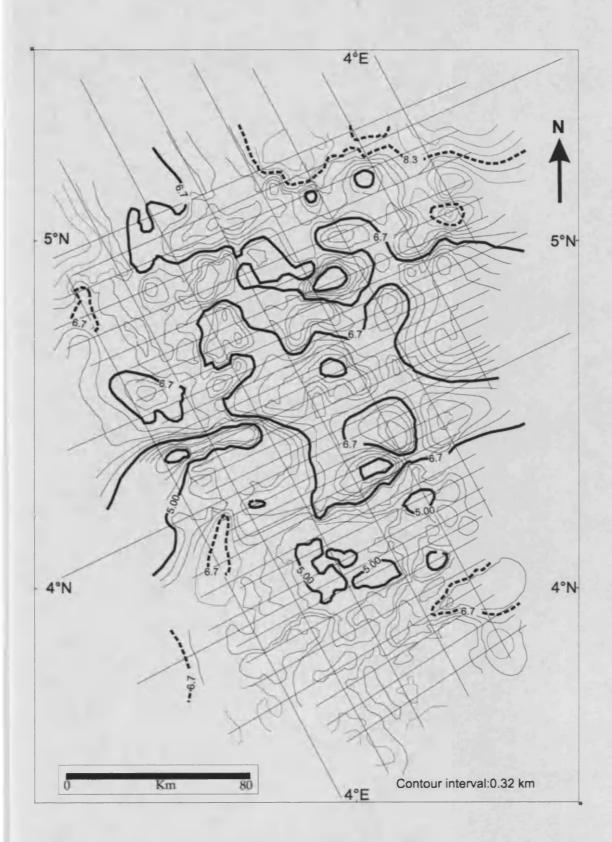
3.5.1.1.4 Unit IV Thickness

Based on our interpretation of Horizon B as the top of the crystalline basement and Horizon M as the reflection Moho, we constructed a time isopach map for the crust

Figure 3.9. Crustal thickness variations under the deepwater west Niger Delta passive margin. Note the correspondence between zones of lower values with tectonic spreading fabric.
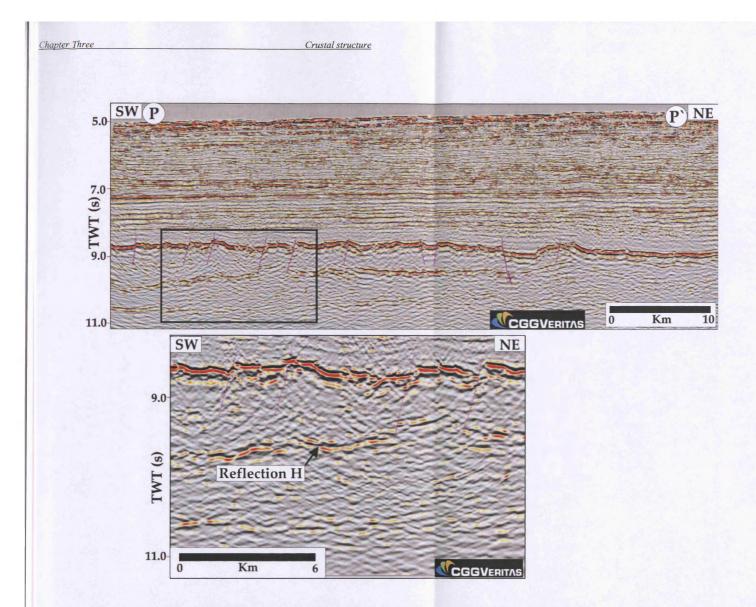
Figure 3.10. Seismic line P-P` showing planar reflections which terminate within the upper part of the crust. The location is shown on figure 3.3.
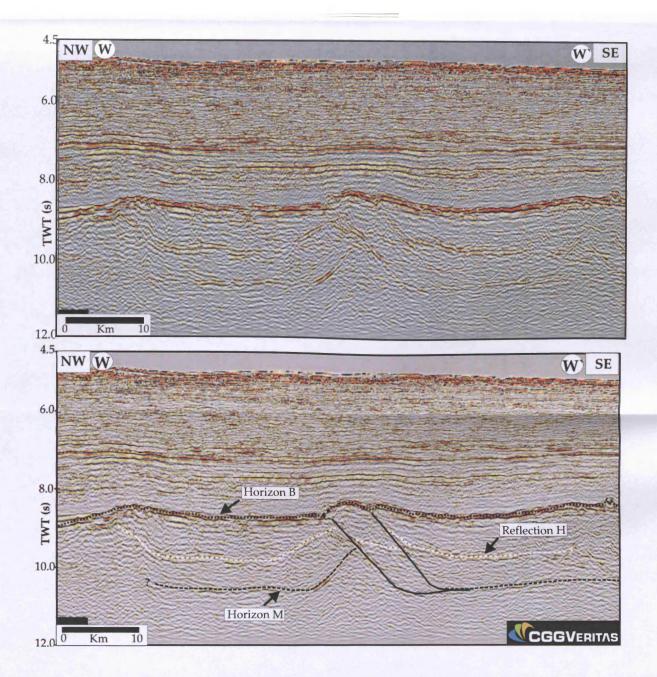
Figure 3.11. Seismic line example of bulge on horizon B due to compressive components of the faults. Strike line example of reflection H is also shown here. Fault cutting through the entire crust with an average dip of 35°. These types of faults are generally compressive in nature.
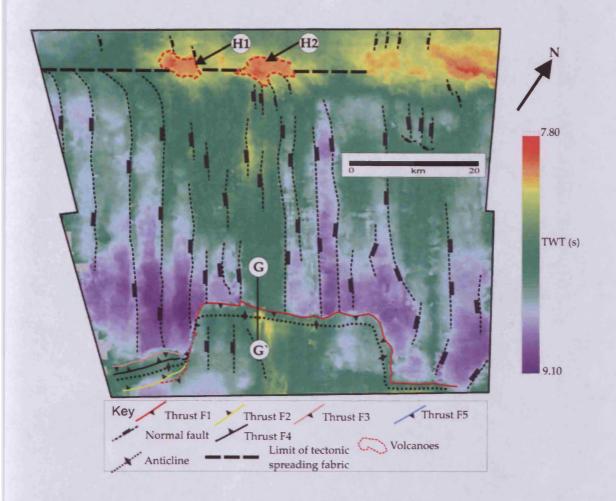
in the study area, and converted this to depth isopach using an average interval velocity of 6000 m/s. As noted above this interval velocity was based on stacking velocities. The large errors (15%) inferred in the stacking velocities due to the low frequency content in this deeper part of the seismic profile precluded any more detailed analysis of lateral velocity variation within Unit IV, but no systematic variation could be observed in the stacking velocities.

The computed crustal thickness map (Fig 3.9) shows that the crystalline crust in the deepwater west Niger Delta is extremely thin overall, ranging from just less 5 km in several regions to just less than 7 km in the more inboard regions and in the vicinity of major transform faults (Figs 3.7AB). Remarkably, the areas with the thinnest crust are located where regular patterns of faults are interpreted to offset Horizon B (see next section) i.e. mostly in the southern part of the study area (Fig 3.9). The lateral variation in thickness is generally quite gradual, suggesting no major structural control of gross crustal thickness that might be expected in a continental margin setting e.g. due to major faults. Areas with rapidly changing thickness are likely to be artefacts, since they are restricted to zones where Horizon M could not be interpreted due to complexities in the overburden geometry and the concomitant attenuation and distortion of the seismic wavefield.

3.5.1.2 Structural elements

3.5.1.2.1 Normal faults

Regular step-like offsets are seen on Horizon B throughout the 2D seismic dataset and from the sense of dip of the discontinuities and the sense of offset are interpreted as normal faults (Figs 3.10 and 3.12). This interpretation is most robust in areas where the concordant package is recognisable beneath Horizon B, but is strongly supported form previous interpretation of similar structures in the
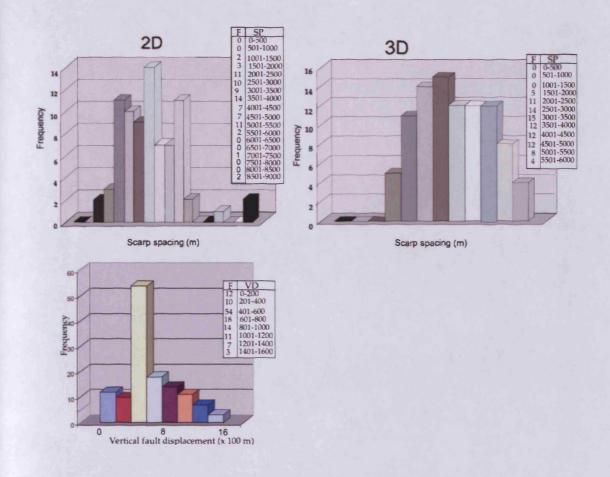
Figure 3.12. A 3D structural map of horizon B showing the termination of fault (dashed black lines) generally termed curved abyssal hill at the major transform structure (Chain fracture zone). The transect G-G` (Figure. 3.14) is a strike line across the uplifted area showing the topographic change across the area.

area of the 3D survey (Davies et al. 2005). The faults have a spacing of between 1-9 km based on the measurement of 172 (79 from 2D and 93 from 3D data set) faults (Figs 3.13AB). The throw values of 129 faults measured showed a range of between 180 and 1520 m but are dominated by faults with throw of between 400-600 m (Fig 3.13C). Where they can be interpreted over a significant depth range, the faults are essentially planar in geometry, dipping mainly southwest, with steep dips in the range 50-70°.

The planform geometry of the normal faults can only really be defined in the area of the 3D seismic survey, although occasionally they can be traced from dip to strike 2D lines, and from this an approximate strike direction can be estimated (Fig 3.3). On the 3D survey area, they are mapped at Horizon B in detail, and strike parallel to one another in a predominantly NW-SE direction (Fig 3.12). Some of these faults terminate abruptly at the Chain fracture zone (Fig 3.12). They curve in strike in a counter-clockwise direction towards the Chain Fracture Zone in a zone of about 2-5 km from this major structure (see Fig 3.12) and terminating at some point on the fracture zone, suggesting a close relationship between the evolution of the fracture zone and the normal faults. This relationship is strongly reminiscent of that seen between oceanic fracture zones and spreading-related faults and basement fabrics (Whitmarsh and Laughton, 1975; Gudmundsson, 1995; Sonder and Pockalny, 1999).

Importantly, the seismic expression and seismic-stratigraphic context of the normal faults identified within the 3D survey area is identical to that seen on the 2D profiles. The quality of the imaging is superior on the 3D seismic data because of the more precise seismic migration of this data. This similarity leads us to infer that the style and timing of the normal faulting is similar throughout the study area. The limited mapping of the faults on the 2D survey also indicates a general uniformity in the regional strike of the normal fault sets, excluding the local changes noted above adjacent to prominent fracture zones.

2D

F	SP
0	0-500
0	501-1000
2	1001-1500
3	1501-2000
11	2001-2500
10	2501-3000
9	3001-3500
14	3501-4000
7	4001-4500
7	4501-5000
11	5001-5500
2	5501-6000
0	6001-6500
0	6501-7000
1	7001-7500
0	7501-8000
0	8001-8500
2	8501-9000

3D

F	SP
0	0-500
0	501-1000
0	1001-1500
5	1501-2000
11	2001-2500
14	2501-3000
15	3001-3500
12	3501-4000
12	4001-4500
12	4501-5000
8	5001-5500
4	5501-6000

F	VD
12	0-200
10	201-400
54	401-600
18	601-800
14	801-1000
11	1001-1200
7	1201-1400
3	1401-1600

Figure 3.13. A graphical picture showing the spacing and vertical displacement of faults measured from 2D and 3D seismic data in the study. Note that F and SP signifies frequency and scarp spacing on the table.
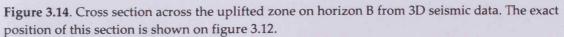
3.5.1.2.2 Transform faults

In the SE part of the area (Fig 3.3), a series of well defined normal faults are observed terminating at a major structure which is oriented orthogonally to the main fault trend (Fig 3.12). This major structure has previously been interpreted as a fracture zone of oceanic-continental transform type by Davies et al. (2005), with the region north of this structure being of highly stretched continental crustal affinity. This interpretation is difficult to reconcile with observations presented in previous sections (see section 3.6).

A series of parallel bathymetric highs are also prominent along the Chain Fracture Zone (Fig 3.12) at positions H1 and H2. These features are buried beneath sediment draped above Horizon B. The highs are between 2 and 5 km wide, 8-12 km long and a maximum elevation of 1400 m above the regional of Horizon B. They have flat tops with cuspate margins clearly mappable with the 3D seismic data. The cuspate features are between 0.5 and 3 km in width. Automatic picking of the high amplitudes within Horizon B presented by Davies et al. (2005) revealed complex ribbon-like patterns of high seismic amplitude that bifurcate and trifurcate downdip from the crests of the observed highs that were interpreted as lava flows. From this interpretation, and the overall geometry, these bathymetric features were interpreted by Davies et al. (2005) as submarine volcanoes developed along the trace of the fracture zone. The prolongation of the Chain Fracture Zone into the study area is highly likely from the position and strike of these bathymetric features. The position of the COB in the area has been interpreted by others to be significantly landward of where Davies et al. (2005) and Morgan (2003) placed it, notable amongst them are the works of Hospers (1965), (1971); Evamy et al. (1978); Whiteman (1982) and Damuth (1994).

3.5.1.2.3 Thrust faults

Figure 3.14. Cross section across the uplifted zone on horizon B from 3D seismic data. The exact position of this section is shown on figure 3.12.

A number of thrust faults have been interpreted from both the 3D and 2D seismic data in the southeastern part of the study area (see chapter four). This interpretation is based on reverse sense offsets of stratal reflections at Horizon B and immediately above and below this marker, linked to distinctive, generally planar fault plane reflections. These strike NE-SW and verging NW, and are characterised by reverse polarity and shallow dips (<40°). The magnitude of the thrust offset is of the order of a few hundred metres, but relief of the associated folds can be up to a kilometre. These inferred fault plane reflections transect the thin basement of Unit IV and appear to detach at the level of the reflection Moho (Horizon M) (Figs 3.11 and 3.14). These reflections are thought to represent a compressional reactivation episode linked to regional inversion in the Late Cretaceous (see Figs 3.11 and 3.14). The detachment level at Horizon M suggests that the base of the crust was mechanically weak.

3.6 Discussion

The nature of the crystalline crust beneath the mid-lower slope of the west Niger Delta has been open to considerable debate. Some workers consider that it is fully oceanic (Hospers, 1965; 1971; Evamy et al. 1978), and place the continent-ocean boundary inboard of the slope, or even as far inland as the Benue Trough (Whiteman, 1982; Damuth, 1994). Others consider that the crust is either extensionally thinned continental crust (Morgan, 2003) or transitional crust i.e. highly stretched continental crust (Davies et al. 2005). This discussion summarises the evidence presented in this paper that has a bearing on this question, and argues the case for fully oceanic crustal composition beneath the study area. This debate has fundamental implications for petroleum exploration and for regional tectonic analysis, and it is timely to assess the crustal structure given the activity in deepwater exploration in the area.

Velocity and Thickness of Unit IV

One of the most remarkable results of our mapping of the two regionally correlatable reflections (B and M), is the realisation that in an absolute sense the crust is very thin, and also very uniform in thickness (Fig 3.9). We have found no evidence for abrupt lateral thickness changes, for example, across any major faults. Even across the landward extension of the main fracture zones, the crustal thickness remains almost unchanged.

The range of thickness values between c. 5-7 km argues strongly for an oceanic crustal affinity for the whole of the study area. Using the uniform interval velocity model of 6000 m/s, these crustal thicknesses compare very well with a compilation of oceanic crustal thicknesses computed from wide angle seismic data in a diverse range of tectonic settings (Table 3.1). Included in this compilation are the interval velocities for the crystalline oceanic crust derived from modelling the wide angle arrivals in these studies, and these show a range of velocities that encompasses our estimated value and its error limit. In particular, our values compare well with other published thicknesses and velocities for oceanic crust outboard of the Atlantic margins such as in nearby Equatorial Guinea or in deepwater Angola (Sage et al. 2000; Wilson et al. 2003)(Table 3.1).

Structure of Unit IV

The observations of the different types of internal reflection identified within Unit IV provide additional support for the interpretation of oceanic crustal type in the study area. The uppermost concordant reflective series within Unit IV ranges in thickness from 0.4 -2 km. This interval has been extensively mapped in the area of the 3D seismic survey, where from attribute analysis; Davies et al. (2005) argued that the seismic facies was characteristic of interbedded lavas and sedimentary

rocks. As such, this layer could certainly therefore be interpreted as oceanic Layer 1, as commonly defined (Raitt, 1963; Christensen and Salisbury, 1975). The common occurrence of normal faults within this layer, with the recognisable thickening of the reflective interval across the faults is also consistent with an oceanic Layer 1 interpretation. This seismic facies is identical to Layer 1 series identified on reflection seismic data from the nearby margin of the Rio Muni (Wilson et al. 2003). This study therefore favour an interpretation of the uppermost part of Unit IV as a complex inter- layering of volcanoclastic rocks, extrusive basaltic lava flows and sediments.

In marked contrast, the lower part of the crust is more homogenous and this is consistent with seismic character observed for Layers 2 and 3 of the oceanic crust elsewhere. The thickness of lower part of Unit IV is within the range for a normal oceanic crust (Table 3.1). The high amplitude, subhorizontal, intracrustal reflections (e.g. H on Fig 3.11) may be related to acoustic impedance contrasts within the oceanic Layer 2 or 3 or may conceivably be picking out the Layer 2/3 boundary (McCarthy et al. 1988). Alternative explanations could include major sheet intrusions, low angle detachments (c.f. Macleod et al. 2002), or hydrothermal alteration fronts (White et al. 1990). Reflective mafic sills can be identified, for example, as acoustically bright discordant sheets within the likely sheeted dyke complex of Layer 2 along the Namibian margin (Clemson, 1997).

The other major group of intra-Unit IV reflections are unlikely to be discordant intrusions because of their large lateral extent and planar geometry. It seems inherently unlikely that they represent hydrothermal alteration fronts, because their strike is parallel to the dominant structural grain as mapped at Horizon B. This latter observation instead points to a more likely interpretation of intra-crustal shear zones, similar to those described by Mutter et al. 1985; McCarthy et al. 1988; Morris et al. 1993; White et al. 1994; Collier et al. 1997. These shear zones cut through the entire crust (Figs 3.11 and 3.14) with average dip of

References	Mean thickness (km)	Comments
Hills, 1957	6.45 +/- 1.92	Atlantic and Pacific, water >4000 m, excluding oceanic trenches.
Raitt, 1963	6.57 +/- 1.61	Atlantic, Indian and Pacific, water >3000, excluding deep trenches, continental slope, flanks of islands, oceanic rises
Shor et al. 1970	6.11 +/- 1.63	Pacific only, water >2500 m, excluding trenches and outer ridge of trenches.
Christensen and Salisbury, 1975	6.36 +/- 1.35	Main basin excluding fracture zones, off ridge rises, plateaus and linear island chains.
Wollard, 1975	6.48	Pacific only, water >3000 m
Houtz, 1980	5.59 +/- 1.30	Atlantic only.
McClain, 1981	5.83 +/- 0.93	Pacific only excluding fracture zones, seamounts, Hawaiian chain volcanics, grossly variable profiles.
McClain and Atallah, 1986	5.86 +/- 0.91	Pacific only
Keen et al. 1990	5.84 +/- 1.12	Atlantic and Pacific, depth anomaly <0.5 km, excluding ocean islands, fracture zone traces, trenches, seamounts, marginal basins.

Table 3.1: Mean crustal thickness for normal oceanic crust from the compilation of slope intercept solutions as modified from White et al. (1992).

35°, detaching close to Horizon M . The Moho is an obvious major mechanical detachment level, and this observation thus strengthens the case that the reflection Moho is a significant lithological boundary.

The most common structure observed throughout the study area are the small to moderate sized normal faults (e.g. Figs 3.4 and 3.10). The study did not observed any large extensional faults detaching within the crust and with major offset of the top of the crystalline crust as would be expected as evidence for major continental crustal extension and as is well seen, for example along the Iberian margin (Whitmarsh et al. 2001). In contrast, the style of block faulting observed in the area is typical of oceanic normal faults at the mid oceanic ridge of newly forming oceanic crust in slow-moderate spreading domains (Searle, 1979, 1983; Laughton and Searle, 1979; Searle et al. 1981) both in the range of displacement values observed at Horizon B, and in the typical spacing. This is particularly clearly seen in the 3D seismic survey area, where the fault system mirrors classical oceanic crustal fault systems at the present day mid-Atlantic ridge (e.g. Minshull and Hall, 1997; Collier et al. 1997; Reston et al. 1996).

The regularly spaced normal faults to the south of the Chain Fracture Zone (see Fig 3.12) are also comparable in planform to well documented examples on either side of oceanic fracture zones (Searle and Laughton, 1977; White et al. 1990). Studies from well mapped ridge parallel transform junctions such as the Vema transform (Macdonald et al. 1996), Clipperton transform faults (Barth et al. 1994), the Siqueiros transform faults (Fornari et al. 1989), Kane transform fault (Auzende et al. 1994) and the Hezeen transform fault (Lonsdale, 1994) indicate that the ridge transform junctions are normally characterised by curved fabrics, as clearly seen for the Chain Fracture Zone (Fig 3.12). Across the Chain Fracture Zone, therefore, the repetition of the same pervasive spreading fabric is critical supporting evidence to suggest that the nature of the crust is also oceanic on the northwestern side of the fracture zone (Fig 3.3). Thus, it is argued here that this is an ocean-ocean fracture zone, with the modification of the tectonic spreading fabric near the

fracture zone, the faults curve in the direction of the ocean-ocean fracture zone offset.

In conclusion, the evidence summarised above makes a powerful case for the interpretation of the crust throughout the study area as being oceanic in origin, rather than transitional or continental. This interpretation explains the abnormally thin and uniform crust, and provides a satisfactory lithological context for the internal reflection character. Most persuasively, it accounts for the regular pattern of the modest normal faults as a tectonic spreading fabric which occurs on either side of the Chain Fracture Zone.

3.7 Conclusions

The interpretation of the seismic reflection dataset complimented with gravity data has allowed the identification and description of some of the most important structural features present in the oceanic crust of the deepwater west Niger delta continental margin. Thus the following conclusions were drawn from this study:

- The abnormally thin igneous crust within the study area is one of the most striking results of this study. More than 90% of the study area is below the global thickness of 7.08 km for a normal oceanic crust (White et al. 1992) but within published values for the Atlantic Ocean normal oceanic crust (Rosendahl and Groschel-Becker, 1999). The anomalously thin oceanic crusts away from the major fracture zone (Chain FZ) can be attributed to three main settings; at very slow spreading ridges (White et al. 1984; Minshull et al. 1991), adjacent to non-volcanic continental rifted margins and at fracture zones (White et al. 1992).

- 2D and 3D seismic reflection data interpretation of the deepwater west Niger Delta has demonstrated the existence of normal oceanic crust in the

area. This is revealed from the thickness map of the crust (Fig 3.9) which shows that the crust here is between 5.0 and 8.3 km.

- The Chain Fracture zone earlier interpreted as Continent-Ocean Fracture zone by Davies et al. (2005) is in fact an Ocean-Ocean fracture zone similar to those observed in the North Atlantic (Rabinowitz and LaBrecque, 1979; Muller and Roest, 1992). This study has also shown that there is no significant difference in the crustal thickness across the fracture zone as the crust on opposite side of the transform is made up of about 5-7 km thick oceanic crust and this is supported by the pervasive tectonic spreading fabric observed on the north across the Chain fracture zone.

- Tectonic spreading fabric terminating at the Chain Fracture zone is clearly diagnostic of a normal oceanic crust. Subsurface scoop-like forms of faults terminating at the Chain fracture zone are generally observable at ocean-ocean fracture zones (Searle and Laughton, 1977)

- The Moho (horizon M) here acts as a detachment surface for some of the listric intracrustal faults in the study area.

- Volcanoes are erupted at the ancient seafloor during the accretion of the crust and the subsequent development of tectonic spreading fabrics.

- The development of the anomalous thrust structure here may be related to the change in the pole of rotation during the Santonian.

- The crust in the study could be divided into 2 layers based on seismic characteristic of the packages within major regional reflectors.

● The Moho reflection in the study area shows a variable reflection pattern, as they are present in some areas and being absent in others. This may be attributable to variation in lateral composition.

Chapter Four: Thrusting in Oceanic crust deepwater west Niger Delta.

4.1 Abstract

2D and 3D seismic reflection data acquired over oceanic crust in the deepwater west Niger Delta reveal convincing evidence for compressional tectonics during oceanic crustal spreading. Using the 3D seismic dataset, numerous inclined seismic reflections that dissect the entire oceanic crust from the top of the crust to the level of the Moho that are interpreted as thrusts are described. Thrust propagation results in the development of associated hanging wall anticlines and footwall synclines. These structures are orthogonal to and clearly post-date normal faults that formed during the accretion of oceanic crust during continental drift and strike at right angles to them.

The Charcot Ridge is located 140 km south of these thrusts and is a significantly larger structure. It is a triangular-shaped uplifted region of oceanic crust measuring 80 by 150 km and is located along trend of the NE-SW oriented Charcot Fracture zone. Two interpretations are possible for the role of the fracture zone in the development of the Charcot Ridge: (1) A thin skinned model whereby the oceanic crust west of the fracture zone has been thrust south-eastwards, with detachment occurring close to the level of the Moho. The ridge forms as a result of translation and folding above a crustal-scale ramp-flat thrust geometry; or (2) A thick skinned model where there is no detachment close to the Moho with the thrust fault being much steeper, penetrating the crust and probably the mantle lithosphere. In this interpretation the structure formed due to the compressional reactivation of the fracture zone. Approximate dating of onlapping reflections on either side

of the ridge constrains the timing of its formation as between 25-120 million years ago. The Charcot Ridge represents one of the largest thrust structures to be identified in a passive margin setting. Many other compressional folds with the same orientation formed to the northeast in the Benue Trough, probably during the Santonian, as a result of a change in the spreading direction during South Atlantic rifting. It is speculated that the same causal mechanism applies for the formation of the Charcot Ridge.

4.2 Introduction

Oceanic crust in passive margins settings is increasingly being imaged by commercial 2D and 3D seismic reflection datasets. In these distal settings, the sedimentary cover sequence is relatively thin and therefore relatively high quality imaging of the extensional and transform faults has been possible (e.g. Davies et al. 2005). These data are revealing structures that are not consistent with passive margin tectonics but instead are indicative of compression. The identification of such structures in a passive margin setting is not new - there is an increasing catalogue of examples of passive margins that show evidence for compressional tectonic activity (e.g. Bull, 1990; Bull and Scrutton, 1992; Masson et al. 1994; Pilipenko, 1994; Dore and Lundin, 1996; Cobbold et al. 2001; Hudec and Jackson, 2002). However high quality imaging of the compressional structures within the crust that overlies these basin is uncommon and clear evidence for the relationships between the

compressional structures and the transform and extensional faults, that are more typical of passive margins, has not been described before.

Relatively well imaged deformational features that cross-cut the oceanic crusts from its surface to the depth of the Moho and potentially deeper were described. These structures are all associated with folding of the crust and the wavelength of the folds can be anything from 1 to 80 km wide. They are imaged on both 2D and 3D seismic data, with the 3D seismic data providing very good evidence for their origin. One of the structures described represents a major compressional structure in the basement, probably the largest of its kind yet to be described in a passive margin setting. The aim of this paper is thus to describe these structures, account for their origin and propose a most likely timing for their formation.

4.3 Compression in Passive Margins

It is well established that the passive continental margins are commonly not tectonically passive (Dore et al. 1997) and have in many cases undergone shortening, sometimes by reactivation of pre-existing faults (e.g. Masson et al., 1994; Bull and Scrutton, 1990; Hudec and Jackson, 2002). Several mechanisms have been invoked to explain the causes of this intraplate deformation at passive margins. For example it has been proposed that there is an alternation of compression and extension that arises because of the non-parallel boundaries (Menard and Atwater, 1968, 1969; Bonatti, 1978; Sykes, 1978; Bonatti and Chermak, 1981; Bonatti and Crane, 1982; Bonatti et al. 1994; Pockalny, 1997; Hudec and Jackson, 2002; Peive, 2006) and (b) ridge push; which is as a result of the topographic effect of cooling and contraction of oceanic lithosphere away from spreading ridges (Wilson, 1993) has also been suggested. Even variations in the activity of plumes have been proposed as a

driving mechanism (Dore and Lundin, 1996). Some of the descriptions of this

phenomenon describe deformation of the sedimentary cover (Dore and

Lundin, 1996) and domal folds. Others (e.g. Cobbold et al. 2001; Hudec and

Jackson, 2002) focus on compression that occurred before the Tertiary age

sedimentary cover was deposited and analyze evidence for deformation in

the underlying oceanic basement rocks.

4.4 Geodynamic Setting

The study area is located in the Equatorial region of the South Atlantic margin

where continental extension started during the Early Cretaceous (Nürnberg

and Müller, 1991; Maluski et al. 1995). Rifting propagated northwards from

the Falkland-Agulhas fracture zone (Fig. 4.1A) so that the ocean opened in a

zipper-like manner from south to north (Le Pichon and Hayes, 1971;

Rabinowitz and LaBreque, 1979; Uchupi, 1989; Nünberg and Müller, 1991).

The emergence of the independent spreading centres in the early to middle

Cretaceous resulted in the development of major shear zones developing

between West Africa and the margins of Brazil that subsequently opened

obliquely forming the Equatorial Atlantic (Fig. 1a). Specifically, Nürnberg and

Müller, (1991) suggested that the first phase of rifting started in the Tithonian

(150 Ma) and by the Aptian (118 Ma) seafloor spreading had extended into the

Equatorial Atlantic and the Benue Trough. At this stage the simple model of

two plates diverging became more complicated with shearing motion along

the Equatorial fracture zones, and continued opening along the South Atlantic

and Benue Trough arm of the essentially Ridge-Ridge-Transform fault (RRF)

triple junction which is situated beneath the present day Niger Delta (Fig.

4.1b) (Burke et al. 1971; Grant, 1971; Whiteman, 1982; Ofoegbu, 1984;

Fairhead, 1988).
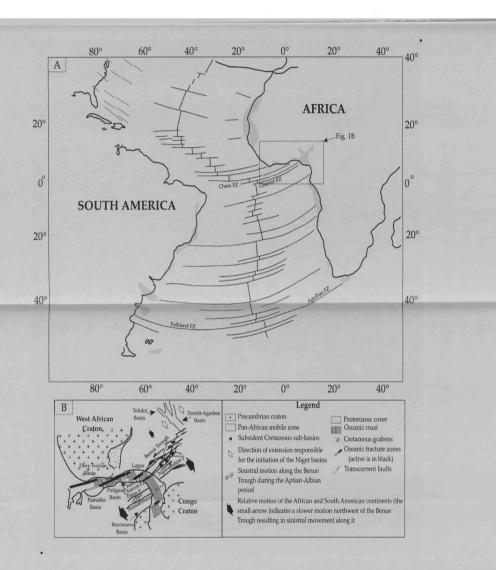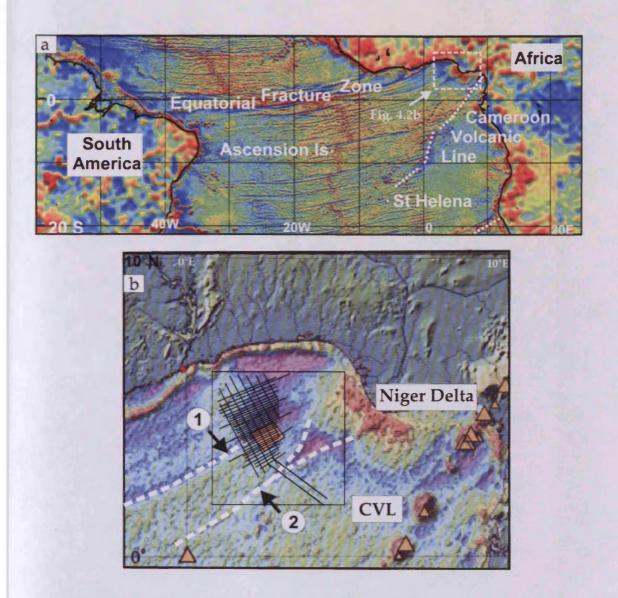
Figure 4.1. (a) Map of the Atlantic showing the location of oceanic fracture zones (modified after Le Pichon & Fox, 1971; Wilson, 1975; Wilson & Williams, 1979). Note the location of the Falkland and Agulhas Fracture Zones. (b) Reconstruction of the Gulf of Guinea during the Albian time showing the Benue trough (modified after Benkhelil et al. 1998).

The Equatorial Atlantic was the location of the intersection of the Central and South Atlantic rifts, and therefore had to accommodate the stresses arising from the differential opening of these two ocean basins. These stresses were dissipated into intra-continental rifts in West Africa and northeast Brazil (Fairhead and Binks, 1991). Once the central and South Atlantic mid-oceanic ridges were linked through the Equatorial Atlantic, the ocean basin began to open as one system. The onset of seafloor spreading in the Gulf of Guinea coincided with the Cretaceous magnetic quiet zone (anomaly M0 to anomaly 34, 118-83 Ma), so the spreading rate in the Gulf of Guinea during the Cretaceous is not precisely known. The absence of magnetic stripes means that fracture zone traces are the main aid to plate tectonic reconstruction in this region.

A gravity map of the South Atlantic (Sandwell and Smith, 1997) shows that it is cross-cut by a large number of subparallel crustal discontinuities identified as oceanic fracture zones occurring on both sides of the mid-Atlantic ridge (Bassetto et al. 2000; Mohriak and Rosendahl, 2003). These discontinuities represent inactive segments of transform faults associated with seafloor spreading axes which can generally be detected by steps in the bathymetry, by displacement of the magnetic anomalies in the oceanic basement and by alignment of gravity anomalies. The area of study covers the eastern terminations of the Chain and Charcot Fracture zones (Figs. 4.1a,b and 4.2a,b). Several other smaller fracture zones are also thought to be present (Babalola, 1985) but are not dealt with here.
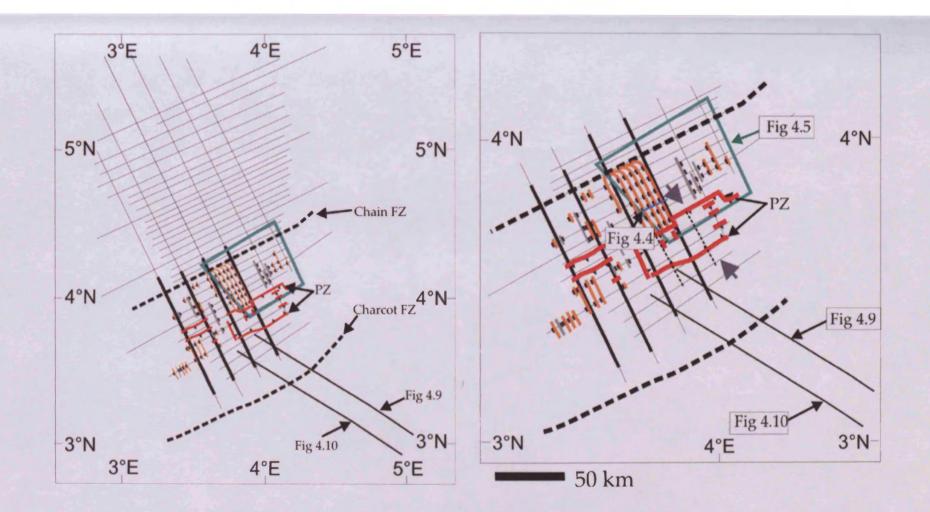
4.5 Data and Methodology

2D and 3D seismic reflection data acquired by CGGVeritas represent the main source of information used in this study. The deep seismic reflection coverage

Figure 4.2. (a) Gravimetric Satellite imagery map of the Central, Equatorial and South Atlantic showing the study area and the position of the major fracture zones in the area (Sandwell and Smith, 1997) but modified after Fairhead and Wilson, 2005. (b) Satellite Gravity map of the study showing the (1) Chain and (2) Charcot Fracture Zones (Sandwell and Smith, 1997) and the approximate position of the 2D and 3D seismic data utilized superimposed on it.

consists of high resolution 120 fold 2D seismic reflection data acquired in 1998, with a 6 km cable length and 12 seconds recording interval, processed using the Kirchhoff bent ray pre-stack time migration. The 3D seismic reflection data were acquired in 1999 and imaged deep levels to approximately 12 s two-way travel time (TWT). The 2D seismic reflection data consist of 2 strike lines of about 320 km combined length which are oriented in a WNW-ESE direction with spacing of 20 km. The rest of the 2D seismic reflection data is made up of 8 strike lines, totalling 1648 km in length, oriented in a NW-SE direction and 33 dip lines of 4089 km length with a SW-NE orientation (see Figs. 4.3 a and b). The 3D seismic data covers an area of 3057 km^2 and were acquired using a 6 km offset length and 12 s record interval, with line spacing of 25 m and has a similar processing sequence to that of the 2D seismic reflection data. These datasets were acquired where the water depth is between 1500-4000 m. The quality of the data is very good due to the application of pre-stack time migration (PSTM) (see Yilmaz, 2001). The data are displayed with a reverse polarity (European convention) so that an increase in acoustic impedance is represented by a trough and is black on the seismic data in all figures presented here. The dominant frequency of the seismic data varies with depth, but it is approximately 10 Hz at the level of interest. A seismic velocity of 6000 m/s for the oceanic crust (based on other areas in the South Atlantic (Sage et al. 2000; Wilson et al. 2003) means that the vertical resolution is estimated to be about 150 m. Satellite derived gravity data from the world database compiled by Sandwell and Smith (1997) which images the Chain and Charcot fracture zones (Figs. 4.2a, b) were also used. The crust in the West Niger delta has never been penetrated by scientific or commercial drilling.

Figure 4.3. Simplified 2D and 3D seismic reflection database overlain by a 2D structural interpretation map of the study area. PZ on the map signifies uplifted (pop-up) compressional fault zone. The red colour features are compressional faults while the orange and grey signifies the position of normal faults but with different dipping direction

4. 5.1 3D Seismic Data

This section starts with a description of a representative seismic line from the

3D seismic survey in order to establish what the key seismic reflections are

within the crust and the general character of the structures that we are

focusing on.

It is followed by a detail description of the deformational structures,

categorizing them as structures that have NW-SE and WSW-ENE strike using

the 3D seismic data as these data provide the highest resolution and interpret

their 3D geometry in the seismic time domain. Once the characteristics of

these structures are established, a description and interpretation of the

related, more equivocal and larger-scale structures on 2D seismic data will

follow.

4.5.1.1 Key reflections

In a representative NE-SW orientated seismic line from the 3D seismic dataset

the Tertiary-age sediments of the Niger Delta form the upper 8500

milliseconds (ms) of the seismic record. At the base of this sedimentary pile,

there is a very high amplitude reflection that forms continuous segments

separated by clear breaks in the reflection event. This reflection is termed

reflection 2 (Fig. 4.4). Approximately 1.5 s below this is a much lower

amplitude, less continuous reflection (termed reflection 1) that can be traced

across most of the 3D seismic dataset. Reflections 1 and 2 are approximately

parallel to each other. Mapping of reflections 1 and 2 as well as line by line

inspection of the 3D seismic dataset reveals two sets of tectonic structures,

one striking NW-SE and the other striking ENE-WSW that are described

below.
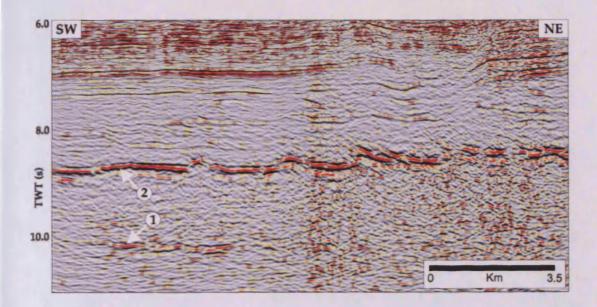
Figure 4.4. A 3D seismic line showing the defined major horizons used in the study.
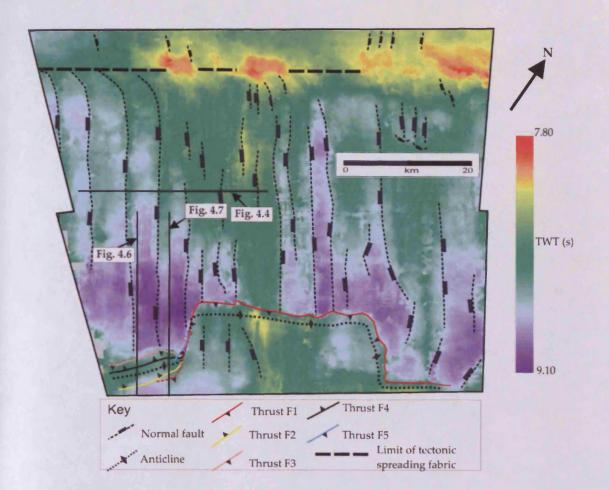
4.5.1.2 Structures that strike NW-SE

Mapping of reflection 2 across the 3D survey shows that the discontinuous character of this reflection is the result of faulting. Faults have a regular spacing of between 1 and 9 km and the lateral tips of these faults curve towards the position of what has been interpreted to be a NE-SW orientated fracture zone (Fig. 4.5) described by Davies et al. (2005). By mapping out the stratal cut-offs of reflection 2 at fault plane intersections, it is clear that the vast majority of the faults with this strike have a normal offset, and their maximum throws range from c. 50-400m. The pattern of faulting is highly consistent over an area of 2400 km^2. Mapping of reflection 1 is more difficult as it is not as continuous as reflection 2. In some cases there is evidence that the normal faults also cut reflection 1, but in most examples no offset is identified.
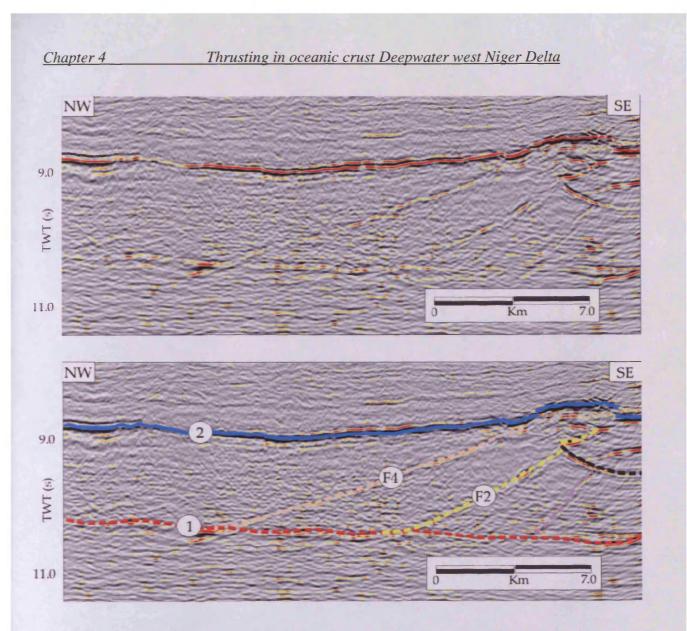
4.5.1.3 Structures that strike ENE-WSW

Representative seismic lines (Figs. 4.6 and 4.7) taken in an NW-SE orientation (Fig. 4.5) again shows reflection 1 and reflection 2, but also reveals dipping reflections that cut the interval between reflection 1 to reflection 2. These reflections are low amplitude but continuous and dip at angles of between 22° and 32° towards the SSE and the NNW. Their strike is at right angle to the normal faults. Some of the dipping reflections form in the same area, one above another, with the terminations of some abutting others that dip in the opposite direction. Above the uppermost dipping reflection is an anticline which is most clearly identified at the level of reflection 2 (Figs. 4.6 and 4.7). In some locations the dipping reflections coincide with reverse offset of reflection 2 (Figs. 4.6 and 4.7). Close examination of the map of reflection 2
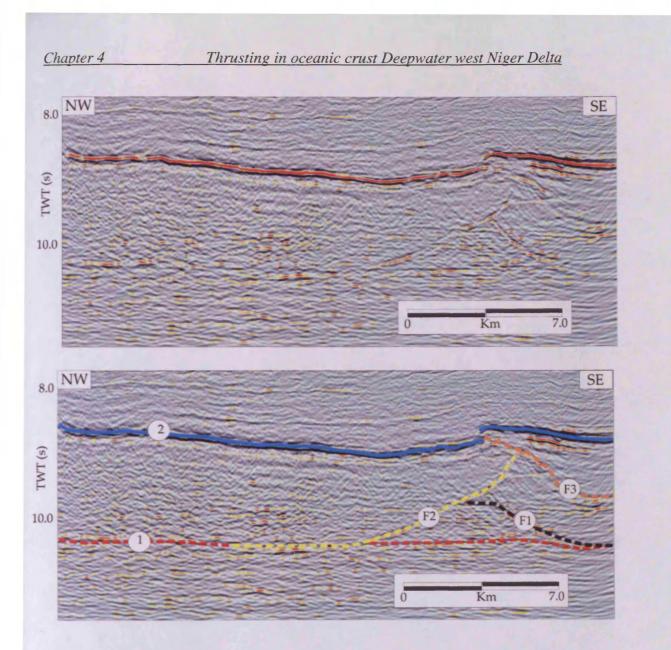
Figure 4.5. Time-Structural map of horizon 2 based on 3D seismic data. Note the curvature of the tectonic spreading fabric towards the trace of the Chain Fracture zone.

Figure 4.6. Interpreted 3D seismic data example of the basement thrust faults F2 and F4 verging in the south.

Figure 4.7. Interpreted 3D seismic data example of the basement thrust faults F1, F3 and F2 verging in the north.
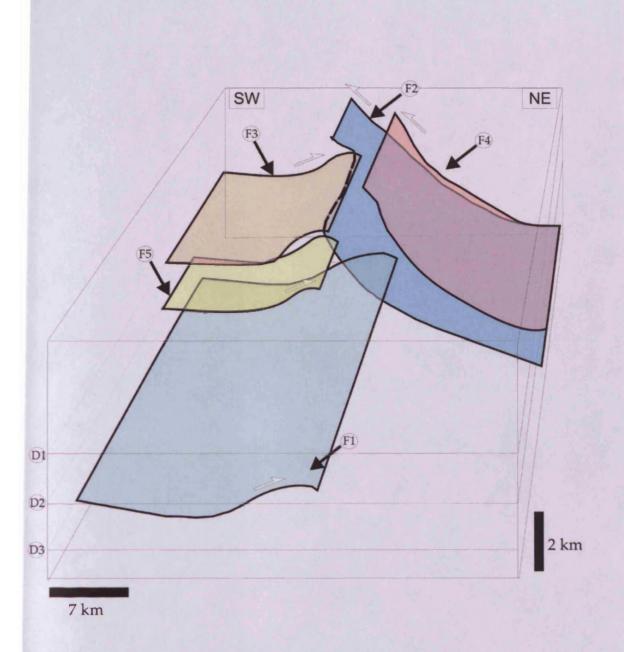
shows that the NW-SE structures that have normal offset are cross-cut by the ENE-WSW orientated dipping reflections.

4.5.1.4 Interpretation

The regularly-spaced normal faults that have a NW-SE orientation and cut through the section have distinctive curved tips as they get close to the Chain fracture zone, which is a typical feature of oceanic crust (Searle and Laughton, 1977) and form during its accretion (Malinverno and Pockalny, 1990). The position of reflection 2 beneath the delta and its high seismic amplitude is consistent with this being the top of the oceanic crust (Davies et al. 2005). We interpret the less continuous reflection located 1.5 s below reflection 2 to be the Moho (Davies et al. 2005; see also section 3.5.1.1.2).

The dipping reflections commonly abut other dipping reflections forming distinctive cross-sectional geometries. The close association that the WSW-ENE dipping reflections have with folds identified at the level of reflection 2 and the reverse offsets identified on reflection 2 are both consistent with the these structures being thrust faults. The folds recognized at the upper tips of these faults at reflection 2 are interpreted as having formed by thrust propagation (c.f. McClay, 1992). We interpret the tendency for the thrusts to abut one another to indicate that the thrusts have been active sequentially and that earlier thrust planes have been cut by later ones. The 3D seismic grid allows for a detailed 3D mapping of the thrusts and their visualization (Fig. 4.8). The thrusts offset the NW-SE striking normal faults and therefore post-date them. Another important observation is that the thrusts strike orthogonally to the normal faults, rather than being sub-parallel or even oblique to them.

The topographic highs on reflection 2 (Figs. 4.5, 4.6, and 4.7) are associated with a broad zone of accommodation faults that are due to the

Figure 4.8. 3D fault surface model of all the five (F1-F5) crustal interpreted faults. This view does not cover the extreme southeast and west of the study area due to the unavailability of dense 3D seismic reflection data here. This view covers all the major thrust faults in the basement that contributes to the formation of the triangle zone. The thrust faults F1, F3 and F5 are verging towards the north while F2 and F4 are south verging. Note the area of basement fault ramp and linkage.

interaction and cross-cutting of the major thrust faults marked F1, F2, F3, F4 and F5 (Figs. 4.5, 4.6, 4.7 and 4.8). The dips of these thrust faults range between 25-32° (Figs. 4.6 and 4.7). Their regular spacing results in local development of complex structures that are similar to those observed in triangle zones (McClay, 1992).

The 3D seismic data suggest that these low angle thrust faults are listric and cut through the entire 5 - 7 km crust to the depth of reflection 1. The general listric geometry and flattening of the thrust faults with depth suggests that reflection 1 acts as a likely rheological boundary where there is most likely a major detachment.

Vergence of these thrusts alternates from SE to NW. The major thrust fault F1, for example, dips to the SE and is associated with NW dipping conjugate backthrusts (F2 and F4), which have resulted in the formation of the pop-up structure (see Figs. 4.5, 4.6, 4.7 and 4.8). These main faults F1, F2 and F4 detach on the regional plane of detachment (see Figs. 4.6, 4.7 and 4.8) which is an acoustic boundary in the case of reflection 1.

Perhaps the most significant observation, however, is the orthogonal orientation of the thrusts with respect to normal fault set. These normal faults are interpreted as being parallel to the sea floor spreading fabric and therefore orthogonal to the spreading direction (c.f. Malinverno and Pockalny, 1990). The orthogonal relationship of the thrusts therefore indicates that they did not form during the initial stages of oceanic crustal accretion but occurred during a later, distinct phase of compression.

4.5.2 2D Seismic data

4.5.2.1 General description

The 2D seismic data reveal similar correlatable seismic reflections within the crust, an upper high amplitude and continuous reflection (again labelled reflection 2) and a lower, less continuous reflection located approximately 1.5 s TWT below reflection 2, which we again term reflection 1. Both reflections can be correlated into the region of the 3D seismic survey using the regional 2D seismic grid, where they are found to match their equivalent reflections 1 and 2 described previously. The two 2D seismic lines are between 195 and 215 km long and at the level of reflection 2 cross a ridge-like structure with a triangle planform. The gravity map of the region (Figs. 4.2 a and b), shows that the ridge-like structure is landwards and along trend of the NE-SW trending Charcot Fracture zone, hence we informally term this feature the Charcot Ridge. At the level of reflection 2, it has a maximum width of 80 km and is 150 km long and has a NE-SW orientation. The seismic data show that it has an elevation of nearly 6–8 km above the regional level of the reflection (Figs. 4.9 and 4.10). We have mapped several other key reflections in the sedimentary succession above and to the north and south of the ridge, termed 3, 4 and 5.

4.5.2.2 Description of the Charcot ridge

The 2D seismic lines (Figs. 4.9 and 4.10) clearly show that reflections 1 and 2 are deformed on the flanks of the Charcot ridge. Reflection 1 has two sub-horizontal segments (marked F on Fig. 4.9), that are connected by low angle dipping segment (marked R on Fig. 4.9). Reflection 2 is probably offset by faults which are located at the crest of the ridge. Although not imaged sharply, at least in this transect, they have strongly listric geometries that would not be transformed into planar structures by depth conversion. The south facing side of the ridge has a scalloped face marked Lf1. Other listric
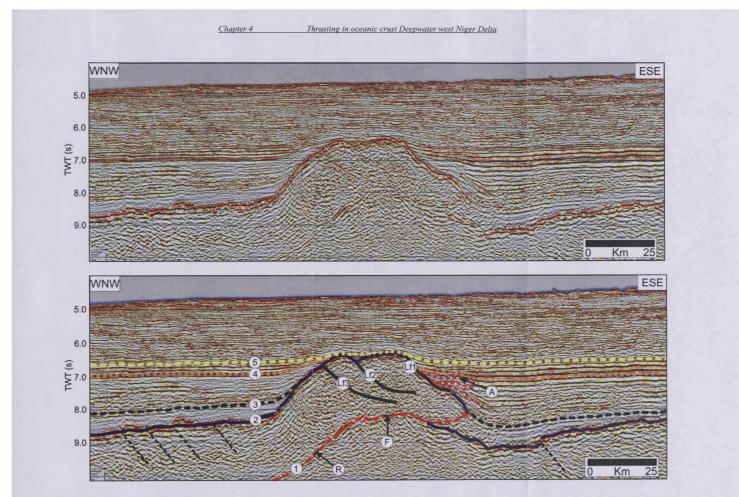
Figure 4.9. (a) Uninterpreted and (b) interpreted WNW-ESE oriented 2D seismic line across the Charcot fracture zone (see Figure 4.2 for the exact position of the line) showing anomalous crustal features. Note that Lf1, Lf2 and Lf3 are due to the lack of lateral support on the fold leading to the development of listric faults surfaces. R and F on reflection 1 correspond to ramp and flat as observed on fault-bend fold models. Also note that the group of reflections marked **A** on this figure are onlap features typical of fold growth.
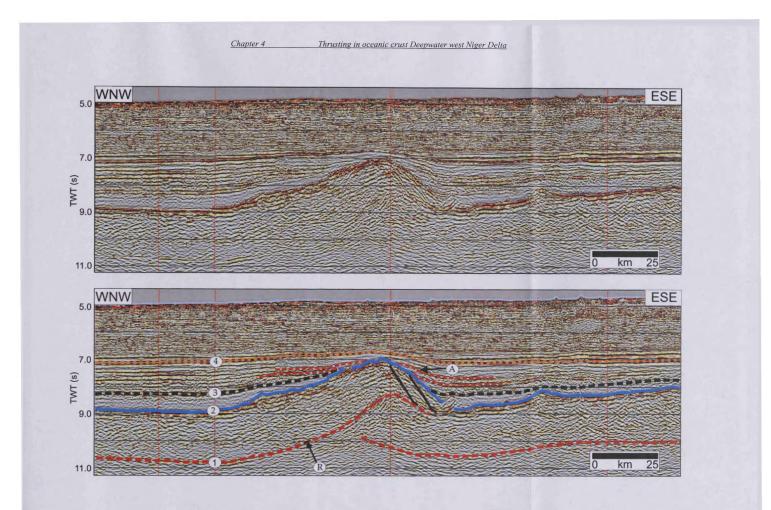
Figure 4.10. (a) Uninterpreted and (b) interpreted WNW-ESE oriented 2D seismic reflection line labelled **B** across the Charcot fracture zone (see Figure 3 for the exact position of the line). This line is about 20 km to the south of the previous figure (4.4) showing yet another perspective of the anomalous basement features.

faults dipping towards the south are also observed and marked Lf2 and Lf3 (Fig. 4.9). One of these faults has a throw of about 300 m.

In contrast, the succession bounded by reflections 2-5 (Fig. 4.9) of 2-4 (Fig. 4.10) defines a sedimentary package that thins almost to pinch-out onto the ridge, with reflection configurations that vary from parallel onlap fill to convergent onlap fill. These onlapping units have had their original geometries distorted by continued deformation or by differential compaction against the dipping flanks of incompactable basement rocks. The gross thickness of this package thins across the ridge from west to east. The onlap patterns are also asymmetric, with the steeper facing, eastern limb of the ridge (labelled **A** on Figs. 4.9 and 4.10) being characterized by highly convergent onlap.

The seismic facies of the units abutting the ridge allows them to be separated into several distinctive units and correlated with units of the same post-rift megasequence elsewhere along the margin. The interval between reflections 2 and 3 is generally low amplitude and lacks any significant internal reflectivity. This interval correlated regionally corresponds to the Late Cretaceous–Palaeocene age Pre-Akata sediment wedge succession described in Morgan, (2003; 2004), Corredor et al. (2005) and Briggs et al. (2006). Between reflections 3 and 4 is an acoustically chaotic, hummocky or transparent seismic reflection package that is occasionally separated by high-continuity reflections typical of hemipelagic drapes. The package between reflections 3 and 5 is most likely equivalent to the Agbada Formation and by regional correlation would most likely consist of intercalations of sandstones and shales (Short and Stauble, 1967; Avbovbo, 1978). The age of this unit has been interpreted by some as pre-Miocene (Chapin et al. 2002) and has been defined elsewhere as Eocene-Pleistocene (Short and Stauble, 1967; Doust and Omatsola, 1990). The base of this unit is marked by a major regional sequence boundary (Morgan, 2003) that corresponds to reflection 3.

The satellite-derived free-air gravity data over the deepwater west Niger delta (Sandwell and Smith, 1997- Figs. 4.2a,b) shows a number of distinctive features. Along the margin is a striking gravity "high" and flanking gravity 'lows' which clearly defines the delta and its flexural depression. This distinct region on the gravity data (fig. 4.2b) that forms a triangular ridge that is 100 km at its widest end narrowing towards the southwest has been interpreted as a gravity high.

4.5.2.3 Interpretation of the Charcot Ridge

Reflection 2, which is high amplitude and continuous and is located below the delta is interpreted to be the top of the oceanic crust firstly because of its acoustic character, and secondly because of its continuity with reflection 2 identified in the area of the 3D seismic survey. Similar reasoning applies to reflection 1. Based on its context and continuity, and its consistent depth and similarity with reflection 1 as mapped on the 3D seismic data, it is interpreted to represent the Moho (Davies et al. 2005; see also section 3.5.1.1.2). Elsewhere in the Gulf of Guinea, Rosendahl et al. (1991; 1992), Meyers et al. (1996a; b) and Rosendahl and Groschel-Becker, (1999) have also interpreted a similar reflection as corresponding to the Moho.

The basement around the southern part of the 3D and also on the 2D seismic reflection data represents the most strongly deformed part of the oceanic crustal basement and has a vertical relief of between 2.0 s (6.67 km) and 2.25 s (7.50 km) (Figs. 4.9 and 4.10), with large low-angle detachment faults accommodating shortening than elsewhere in the study area. Classical pop-up structures and triangle zones are commonly developed in this area (see Fig. 4.8). The structure of the anomalous ridge was not supported, thus allowing it to undergo some gravitationally driven collapse (marked Lf1 and Lf2) and later Lf3 which has already been removed and deposited between

reflections 2 and 4. This feature is akin to positive relief structures that are subaerially exposed as thrust front ranges in many mountain belts.

Because only 2 seismic lines across the structure are available, two alternative structural interpretations that reflect the uncertainty due to this lack of seismic data coverage have been developed. Based on the very strong evidence from the 3D seismic data for NE-SW striking compressional structures (the thrusts and associated thrust propagation folds) and given the observations from the 2D seismic lines, both interpretations outlined here consider the Charcot Ridge to be a compressional structure, but vary on whether this compressional structure is thick- or thin-skinned. In the following sections we outline the key elements of both interpretations.

4.5.2.3.1 Thin-skinned

In this interpretation, reflection 1 is traced from the northwestern end of the seismic line. but in continuing to trace it towards the southeast we track it along a dipping reflection that either represents reflection 1 or an event that is very close to it (marked R on figs. 4.9 and 4.10). By simply continuing to track this reflection to the southeast, a ramp and flat geometry is defined (Fig. 4.9). The continuation of this reflection is termed reflection 1a. Between reflection 1 (and its continuation - reflection 1a) and the much shallower reflection 2, the thickness of the crust is seen to be relatively constant on both the horizontal and sub-horizontal segments of the ridge. In the thin-skinned interpretation (Fig. 4.11a) the ramp and flat section of reflection 1a are considered to be ramp-flat sections of a southeastward propagating thrust (see Rich, 1934; Davis and Reynold, 1996).

The evolution of the structure is divided into three stages. Stage 1 involves the accretion of the oceanic crust, which in this region of the South

Atlantic is late Aptian to late Albian in age (Gradstein et al. 1995; Wagner and Pletsch, 1999; Macgregor et al. 2003). Following this stage and prior to any significant sedimentation, was compression and shortening of the crust by the propagation of a thrust. The crust has been thrust horizontally for a distance of 8-10 km. There may have been a later compressional event, based upon the identification of differential growth packages (reflections onlapping the Charcot Ridge between reflections 3 and 4 (labelled A on Fig. 4.9). Lf1, Lf2 and Lf3 are interpreted to be listric faults. They probably formed because the structure had insufficient lateral support, thus developed into the collapse feature. The lower part of the scalloped face on fault Lf1 is the first to develop followed by Lf2 and later by Lf3 (Fig. 4.9) and that was prior to or during the deposition of reflection units S1 to S2. During Stage 3 the structure was buried, however, the reactivation of this structure is difficult to accomplish. Some of the relief identified on reflection 1 is likely to be due to the effect of velocity pull-up due to higher velocity basement rocks forming the core of the fold.

4.5.2.3.2 Thick-skinned

In the thick-skinned interpretation (Fig. 4.11a), reflection 1a would not be interpreted as merging with reflection 1 in the northwestern end of the seismic line (see Fig. 4.9). Instead, based to a large extent upon the knowledge that the Charcot Ridge is located along trend of the Charcot Fracture Zone, thus can be interpreted it to be a vertical fracture zone beneath the centre of the Charcot Ridge. The thrust seen at shallow structural levels would steepen and become sub-vertical at depth. This interpretation of the structure is in part driven by the occurrence of the Charcot Fracture zone and there is less direct evidence to support the interpretation of the thrust in this way. This possibility is included. However, it is recognized that the resolution of the
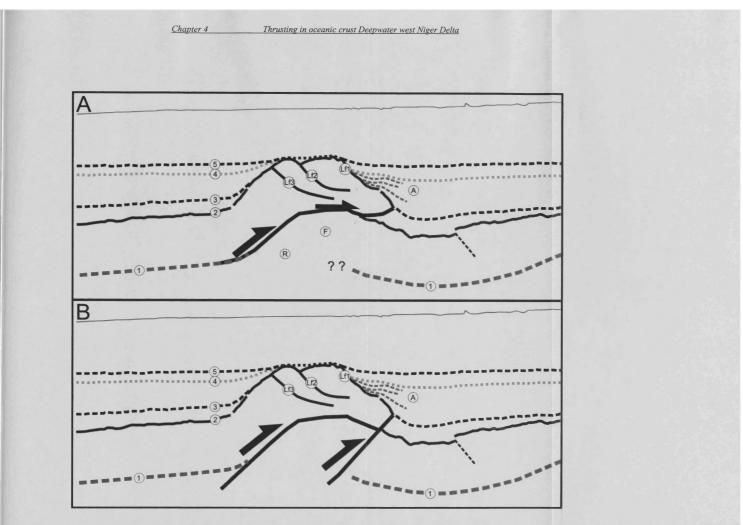
Figure 4.11. A line drawing of figure 4.9 illustrating the two possible interpretations of the same data over the Charcot ridge structure. (a) Shows thin-skinned model with the ramp-flat (marked as R and F) thrust fault detaching within or near the Moho marked as reflection 1. (b) Shows a thick-skinned model with the thrust actually continuing at depth after displacing the Moho.

data and the fact that only two lines were available mean that there are uncertainties in the interpretation. In this interpretation the thrust is also interpreted to have propagated southward.

4.6 Discussion

The previous sections have documented significant evidence for a phase of shortening in the region covered by the study area, both within the area of the 3D seismic survey and the regional grid over the Charcot Ridge. Irrespective of whether this phase of shortening was through a thin- or thick-skinned deformational regime, it is clearly important to place this shortening within a broader plate tectonic context, particularly in light of the rather few examples published previously that document such significant compressional deformation along a passive continental margin.

4.6.1 Timing and Context

Several lines of evidence can be used to date the compressional activity in the area. Firstly, there are long range seismic correlations of the stratigraphic units that onlap the Charcot Ridge to seismic-stratigraphic units that are dated biostratigraphically in an upslope position. Morgan (2003) proposed that these units are between Oligocene and Early Cretaceous in age and that they predate the development of the Niger Delta. Secondly, the geometry of the thickness change noted between reflections 2 and 4 between the northwest and southeast indicates that most of the growth in the structure occurred during the deposition of this unit implying that this interval defines the syn-kinematic period. The age of the compressional event could on this basis be constrained loosely to some time between the time of plate break-up to the

time equivalent of the Akata and Agbada Formation, i.e. approximately between 120Ma and 30Ma. Thirdly, the orthogonal relationship between the thrusts and the normal faults in the area of the 3D seismic survey demonstrates conclusively that the thrusts post-date oceanic crustal formation. By analogy, if the thrusting post-dates break-up and early crustal formation in the 3D area, then it is likely that the compressional development of the Charcot Ridge, only 150km to the southeast was also of the same general compressive phase.

Faced with such an uncertainty in the dating of the syn-kinematic package, further insight into the likely timing of this compressional event must therefore be sought from the regional tectonic history. In a regional context, compressional activity has been noted in the post-break up period by a number of authors. A compressional episode that is the first post-break-up event has been identified in the Benue Trough (Burke, 2001) and has been generally reported in the Equatorial Atlantic during changes in the pole of rotation (Anomaly 34, 84 Ma). This is a major folding event, caused by the India/Asia motion and in the South Atlantic (Dewey and Burke, 1974; Guiraud et al. 1992; Janssen et al. 1995; Guiraud and Bosworth, 1997; Hudec and Jackson, 2002; Fairhead and Wilson, 2005).

Elsewhere in the basins of Central West Africa the compressional events within this time frame have been observed and described as associated with the development of transpressional anticlines in the Benue trough and in the Central African rift (Fairhead and Binks, 1991; Genik, 1992; Guiraud and Maurin, 1992). In North of the Rio Muni basin, these same structures have been interpreted as resulting from transpressional inversion of the NE trending extensional faults, subparallel to those observed in Rio Muni (Dailly, 2000). Throughout the Equatorial African margin, this event generally occurs between late Turonian and early Campanian time. This event was described to be coincident with the change in spreading direction during opening of the

Atlantic Ocean at anomaly 34 (84 Ma) (Fairhead and Binks, 1991; Fairhead and
Wilson, 2005) as can be recognized from the change in flow line direction
reflected in fracture zone geometry (Haxby, 1985; Klitgord and Schouten,
1986; Fairhead, 1988; Binks and Fairhead, 1992).

These events are very well defined in the Central and South Atlantic
(Fairhead, 1988) as associated with the reactivation of the Equatorial Atlantic
fracture zones which can be recognized by their enhanced gravity signature
away from spreading ridges (Fairhead and Binks, 1991). This event may also
be the cause of the reactivation of transform zones and the development of
Aptian cored inversion anticlines in the Rio Muni Basin (Dailly, 2000). Given
the large number of studies that have reported compressional activity
associated with changes in plate vectors in the Late Cretaceous, it seems most
likely to us that the genesis of these compressional event observed within the
study area is contemporaneous with these events observed in other areas of
the eastern Atlantic borderlands.

4.6.2 Consideration of other interpretations

Other possibilities that are also envisaged to have led to the formation of
compressional structures in the crust include leaky transform and strike-slip
movements, but more data would be needed to investigate this further for the
study area. Specifically, the following possible mechanisms should not at this
stage be ruled out (1) compressional structures along bends of strike-slip
faults (restraining doubled bend or restraining stepovers (Schreurs, 1994;
Stone, 1995; Sylvester, 1988; McClay and Bonora, 2001), (2) volcanism related
to leaky transforms (Sykes, 1978; Meyers and Rosendahl, 1991; Bonneville and
McNutt, 1992), (3) compressional thrust faulting with the directional of
maximum compressional stress normal to the strike of the fracture zone

(Sykes and Sbar, 1974; Bonatti et al. 1994) and (4) volcanic complexes (Bull and Scrutton, 1992).

These possibilities are less appealing at present because they do not match the current limited observation set. It is noted for example, that a restraining double bend might be expected to lead to an uplift structure with compressional faults at the flanks and opposing reverse faults at the centre of the structure, while that of restraining stepover would result in a pop-up structure. In contrast, the Charcot Ridge is demonstrably asymmetric. Many large intraplate strike-slip systems do however produce anticlinal uplifts in the overlying sedimentary section with older strata or basement exposed in the core (McClay and Bonora, 2001). Strike-slip faults can have significant vertical components of motion for a relatively small transpressive component i.e. the slip vector is slightly oblique to the dominant trend.

Not everywhere in the ocean are plate motions exactly parallel to transform fault. In places where a component of opening motion occurs across the transform, volcanic activity may result and the fracture zone is termed a "leaky transform". Some studies attribute the formation of volcanoes to a leaky transform fault associated with the opening of the Atlantic Ocean. Meyers and Rosendahl (1991) pointed out that magmas and uplift that formed the main volcanic centres seem to occur preferentially where major fracture zones transect the proposed Cameroon volcanic line, suggesting that the South Atlantic plate had a major reorganization at the time of seamount formation, allowing magma to leak through the fracture zones and forming the volcanic chain. Sykes (1978) also arrived at the same conclusion and that the reactivation of the fracture zone is dated at the early opening of the South Atlantic. Plate reorganization is of great importance, since transform faults can be reactivated (made leaky) and create linear volcanic chains (Sykes, 1978; Bonneville and McNutt, 1992). Weak spots along fracture zones can be linked to regions of excessive volcanism and major plate reorganization with large

changes in direction are not necessary to trigger (or suppress) such volcanism. With such limited data, it is not right to infer whether or not the Charcot Ridge has an element of magmatic uplift. The case of volcanic complexes is not supported here because of the continuity of the moho reflection.

In summary, the evidence at present favours the origin of the Charcot Ridge as a thin-skinned structure and this is the preferred model. It is speculated that it is Santonian in age, because there are many other compressional features in the Benue Trough, about 600 km away that formed during the Santonian. The Santonian compression event occurred due to a change in oceanic spreading direction. It is also suggested that the genesis of the compressional event observed within the study area is contemporaneous with similar deformational events observed in other areas of the Atlantic and results from changes in plate motion, but much additional work is required to overcome the current limitation of poor constraint on the exact age of these deformations.

4.7 Comparison to other structures

The Charcot fold is a longwave-ondulation of the oceanic basement that affects the sedimentary cover but without a seafloor deformation. On seismic section and gravity map, the wavelength is seen to be around 60 km with a significant vertical relief of 6.7-7.5 km and this deformation occurred during the Cretaceous. Compared to other areas like the central Indian Ocean (Bull, 1990; Bull and Scrutton, 1992; Krishna et al. 2001) and ridge system such as the Wyville-Thompson ridge west of Shetland. In the central Indian Ocean, the folds have wavelengths of between 130 and 250 km with a mean of around 190-200 km and the amplitude of their undulations is 1-2 km with a clear cut deformation of the seafloor. The undulations across fracture zones here were initially noted by Bull (1990) as being consistent to a combination of

an approximate N-S compression and strike-slip motion indicated from earthquake. The Wyville-Thompson ridge which is a bathymetric feature of the North Atlantic Ocean floor is about 200 km in length and amplitude of 2 km, located between the Faroe Islands and Scotland. The shortening here was formed during the Eocene to Miocene period. The fold is interpreted to have formed by the reactivation of a pre-existing fault and thus could be classified as an inversion structure (Boldreel and Andersen, 1993).

4.8 Conclusions

1. Two distinct structural styles have been identified in the basement. These are normal faults which form the northwest-southeast trending tectonic spreading fabric which formed due to the accretion of oceanic crust and compressional faults that formed during a later phase of compression and have a northeast-southwest orientation.

2. Two-scales of thrust fault have been identified, several folds with wavelength of a few kilometres and one much larger structure which is 60 km wide.

3. In the case of the small-scale thrusts there is evidence for thrust faults cross-cutting the entire oceanic crust, possibly soling-out near to the Moho.

4. The moderate quality of the seismic data over the Charcot Ridge means that the detailed interpretation of this structure is problematic. Our preferred interpretation is that it represents a major crustal scale thrust, which has a thin-skinned, origin, again with the soling-out of the main thrust occurring near the Moho.

5. The Charcot ridge forms a major structural high that splits the Niger Delta into western and southern lobes. It probably formed due to the thrusting of oceanic crust to the north of the Charcot Fracture zone over crust to the south of it.

6. The Charcot structure also represents one the largest compressional structures in basement rocks to be identified in a passive margin setting

7. Very approximate age dating based upon the long range seismic correlations of others indicates that the compressional phase is of Cretaceous age. It may be equivalent to the Santonian event, and caused by a change in spreading direction during continental drift.

Chapter Five: The Role of Multiple Detachment levels in the Fold and Thrust Belts of the Deep and Ultra-deepwater West Niger Delta

5.1 Abstract

Interpretation of recently acquired 2D and 3D seismic data from the contractional domain of the Tertiary deepwater west Niger Delta which is an area of current hydrocarbon exploration and development to show that during its gravitational collapse, multiple detachments were active. Detachments are located within (1) what is herein referred to as the 'Dahomey unit', (2) the transition between the Agbada and Akata Formations (Top Akata), and (3) the Akata Formation. Seismic interpretation and quantitative measurements of fault displacements show that the utilisation of different detachments results in contrasting styles of thrust propagation and fold growth. Two geographical zones are defined. In zone A, (NW sector of the study area), the stratigraphically shallowest Dahomey detachment is dominant and is associated with *thrust truncated folds*. In zone B, (SE sector of the study area) a stratigraphically lower detachment approximately at the Agbada-Akata Formation boundary is associated with *thrust propagation folds*. A third detachment, within the Akata Formation is locally developed and is also associated with *thrust propagation folds*. The different deformational histories are probably related to the mechanical stratigraphy and the pore-pressure characteristics of the succession.

5.2 Introduction

Deformation caused by gravity tectonics is common to many deepwater passive margins (Bruce, 1973; Dailly, 1976; Evamy et al. 1978; Doust & Omatsola, 1990; Marton et al. 2000). As petroleum exploration becomes increasingly focused on these deepwater settings, insights into the evolution of the contractional deformation structures that are located in the toe regions of the gravity tectonic system and their suitability as hydrocarbon traps has become important. The deepwater west Niger Delta region (Fig. 5.1a) is predominantly a compressional structural domain that has recently become the focus of significant oil and gas exploration activity. However, there is currently no documentation of the variability of the fold styles across the area and their structural evolution. This has been due to the historical lack of extensive 2D and 3D seismic reflection data and well bore calibration of the stratigraphy. Earlier studies were based largely on a few widely spaced reconnaissance seismic lines (Burke, 1972; Delteil et al. 1974; Emery et al. 1975; Mascle, 1976; Lehner and De Ruiter, 1977; Damuth, 1994) and focused upon the mapping of fracture zones and other basement structures while recent publications (Ajakaiye and Bally, 2002a, b; Shaw et al. 2004; Bilotti and Shaw, 2005; Corredor et al. 2005a, b) have focused on studying the gravitational structures (Fig. 5.1b). Specifically, Corredor et al. (2005a) have carried out structural reconstructions of the progressive development of the fold and thrust belts, describing the style of thrusting and associated folding. They drew links between detachment level to structural style but did not focus on the deepwater west Niger Delta.

Thrust-related folds can evolve in many ways (e.g. McClay, 2004). These can be distinguished based upon (a) the shape of the thrust that underlies the fold and the relationship between folding and the kinematics of the thrust tip or (b) whether they have formed above a thrust with no ramp; a

lower flat and ramp; or a lower flat, ramp and upper flat. They can also be differentiated kinematically depending on whether they have formed from a fixed tip, a propagating tip, or from a thrust that continues beyond the fold (Wallace and Homza, 2004).

The seismic data used in this study were acquired over what are herein termed the (a) inner (proximal) fold and thrust belt, (b) detachment (inter thrust) fold belt and (c) outer (distal) fold and thrust belt of the deepwater west Niger Delta (Fig. 5.1a). This work complements that of Corredor et al. (2005a) who carried out structural reconstructions in 2D over selected cross sections across the delta. The aim of this paper is to document regional variations in thrust and fold styles and relate these to the stratigraphic characteristics of different detachment levels.
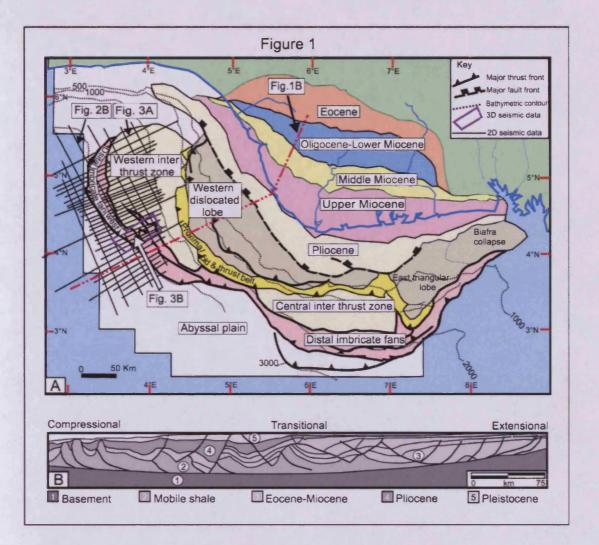
5.3 Previous research on detachment zones

The structural styles of deepwater fold and thrust belts are influenced by a number of parameters including the original mechanical stratigraphy (Erickson, 1996) and the fluid pressure distribution (Ramsay and Huber, 1987). The strength and thickness of the competent layer being deformed control the wavelength, amplitude, and asymmetry of thrust-related fold structures (Erickson, 1996). As such they control the location of a thrust or fold within a multilayered stratigraphic package.

Pore fluid pressure plays a key role in the development of deepwater fold and thrust belts particularly where there are no evaporitic sediments capable of localising a detachment surface. According to the Mohr-Coulomb failure theory, an increase in pore pressure will reduce the effective normal stress, thereby lowering shear strength. The occurrence of excess fluid pressure helps to account for the phenomenon of weak faults in general (Sibson, 1981; Byerlee, 1993) and this mechanical principle can also be applied

Figure 5.1. (a) Map of the Niger Delta showing the different structural domains (modified after Damuth, 1994). Note IFTB, DFB and OFTB are equivalent to the inner fold and thrust belt, detachment fold belt and outer fold and thrust belt respectively (b) Regional dip line extending across the onshore into the deepwater west Niger delta. Modified after Haack et al. (2000). Vertical exaggeration = 2.0

to the localisation of detachment surfaces in thrust domains (Hubbert and Rubey, 1959).

Previous work on fold belts such as that of the Western Gulf of Mexico (Peel et al. 1995) and the Niger Delta (Doust and Omatsola, 1990; Morley and Guerin, 1996; Wu and Bally, 2000) considered detachment to occur on overpressured shales. Where multiple overpressured levels exist in passive margin deepwater settings, multiple detachment levels are not uncommon. Some compressional belts have developed above multiple detachment levels composed of either shale (Rowan et al. 2004), rock salt or other evaporites (Grelaud et al. 2003) or a combination of these (Peel et al. 1995). This has resulted in complex thrust-related fold geometries (Davis & Engelder, 1985; Cobbold et al. 1995).
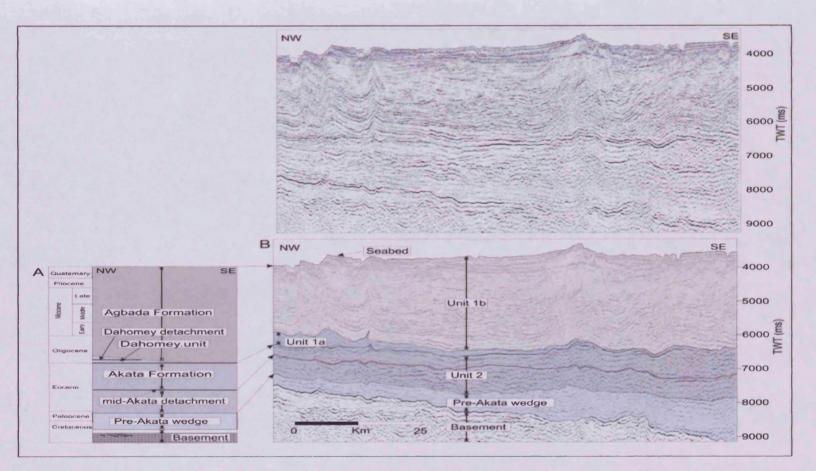
5.4 Geological setting

The Niger Delta is one of the largest modern deltas in the world (Doust and Omatsola, 1990; Hooper et al. 2002). It is situated at the southern end of NE-SW folded rift basin, the Benue trough which formed during the Cretaceous opening of the South Atlantic, when the equatorial parts of Africa and South America began to separate (Burke et al. 1971; Whiteman, 1982; Fairhead and Binks, 1991). During the opening of the Equatorial Atlantic in the late Early Cretaceous (Nünberg and Muller, 1991; Maluski et al. 1995), the trough became filled progressively with Albian and younger post-rift deposits. By the Late Eocene, a delta had began to prograde over the continental margin following the end of the Paleocene marine transgression when the Imo Shales were deposited (Damuth, 1994). The delta now consists of a sedimentary prism some 12 km thick with a subaerial extent of about 75,000 km^2 (Fig. 5.1a).

5.4.1 Stratigraphy

The Tertiary Niger Delta can be stratigraphically divided into three diachronous units of Eocene to Recent age that form a major regressive cycle that is broken up into series of offlap cycles named the Akata, Agbada and Benin Formations (Short and Stauble, 1967; Avbovbo, 1978; Evamy et al. 1978; Whiteman, 1982; Knox and Omatsola, 1989; Doust and Omatsola, 1990). The delta prograded over both oceanic and continental basement (Davies et al. 2005) (Figs. 5.2ab and 5.3ab). This basement includes a syn-rift and post-rift succession that fills a northeast-southwest and WNW-ESE trending rift structure that formed during the Cretaceous, probably during Aptian rifting of the Equatorial Atlantic (Gradstein et al. 1995; De Matos, 2000; Macgregor et al. 2003). An unconformity (mid Aptian break-up unconformity) separates the syn-rift and post-rift sediment fill. Above this lies a low reflectivity package thought to be of Late Cretaceous to Palaeocene age.

In addition to the previously described subdivisions, informally defined are two major seismic-stratigraphic packages (units 1 and 2) based upon contrasting seismic amplitude, seismic facies and deformational characteristics. Unit 2 is about 3-4 km thick and comprises a low reflectivity package, which lacks internal reflection except for a single mid-level high amplitude reflection (Fig. 5.3b), that may be related to a detachment (Corredor et al. 2005a). This unit onlaps the older Late Cretaceous to Palaeocene succession is of marine origin and at the base of the delta and corresponds to the Akata Formation of Avbovbo (1978) and Knox and Omatsola (1989). It is mainly composed of marine shales believed to be the source rock for hydrocarbons and some locally developed sand and silt beds. This unit exhibits anomalously low P-wave seismic velocities (~2000 m/s) that may reflect regional fluid overpressures (Bilotti and Shaw, 2001). It provides a

Figure 5.2. Chronostratigraphic diagram showing the regional variability in stratigraphy along a NW-SE transect across the deepwater west Niger Delta.. 2D seismic line showing the abrupt change in stratigraphy between units 1a, 1b and unit 2. Note that BSM, PASW, Unit 2, Unit 1a and unit 1b corresponds to the basement (Ajakaiye & Bally, 2002), pre-Akata sediment wedge (see Morgan, 2003, 2004), Akata Formation (Avbovbo, 1978; Knox & Omatsola, 1989), Dahomey wedge (Morgan, 2003; 2004) and Agbada Formation (Short & Stauble, 1967; Avbovbo, 1978) respectively.

detachment horizon for large growth faults, located up dip of the study area (Knox and Omatsola, 1989).

Unit 1 is further subdivided into Units 1a and 1b (Figs. 5.2b and 5.3a). Unit 1a is a distinct package of between 300-600 m thick, consisting of semi-continuous to continuous low amplitude reflections that are deformed into series of folds which are clearly evident in the NW of the deepwater region (Figs. 5.2b and 5.3a). It thins southwards until it is below seismic resolution (~ 20 m) (Fig. 5.3b). It is herein termed the Dahomey wedge and is believed to have been sourced from the Dahomey trough of the onshore Guinea basin in the north of this study area (Morgan 2003; 2004). Unit 1b is about 3 km thick below a water depth of over 4000 m and corresponds to the Agbada Formation that has been described by Short and Stauble (1967) from the Agbada-2 well and by Avbovbo (1978). It consists of alternating sandstones and shales deposited by channelised turbidites, debrites and hemipelagites (e.g. Davies, 2003; Deptuck et al. 2003). The sands constitute the main reservoirs in this part of the delta. Sand to shale ratio generally decreases downwards as the formation passes gradually into the Akata Formation. The age of this formation is Eocene to Pleistocene (Short and Stauble, 1967; Doust and Omatsola, 1990). The Benin Formation, as described from the Elele-1 well by Short and Stauble (1967), is not encountered in the deepwater region of the Niger Delta (Morgan, 2003).

5.4.2 Structure

The Niger Delta tectonic province is a typical example of a linked regional gravity tectonic system where horizontal translation of the post rift cover is driven by gravitational failure of the margin. This is accommodated by thin-skinned tectonics with extensional, intermediate transitional and downdip compressional domains (Fig. 5.1b) above one or more detachment levels.

Extension occurs on the shelf and is accommodated by growth faults (Weber and Daukoru, 1975; Evamy *et al.*, 1978; Whiteman, 1982; Knox and Omatsola, 1989). A transitional domain is located basinwards of this and is characterised by shale diapirs and their associated inter-diapir depocentres. The region has been subdivided into three structural domains (Connors et al. 1998; Corredor et al. 2005a)

(a) *Inner fold and thrust belt* (Fig. 5.1a), characterised by higher structural dip with an average distance between imbricated thrust sheets of between 1-2 km and with the formation of occasional piggy-back basins (Corredor et al. 2005a). The data set does not extend over this domain.

(b) *Detachment fold belt* (Fig. 5.1a), characterised by large areas of minor deformation from thrust or shale induced folding (thrusting and folding due to shale swelling), with along transport thrust sheet dimensions ranging from 2-5 km (Fig.5.3a).

(c) *Outer fold and thrust belt* (Fig. 5.1a), comprised of local depocentres and both basinward and hinterland verging thrusts. This domain is situated further downdip, with channelised turbidite sands trapped in broad wavelength anticlines above incipient thrust propagation zones (Fig. 5.3b).

The study area was divided into two zones, A and B (Fig. 5.4), according to structural styles. Zone A is in the detachment fold belt located in the NW of the delta and is characterised by the presence of a group of open folds with asymmetric to symmetric geometry, and with minor thrust faults on the steeper limbs. Further to the SE, and along structural strike from Zone A, a second set of thrust faults have been defined that are coupled with strongly compressional domains may be due to detachment zones that underlie the wedge shaped fold and thrust systems.

5.5 Data and methodology

Zone B is partially covered by 1970 km² of high quality 3D seismic data

acquired in 1999 over water depths of between 1500-4000 m and a 1998

vintage of 2D seismic data that has a combined length of 5230 km. Zone A is

however, only covered by 2D seismic data. These data have a dip and strike

line spacing of 4 km and 10 km, respectively, with a data record interval of 12

seconds and a 6 km cable length with an airgun source. These data were

processed using a Kirchhoff bent ray pre-stack time migration. The 3D dataset

has a 6 km offset length and a 12 seconds record interval. Its processing

sequence is similar to that of the 2D data. The datasets are displayed with a

reverse polarity (European convention) so that an increase in acoustic

impedance is represented by a trough and is black on the seismic data in all

figures presented here. The data are displayed in seconds two-way-travel

time (TWT). The vertical and lateral resolutions are estimated to be between

10-20 m at the top of unit 1 and 100 m at the base of unit 2. Stacking velocities

obtained from Morgan (2003) were used to depth convert the seismic data (see

Yilmaz, 2001). The overall seismic data quality is considered to be good

within the Tertiary section; seismic noise is however noted in the dataset,

occasionally due to poor migration of seismic energy in areas where there are

abrupt lateral velocity changes i.e. in the footwall regions beneath the major

thrust planes.

Regional mapping was undertaken to subdivide the seismic-stratigraphy

into Units 1a, 1b and 2 (Figs. 5.2b and 5.3ab). High amplitude continuous

reflections were then mapped to further subdivide the stratigraphy. These
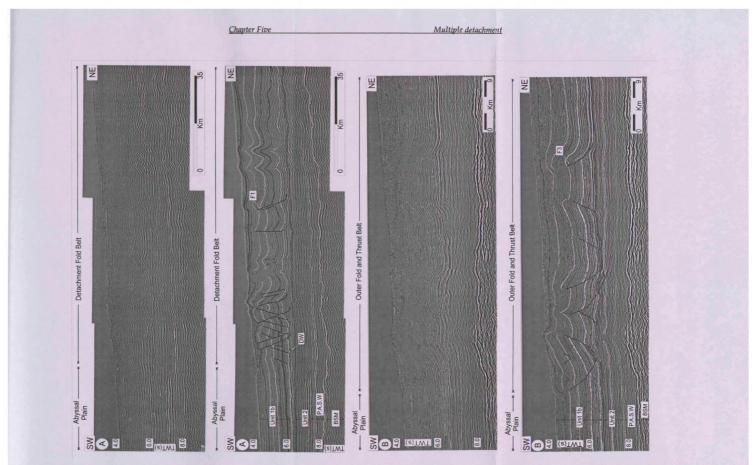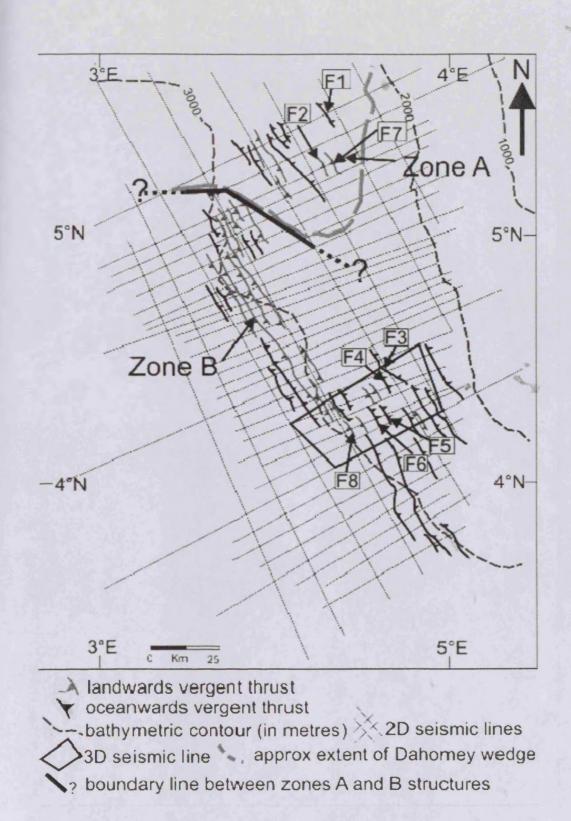
Figure 5.3. Non-interpreted and Interpreted seismic lines from (A) the 2D dataset (B) the 3D dataset, showing the major stratigraphic subdivisions of the deepwater west Niger delta. The major reflectors defined in this section are the BSM, the PASW, unit 2 corresponding to the Akata Formation, unit 1A which is the Dahomey detachment unit, and unit 1b which defines the Agbada Formation. Note the sinusoidal geometry of the Dahomey unit that thins towards the SW direction here and in the SE direction on Fig. 5.2 but becomes relatively thicker towards the NE. The compressional faults tip out from the thick units marked DW. Older inactive fold features are observed buried without seafloor expression.
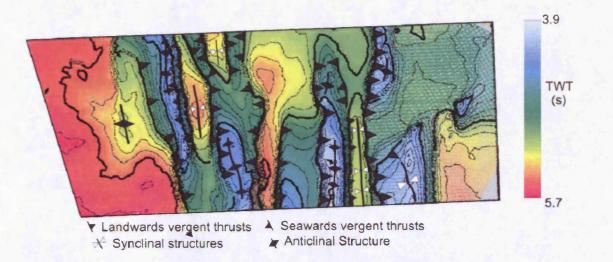
Figure 5.4. Location map of the study area showing the 2D and 3D seismic database, the approximate demarcation of zones A and B and the location of faults F1 – F8 described in this study. It also shows the approximate extent of the Dahomey wedge.

reflections have provided a basis for time stratigraphic interpretation throughout the study area because of the ease with which they can be correlated. This stratigraphic framework was then used as the basis for measuring fault offsets. The high continuity of the mapped reflections was invaluable in aiding correlation across thrust faults within the 3D survey area in particular, because the lateral tips of the thrusts were found to tie beyond the limits of the survey area. Further constraints on the correlation between footwalls and hangingwalls were obtained by linking the regional 2D data to the 3D seismic data.

To analyse the faults, the "displacement-distance" method developed by Muraoka and Kamata (1983) and Williams and Chapman (1983) was adopted. This graphical method provides a primary visual representation of the displacement distribution along the fault trace and provides important constraints for the growth history of the thrust (Watterson, 1986; Ellis and Dunlap, 1988).

Depth converted sections were constructed for each fault analysed. For thrust faults in Zone A, the faults were mapped using the widely spaced regional 2D seismic grid, and specific profiles were selected for depth conversion on the grounds that they were most orthogonal to the strike of the thrust faults. It was assumed that because in the better-constrained distal parts of the region, fold axes were mapped parallel to the strike of the thrust faults, the likely motion vector on the thrust faults was orthogonal to fault strike. Hence the seismic profiles selected are likely to be in or close to the transport direction. This interpretation accords well with what is known of the regional kinematics of the gravity tectonic system as a whole (e.g. Bilotti and Shaw, 2005). For thrust faults in Zone B, profiles were selected based on mapping of the thrusts and associated folds using the dense line spacing of the 3D seismic survey (Fig. 5.5). The parallelism observed on structure maps

Figure 5.5. Time structural map of Miocene (10.3 Ma) showing the parallelism between fold axes and the strike of the thrust faults. The figure is dominated by dip-slip regime. The measurements of the fault displacements were made on profiles that are generally parallel to the likely transport direction.

of the 3D survey area between fold axes and strike of thrust faults again strongly argues for a dominantly dip-slip regime, and hence the need to select profiles that were considered parallel to the likely transport direction.

The displacement (D) values were measured directly from the depth converted, true scale sections using 2DMove structural restoration software that allows for depth converted seismic profiles to be displayed at any scale.

Displacement values were plotted graphically against the distance (X) measured along the thrust fault plane from the upper fault tip to the midpoint position between footwall and hangingwall cutoffs for each specific marker horizon. Displacement values were only recorded for those markers where there was a high confidence in the accuracy of the cross-fault correlation. This method ensured that distortions due to fault plane listricity were not introduced into the graphical display, thus preserving the value of the displacement gradients that can be derived directly from the plots. This approach differs from that used in displacement analysis of extensional faults, where it is more conventional to plot displacement or throw against a distance ordinate measured by projection onto a vertical plane (Walsh and Watterson, 1987).
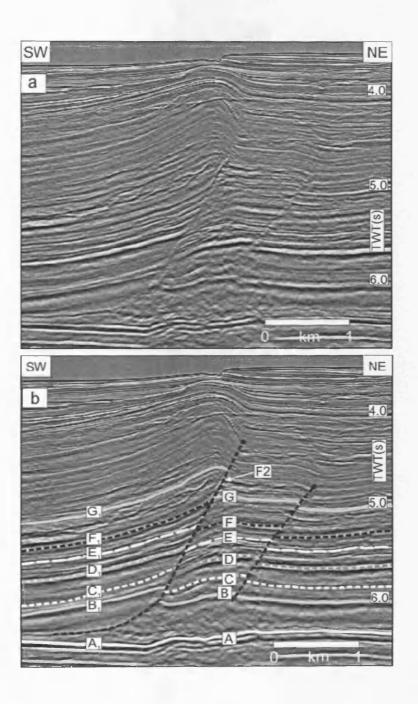
5.6 Observations

In this section, representative 2D (Figs. 5.6 and 5.7) and 3D (Figs. 5.8 and 5.9) seismic lines to illustrate the structural interpretation, pertinent features of the structural geology of the deepwater region, and to demonstrate the location of the detachment levels. The displacement distribution of individual thrusts is presented and discussed as a guide to reconstructing the structural evolution.

5.6.1 Fault interpretation and detachment level

Figure 5.6. Uninterpreted (a) and interpreted (b) representative seismic section from zone A showing a typical fault (F1) detaching within the Dahomey wedge. (c) An enlarged section of the sole segment where the fault plane reflection terminates within a bedding parallel layer marked as BPR.

Figure 5.7. Uninterpreted (a) and interpreted (b) representative seismic section from zone A showing a typical fault (F2) detaching in the Dahomey wedge.
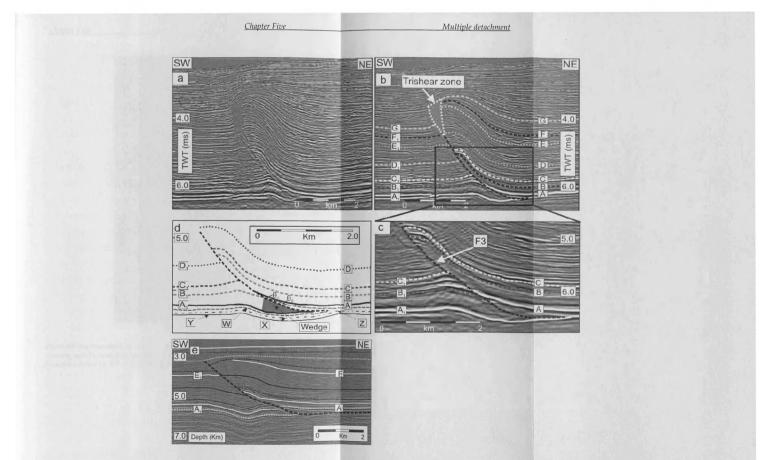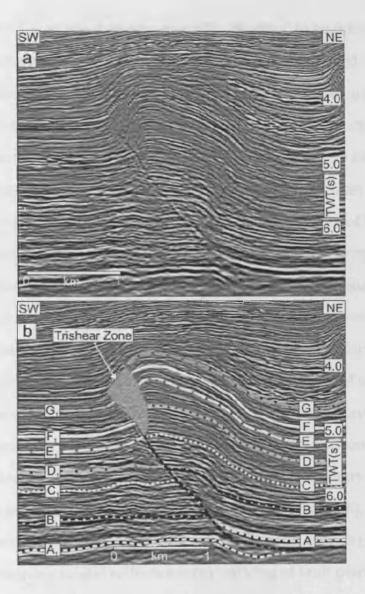
Figure 5.8. Representative (a) Uninterpreted and (b) interpreted seismic section from zone B showing fault F3. Note how the thrust ramps up forming a thrust wedge. Also observed is the amount of displacement between the footwall and hanging walls. The upper tip is invisible within a trishear zone (c) A section of the sole segment defining the exact position of the detachment layer (d) Line drawing of the sole segment describing the relationship between the reflections (e) A depth converted seismic section showing fault F3 from which actual displacement measurements were made.

Figure 5.9. Representative (a) non-interpreted and (b) interpreted seismic section from zone B showing fault F4. Note how the thrust ramps up forming a thrust wedge on the top Akata Formation define by A-A. The upper tip of the thrust is invisible within the trishear zone.

The thrust faults in the study area are generally observed to be oceanward verging and striking in a NW-SE direction, but some are landward-verging and out-of-sequence (Morley, 1988). In general, the thrust planes are listric (concave upwards), steepening upwards to a more planar geometry in the upper parts of the fault planes (Figs. 5.6-5.9). The listric geometry of these thrust faults and the generally asymptotic relationship of the thrust planes with the regional stratigraphy at their base is strongly indicative of the presence of a detachment surface (McNeill et al. 1997). The upper tips are well defined by the smallest resolvable offset of seismic markers, although loss of signal coherence in shallow reflections around the upper tips sometimes obscures its precise location (Figs. 5.8 and 5.9). Individual fault planes range in dip from sub- horizontal, close to the inferred detachment level to c. 40° close to the upper tip. The steepest, more planar sections of the thrusts were observed to be generally steeper for faults in Zone A in comparison with those in Zone B. Depth conversion showed that the listric geometry is not simply due to an increase in seismic velocity with depth (Fig. 5.8E).

Fault planes were interpreted based on the following criteria (a) abrupt offset of steeply dipping stratal reflections, (b) tracking of fault plane reflections, (c) juxtaposition across the fault plane reflection of dissimilar units and (d) a deterioration in the data resolution beneath the faults as a result of the juxtaposition of faster velocity rocks in the footwall juxtaposed laterally against slower velocity rocks in the hanging wall.

The majority of the thrust faults could be traced from a detachment level at depth upwards to close to the seafloor (e.g. Figs. 5.6a, 5.7a, 5.8a and 5.9a). The detailed geometry of seismic reflections at the sole of the thrusts is critical for the determination of the detachment levels in Zones A and B. The quality of the seismic data generally allows the detachment level to be delineated within a vertical resolution limit of less than 25m thickness (Figs 5.6-5.9), and hence contrasting detachment levels observed from faults in Zones A and B

can be resolved with confidence. The detachment level is defined based on tracing the discordance between reflections in footwall and hangingwall to a position where there is no longer any visible discordance (see Fig. 5.6c). In the following sections examples of faults in Zones A and B were examined in more detail to illustrate the interpretational approach adopted to identify detachment levels.

5.6.1.1 Faults in Zone A

The general approach was illustrated with reference to a representative example of a fault from Zone A (Fig. 5.6). All angular relationships were measured from true scale depth converted profiles. It is noted that the fault plane exhibits an acute cutoff for reflection B but not for reflection A. Reflection B has a greater cutoff angle with the fault (c. 28-30° - labelled θ_1 on Fig. 5.6c), than reflection U (c. 18-20° - labelled θ_2 on Fig. 5.6c) and reflection W (c. 12-15° labelled θ_3 on Fig. 5.6c). Similar relationships are identified elsewhere (Fig. 5.7). The fault then shallows in dip asymptotically so that the discordance between hangingwall and footwall stratal reflections diminishes to the point where the units are concordant, which in this case is coincident with reflection X (Fig. 5.6c). This is where I pinpoint the junction between the thrust fault and the strata-parallel detachment which is labelled Z on Fig. 5.6c, and is the basis for our method of identifying the detachment level. It is found that the detachment is often marked by a reflection that has variable and often high amplitude. Similar relationships are identified for most of the faults that were examined (e.g. Fig. 5.7).

5.6.1.2 Faults in Zone B

In the fault displayed in figure 5.8, reflections A and B both exhibit acute cutoffs. The footwall cutoffs were observed at reflection W, but none for reflections W and X (Fig. 5.8). Again, reflection A has a greater cutoff angle (c. 20-25° - labelled θ_1 on Fig. 5.8d) and this reduces downwards to c. 12-15° (marked labelled θ_2) on figure 5.8d. It is also evident that the point where the thrust is interpreted to become layer parallel with stratal reflections (i.e. the point at which it becomes a detachment) defines the apex of a wedge-shaped element (Fig. 5.8d). Similar geometries have been described by Cloos (1961) and Mitra (2002b). Similar wedge elements are observed at the base of the footwall in figure 5.9. In marked contrast, there are no comparable 'wedges' of this type associated with faults in Zone A. Also it is observed that the upper tips of the faults in Zone B are characterised by upward-widening triangular region of markedly reduced amplitude (Figs 5.8 and 5.9). These low amplitude regions bear a striking resemblance to tip-related shear zone called the trishear zone identified in many outcropping thrusts (Erslev, 1991; Allmendinger, 1988).

5.6.2 Displacement-distance characteristics
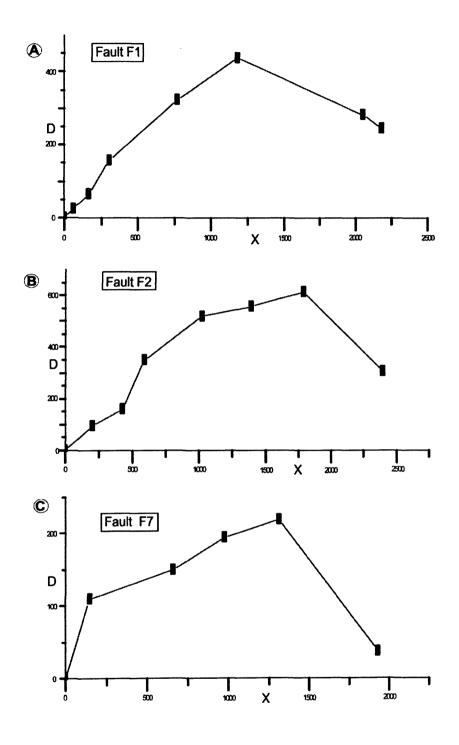
Displacement measurements for eight faults (F1, F2, F3, F4, F5, F6, F7 and F8) (located in Fig. 5.4) were plotted against their stratigraphic position. Faults F1 (Fig. 5.6), F2 (Fig. 5.7) and F7 are located in Zone A whereas faults F3 (Fig. 5.8), F4 (Fig. 5.9), F5, F6 and F8 are situated in Zone B. Graphical plots of displacement (D) versus distance (X) are presented in Figures 5.10 and 5.11. Errors amounting to c. 10% in these measurements include the sampling interval of 4 milliseconds, the errors in positioning due to uncertainty in the migration velocities, and interpretational errors.

5.6.2.1 Zone A
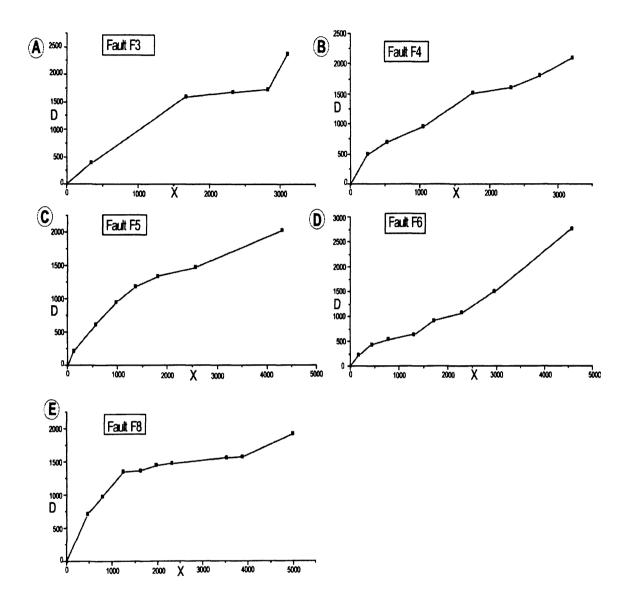
All the thrust faults in Zone A are characterised by displacement-distance plots that show an increase in displacement from the upper tip, to a position approximately midway down the main thrust ramp, where the displacement is a maximum, and from which point to the detachment position, show a clear decrease in displacement values. Three examples of this type of pattern are presented in Figure 5.10. In the case of fault F1, for example (Fig. 5.10a), the displacement maximum recorded at the mid-ramp position is 438 m and decreases to 247 m at the deepest horizon prior to the detachment. This reduction in displacement downwards is too large to be within the error range, and thus appears to be a genuine feature of this example. Similar patterns of asymmetrically peaked displacement-distance patterns can be seen for faults F2 and F3 (Figs. 5.10b and c), where there are even more pronounced downward decreases in displacement values from the maximum position. These observations are highly significant in the context of overall kinematic analysis (Williams and Chapman, 1983), in that the displacement clearly decreases as the detachment is approached.

5.6.2.2 Zone B

In contrast to the thrust faults in Zone A, those in Zone B are characterised by displacement-distance plots that show an increase in displacement from the upper tip downwards to the last measurable horizon offset close to the detachment position. Five representative examples of displacement-distance plots for Zone B faults are presented in Figure 5.11. The general increase in displacement values downwards from the upper tips can either be quite linear with a constant displacement gradient (e.g. upper part of Fig. 5.11a), or more step-like (Fig. 5.11b), or bipartite, with a larger upper gradient, and a smaller deeper gradient (Fig. 5.11b and c). The displacement gradients are similar to those reported for normal faults, and range from 0.2 to over 3.0. The larger values are almost certainly indicative of stratigraphic thinning in the region of

Figure 5.10. Displacement-distance plots for thrusts F1, F2 and F7 from zone A. The origin (0;0) of the plots are equal to the upper tip of the faults.

Figure 5.11. Displacement-distance plots for thrusts F3, F4, F5, F6 and F8 from zone B as represented on a-e respectively. The origin (0;0) of the plots are equal to the upper tip of the faults.

the upper tip, rather than the result of ductile strain associated with fault propagation. The deepest values in all cases were measured quite close to the detachment, so the progressive increase in displacement as the detachment is approached stands in marked contrast to the reduction in displacement observed at the same position for Zone A faults. This contrast in displacement characteristic is universal for the faults in the two zones, respectively, and is considered further below with a view to explaining the difference in behaviour.

5.7 Discussion

5.7.1 Multiple detachments

One of the most important observations made from the seismic interpretation is that the thrust planes are seen to detach into two separate levels in the deepwater region of the west Niger Delta. A third (mid Akata) detachment has also been identified but has only local significance in Zone B. These detachments are interpreted to be located within spatially extensive and mechanically weak units, based on long range correlations of the stratal units containing the regional detachment levels. Over 95% of the combined fold-thrust structures mapped on the regional 2D and 3D seismic data detach into either of these two levels. These two detachments are informally termed the Dahomey and Top Akata Detachments. The Dahomey Detachment (within the Dahomey 'wedge') is a zone rather than a narrowly defined level, with a thickness of between 100-120 m. It is characterised by parallel internal reflections with some bedding parallel slip producing minor deformation and allowing the definition of the detachment interval. This thick detachment 'zone' is conceivably due to the presence of a specifically weak lithology, such as a condensed interval with high organic content, or due to specific clay

mineralogy (e.g. smectite rich). In contrast to the Dahomey Detachment, the Top Akata detachment shows no buckle-type minor deformation. It has a thickness of between 40-70 m.

5.7.2 Displacement patterns

The displacement-distance profile exhibited by faults in Zone A (Fig. 5.10) have been shown to be characterised by a distinct peak in displacement value some distance above the detachment. It is not possible to constrain whether the displacement continues to diminish along the flat portion of the detachment, possibly even to a lower tip zone, as has been suggested for some thrust faults (Eisenstadt and De Paor, 1987; Pfiffner, 1985). What is clear, however, is that the peak value occurs approximately midway up the post-detachment stratigraphy, relative to the overburden present at the onset of thrusting. The displacement-distance plots of these faults thus bear some resemblance to the 'C' type plots described from small normal faults by Muraoka and Kamata (1983) and for thrust faults by Williams and Chapman (1983).

The 'C' type of displacement-distance plot implies that the thrust fault loses displacement both updip and downdip from a point near the centre of the thrust, with considerable displacement gradients in both directions (and presumably, therefore, laterally too). Small variations in the profile are attributed to lithological effects such as bed pervasive ductile thickening within weaker shale layers. The relative smoothness of the profile could be interpreted to indicate an essentially uniform lithology throughout the section consistent with the deepwater depositional setting. The recognition of displacement gradients implies that the wall rocks must be strained in order to accommodate the displacement variation (Walsh and Watterson, 1987), which raises interesting questions about discrimination between thinning due

to wallrock strain versus thinning due to syn-kinematic changes in accommodation space.

Previous studies have linked the recognition of a 'C' type of displacement pattern to a specific propagation and growth model, in which the site of initiation of the fault coincides with the locus of maximum displacement on the fault (Walsh and Watterson, 1987). More recently this concept has been challenged in cases where strong rheological contrasts in the faulted succession have been shown to skew the position of maximum displacement away from the initial locus of propagation (Wilkins and Gross, 2002). In some previous models for thrust nucleation, analysis of this type of displacement pattern has been equated with initial propagation in the ramp region of a ramp-flat thrust structure, with both updip and downdip propagation as strain accumulates (Eisenstadt and De Paor, 1987; Pfiffner, 1985), and this interpretation was followed in suggesting that the 'C' type patterns observed are probable indicators of a localised nucleation site above the detachment, with later propagation of the thrust downwards into the detachment. This propagation sequence is thought by some workers to be characteristic of faulted detachment folds (Mitra, 2002b), alternatively referred to as thrust truncated folds (Wallace and Homza, 2004). This interpretation is similar to that proposed for a thrust and fold in the inter thrust sub-domain of the eastern part of the deepwater Niger delta which was termed a 'thrust-faulted detachment-fold anticline' (Shirley, 2002).

In marked contrast faults in Zone B (Figs. 5.8 and 5.9) show a steadily increasing pattern of displacement with distance from the upper tip to the last measurable point close to the detachment level (Fig. 5.11). As with faults in Zone A, the distribution of displacement on the flat portion of the detachment is unknown. Because the displacement values are unconstrained along the detachment, we cannot infer anything about nucleation and propagation other than to link the distinctive displacement gradients across the entire

post-detachment stratigraphic section to thrust propagation in the transport direction. As noted earlier the folds in Zone B are seen to have be more open than folds in Zone A, which could possibly be linked to the differences in displacement patterns on the thrust faults associated with the folds in the two areas, and the relative partitioning of contractional strain between the thrusts and the folds. The parts of the displacement-distance plot with zero slope may be indicative of fault segments that have propagated with little associated wall strain (Muraoka and Kamata, 1983; Suppe and Medwedeff, 1984; 1990).

In summary, it can be concluded that there are substantial differences between the thrusts in the two zones, both in their displacement patterns and in their relationship to associated folds. Before addressing the key question of why there are differences between these two zones, I first present a model for thrusting and folding in Zones A and B based on my kinematic observations linked to those of previous workers.

5.7.3 Descriptive model for thrust propagation and fold style development

5.7.3.1 Zone A
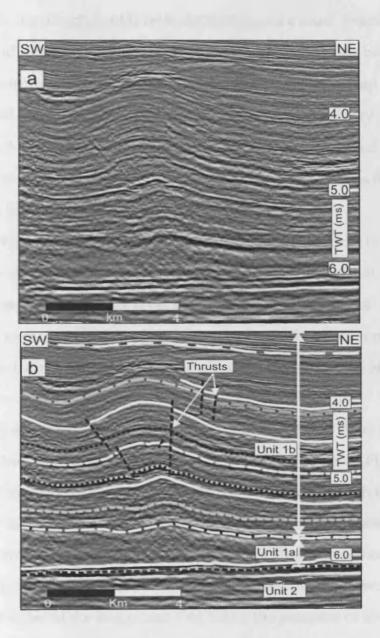
In this zone, the dominant structural fold type is the thrusted detachment fold which is suggested to result from buckling of a stratified succession, and which initially bent without rupture, leading to the formation of an open anticline and syncline pair. It is proposed that the fold then tightened and became more asymmetric as deformation progressed. When the fold could no longer accommodate the strain by folding, ruptures localised and linked on the steeper limb producing a thrust that broke through the forelimb of the fold and finally connected to a mobile detachment layer within the Dahomey unit. These types of structure have been called break-thrust folds (Dixon and Liu, 1992; Fischer et al. 1992); thrusted detachments folds (Mitra, 2002b) or

thrust truncated folds (Wallace and Homza, 2004) and have been described mainly from kinematic models. The term fold-accommodation fault (Mitra, 2002a) would not be appropriate as these type of faults do not connect to a major detachment, which these structures do. This is critically supported by several examples of thrusts faults on the limbs of detachment folds that are at an early stage in their development (Fig. 5.12), in which the thrust has not propagated downwards to connect with the detachment. The presence of this buckled bed with lack of a thrust during shortening may be modified by later truncations of a fault (Jamison, 1987; Mitra, 1990; McNaught and Mitra, 1993). The difference is also shown by the variation in nucleation pattern and the stratigraphic position of the detachment.

5.7.3.2 Zone B

In Zone B, it is suggested that in contrast to Zone A, the fault propagation folds developed coevally with thrusting and consumed slip at the tips of blind thrusts (Suppe and Medwedeff, 1984; Suppe, 1985; Marshak and Wilkerson, 2004). As the thrust tip migrated, strata are folded in front of it and are eventually breached by the thrust. The upward decrease in displacement observed on the displacement-distance plots is quite typical of a thrust-propagation fold but is not really diagnostic of this class of structure (Mitra, 2002b; Wallace and Homza, 2004). Here the folds develop in front of the upper tip of the developing thrust as the ramp propagated up section (see Mitra, 1990; 2002b).

5.7.4 Controls on detachment level

The detachment layer in Zone A is the unit referred to as the Dahomey 'Wedge' is over 100m thick beneath the entire main structures in the area, and is clearly a mechanically weak unit that relates in some way to its lithology. In

Figure 5.12. Non-interpreted (a) and interpreted (b) seismic section showing early stage of development in a faulted detachment fold. Fault and deformation zones form on steeply dipping rotated segments on both limbs resulting in pop-up like structures.

contrast, in zone B, the detachment level is defined across a much thinner interval corresponding to the Top Akata. This detachment level may be due to the presence of overpressure build-up as revealed from a velocity drop (Morgan, 2003) and shown by the high amplitude and reverse polarity reflections (figs. 5.8 and 5.9). Wells drilled in nearby areas have proved this to be the case (large pressure ramp at the Top Akata). So overpressure is the likely mechanism for the Top Akata detachment level.

Stewart (1996) argued that detachment layer thickness played a critical role in the style of shortening in contractional settings. He showed that if a detachment occurred within a thick layer significant fold amplification could be expected prior to thrusting. If the detachment layer is thin, shortening quickly leads to thrust nucleation and thrust propagation folds could be expected thereafter.

Combining the mapped distribution of detachment folds of Zone A with the regional distribution of the Dahomey Wedge detachment 'layer' (Fig. 5.4), it can be seen that the zone of detachment folds coincides exactly with the mapped extent of the Dahomey Wedge. Adopting the argument advanced by Stewart (1996) on the influence of detachment layer thickness, I can therefore simply propose that the main factor controlling the development of two distinct structural styles in the deepwater fold belt is the presence or absence of a thick detachment layer. Where present, detachment folds develop, with differing degrees of associated thrusting out of the limbs. Where absent, instead the shortening slope sediments detach at the Top Akata pressure ramp, which forms a discrete and thin detachment level, above which the nucleation of early thrusts is encouraged, which evolve into the distinctive high strain, thrust propagation folds.

By analogy with the results of numerical and analogue modelling of the factors affecting fold style such as differences in competency and stratigraphic thickness between the upper Dahomey detachment and the underlying Akata

detachment units have probably affected the style of folding that is observed. The Dahomey unit is relatively incompetent, and thus is able to move into the cores of the developing anticlines from the adjacent synclinal hinge. I suggest that this incompetent unit allowed the growth of the fold by flexural slip while maintaining parallel folding, bed length and thickness. The deformation from the top Akata unit may be primarily due to internal ductile strain or flexural slip as indicated by thickness changes across fold limbs and widely spaced bed parallel slip surfaces.

5.8 Implications
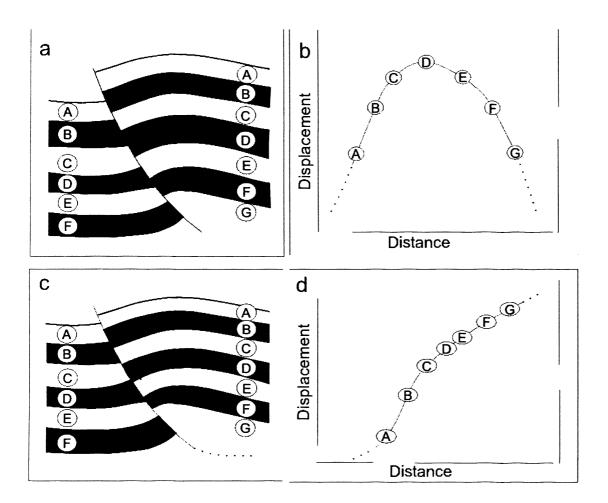
Understanding the evolution of structures in the deepwater west Niger delta is necessary in order to avoid the improper assessment of not only the trap geometry, location, shape, size, depth and vertical extent but also the reservoir, seal, source and migration. It is found that fault propagation folds generally form tighter anticlines than thrusted detachment folds and as such would have different type and size of trap. This may be supported by the fact that most of the world class discoveries are located within Zone A where the thrusted detachment folds are the dominant structure with low relief and high area as compared to Zone B which is dominated by thrust propagation folds which have higher relief but with smaller area.

The interpretation of these different structures will have contrasting implications for the presence and geometry of the fault type whether they impede the migration of fluid or result in compartmentalisation of the reservoirs. The structures are likely to control hydrocarbon migration in that in the Zone A area, there may be no fault linking source to trap and reservoir, whereas elsewhere (Zone B) there generally would be a link. Therefore, it is propose that the risk of a trap not being on a migration pathway is higher in Zone A structures. This is particularly true for the early developmental stages

of thrusted detachment folds, where a through-going fault linking trap to source has not fully developed.

5.9 Conclusions

This study has shown that in the deepwater fold and thrust belt of the Niger Delta there is a strong dependence of structural style on the thickness and lithology of the detachment unit. In Zone A, folds formed in response to ductile deformation of the inherently weak Dahomey wedge, which was susceptible to flow due to the regional overpressure developed at or around the top of the Akata Formation and shown from the greater amount of shortening that could be due to lithologic changes. In Zone B, the folds are more clearly linked to thrust propagation.

This study has shown that two distinct structural patterns are possible within the deepwater west Niger Delta. They are the thrusted detachment folds in Zone A and the thrust propagation folds in Zone B. The two structural styles can be distinguished on the basis of markedly contrasting displacement-distance plots (Fig. 5.13). More symmetrical displacement patterns with a discrete maximum in the mid-ramp position are found for all the thrusts in Zone A associated with detachment folds, whereas the thrust propagation folds are associated with a downward increasing pattern of displacement towards the detachment.

Figure 5.13. Model showing thrust related fold types and their associated displacement-distance profiles. (a) Thrust related fold type with apparent nucleation point at the centre of the fault. (b) Idealised displacement-distance pattern from a "C-type" fault (after Muraoka and Kamata, 1983). (c) Thrust related fold type showing nucleation point at the base of the fault. (d) Idealised displacement-distance pattern from a type II fault. Note here that the nucleation point corresponds to a detachment level. Displacement values are projected from a perpendicular down to a horizontal line from the midpoint between the hanging wall and footwall cut-offs.

Chapter Six: Summary and discussion

6.1 Introduction

In this study, the integration of industry seismic (2D and 3D) reflection data as well as gravity data have been utilised in order to have a proper understanding of the structural evolution of the deepwater west Niger Delta passive margin. This research has focused on the crustal structure of the Niger delta **(Chapter 3)**, seismic evidence of anomalous crustal-scale thrust structure in oceanic crust **(Chapter 4)** which is a complete departure of what is expected at other passive margins, while the role of multiple detachment levels in the west Niger Delta fold belts is also studied **(Chapter 5)**.

The main aim of this present chapter is to draw together the key scientific results presented in the preceding chapters inorder to erect an integrated model for the phenomenon of the structural evolution of this margins. The previous chapters were structured in three semi-independent units, in a format resulting from the different emphasis required to address the key problems raised during the research. In this chapter, therefore, it is intended to integrate the observations and analysis undertaken during this study with regard to establishing the link between them. This chapter commences with a summary of the most notable results and findings of this thesis which were described in **Chapters 3, 4 and 5**. The main arguments of this chapter is subsequently developed through discussing in chronological order the tectono-stratigraphic evolution of the study area.

6.2 Summary of results

6.2.1 Results from the crustal structure (chapter 3)

Chapter 3 presented a pioneering work on the crustal structure of the deepwater west Niger Delta margin that had not previously been documented from 3D seismic reflection data and complimented with 2D seismic reflection data. The principal objective of this chapter is to describe the crustal structure, thickness and distribution of the crust. A resultant aim is to examine the possible implication of the result to the delineation of the Continental from the Oceanic crust in the delta. The summary of the findings in **Chapter 3** includes the following.

- The abnormally thin igneous crust within the study area is one of the most striking results of this study. More than 90% of the study area is below the global thickness of 7.08 km for a normal oceanic crust (White et al. 1992) but within published values for the Atlantic Ocean normal oceanic crust (Rosendahl & Groschel-Becker, 1999).

- The anomalously thin oceanic crusts away from the major fracture zone (Chain FZ) can be attributed to three main settings; at very slow spreading ridges (White et al. 1984; Minshull et al. 1991), adjacent to non-volcanic continental rifted margins and at fracture zones (White et al. 1992).

- It has demonstrated the existence of normal oceanic crust in the area. This is revealed from the thickness map of the crust which shows that the crust here is between 5.0 and 7.0 km.

- The Chain Fracture zone earlier interpreted as Continent-Ocean Fracture zone by Davies et al. (2005) is in fact an Ocean-Ocean fracture zone similar to those observed in the North Atlantic (Rabinowitz and LaBrecque, 1979; Muller and Roest, 1992). This study has also shown

that there is no significant difference in the crustal thickness across the fracture zone as the crust on opposite side of the transform is made up of between 5 and 6.67 km thick oceanic crust, and this is supported by evidence of pervasive tectonic spreading fabric observed on the northern part across the Chain fracture zone.

- Tectonic spreading fabric terminating at the Chain Fracture zone is clearly diagnostic of normal oceanic crust. Subsurface scoop-like forms of faults terminating at the Chain fracture zone are generally observable at ocean-ocean fracture zones and this has been confirmed by Searle and Laughton, 1977.

- The Moho (horizon M) acts as a detachment surface for some of the listric intra-crustal faults in the study area.

- Volcanoes are erupted at the ancient seafloor during the accretion of the crust and the subsequent development of tectonic spreading fabrics.

- The development of the anomalous thrust structure here may be related to the change in the pole of rotation possibly during the Santonian.

- The crust in the study could be divided into 2 layers based on seismic characteristic of the packages within major regional reflectors.

- The Moho reflection in the study area shows a variable reflection pattern. They are present in some areas while they are absent in others. This may be attributable to variation in lateral composition.

6.2.2 Results from thrusting in oceanic crust (Chapter 4)

Chapter 4 provides a comprehensive examination of anomalous crustal faults.

- Two distinct structural styles are evident and related to the basement architecture in the study area, (a) the dominance of planar normal faults defined mostly by tectonic spreading fabrics are observed in the northern part and (b) compressional faults are mostly observed in the south.

- There is ample evidence that suggest widespread deformation of the oceanic crust. This compressional deformation in this area may be related to changes in motions across the highly sheared boundaries between the Africa and South American plates.

- The interpretation of basement thrust faults in the area are indicative of compression within oceanic crust. Their origin is understood as owing to numerous thrust sheets in the crust. The investigation of the fine structure of the oceanic crust revealed some crustal scale accretionary forms that may be due to tectonic compression during the late stage of the Atlantic opening.

- The crustal basement includes structures of tectonic compression that slightly affects the overlying sediment cover.

- The crustal topography in the deepwater west Niger delta is thought to have been formed by tectonic movements of different directions and amplitude owing to volcanic activities. These movements are

important in the formation of transform fracture zones and anomalous

crustal features at both the mid Atlantic ridge and deep basins.

6.2.3 Results from the role of multiple detachment levels in the fold belts (Chapter 5)

Chapter 5 presents an analysis of folds styles in the deepwater west Niger

Delta. The research effort here was focused on the linking the fold style to the

level of the detachment onto which they detach in the stratigraphy. This was

achieved with the application of 3 independent approach that includes the

adoption of the displacement-distance method that was developed by

Muraoka and Kamata (1983) and Williams and Chapman (1983), regional

mapping to subdivide the stratigraphy and within this constrained

stratigraphy, locate the position of the detachments from a critical analysis of

the reflection patterns at the sole of the thrust fault.

- The result obtained from the displacement-distance measurement
  revealed that the faults from zone A are characterised by a distinct
  peak in the displacement values some distance away from the likely
  position of the detachment. This is a deviation of the characteristics
  curve obtained for displacement-distance profiles in zone B which
  shows a steadily increasing pattern of displacement.

- Results of the study indicate that multiple detachment play a major
  role in the evolution of a thrust system, in response to the great
  importance of mechanical stratigraphy. The most important result of
  chapter 5 is that different detachment levels produce different sets of
  structures, with different size, deformation history and importance. In
  zone A, the presence of the upper (Dahomey) detachment is

synonymous with the development of thrusted detachment fold, while

zone B is characterised by the growth of thrust propagation fold

evolving from the relatively lower Akata detachment level.

- These two structures can easily be distinguished by their characteristic displacement-distance profiles.

6.3 Cretaceous to Recent tectono-stratigraphic evolution of the Deepwater West Niger Delta

In the absence of direct stratigraphic controls from well data, the stratigraphy

of the deepwater west Niger delta margin has been analysed tectono-

stratigraphically i.e. in terms of major sequences. It should be noted here that

the author does not view this approach as an alternative to seismic

stratigraphy or sequence analysis but rather as an essential framework

builder.

6.3.1 A tectonic model for the Deepwater west Niger delta
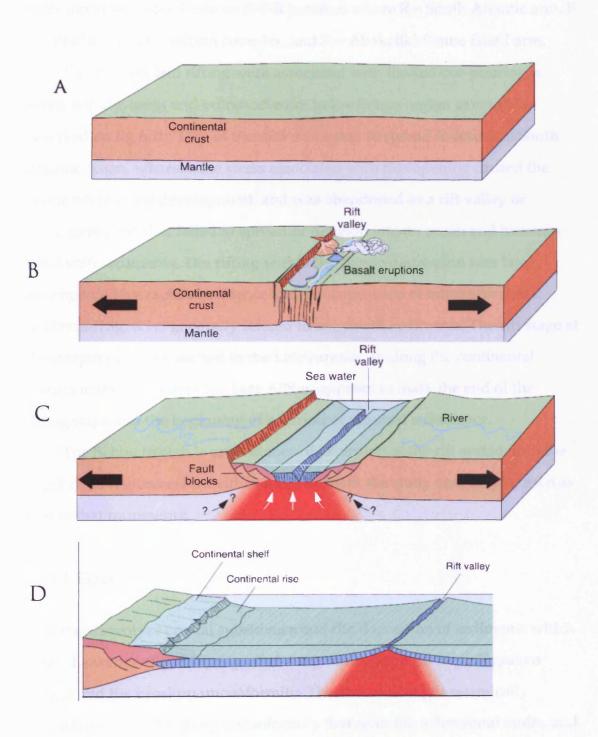
Reconstructions and development of the Gulf of Guinea margin has been

given by several authors (e.g. Burke et al. 1971; Emery et al., 1975; Whiteman,

1982). A tectonic model involving the rise and cessation of mantle plumes is

proposed for the study area. The mantle plume concept was first defined by

Wilson, 1965 and enlarged by Morgan, 1971, Wilson, 1973 and was also

applied to the plume –generated triple-plate junctions (Burke and Dewey,

1973). As continental spliting may be the response of a continental lithosphere

to the development of a hot region (leading to upwelling) in the underlying

upper mantle at periods when it is subjected to widespread tension. In the

following section, the evolution of the delta would be described based on the

grouping of events as stages. The evolutive stages starts with an initial one which shows the continental crust and the mantle (fig. 6a).

6.3.1.1. Stage 1

The initial stage in the evolution of the study area involved persistent tensional stresses in the continental lithosphere (fig. 6.1b) caused by the trench suction force acting on opposite sides of a continental plate rather than by uplift (Bott, 1982), and the rise of a mantle plume beneath the stretched continental lithosphere as a result of local convective upwelling of mantle material causing crustal doming. The overlying part of the lithosphere thins possibly as a result of penetration of magma followed by wholesale foundering of blocks of cool lithosphere as hot asthenosphere material upwells to replace it. The lithospheric thinning and weakening causes increased tension above the hotspot, leading to rifting and possible dyke intrusion and possible eruption of basalt.

6.3.1.2. Stage 2

This increased tension thus results in rifting (faulting) (fig. 6.1c) and the subsequent development of a rift-rift-rift (rrr) triple plate junction which involves the Abakaliki-Benue arm, the Gulf of Guinea arm and the South Atlantic arm during Aptian to early Albian times. This has previously been described in Burke et al., 1971; Grant, 1971b; Burke and Whiteman, 1973; Petters and Ekweozor, 1982; Whiteman, 1982; Ofoegbu, 1984. The Gulf of Guinea arm later evolved into a complex long ridge-ridge transform arm while the South Atlantic arm evolved as a short ridge-ridge transform. The Abakaliki-Benue arm opened slightly and then closed during the Santonian (Burke et al., 1971; Whiteman, 1982). Later during the Cretaceous, the R-R-R

A

B

C

D

Figure 6.1: A simplified model describing the initial phases in the evolution of the study area. (A) Shows the initial stage before the development of the evolution. (B) The continent undergoes extension. Here the crust is thinned and a rift valley forms continental separation, as the continent edges are faulted and uplifted basalt erupts from the ocean crust. (C) This shows the development of rifts due to the upwelling of mantle materials (D) shows a wider coverage of the evolution and how it develops into continental and oceanic segments.

triple junction evolved into an R-F-R junction where R = South Atlantic arm, F = Gulf of Guinea transform complex, and R = Abakaliki-Benue failed arm.

The doming and rifting were associated with limited out-pouring of alkaline-mafic lavas and volcanoclastics in the Benue region as could be observed on fig 6.1b. Two of the rifts continued to spread to form the South Atlantic ocean, whereas the stress associated with this opening caused the Benue rift to cease development, and was abandoned as a rift valley or aulocogen; a rift that failed to spread or develop into an ocean and becomes filled with sediments. The rifting within the Benue depression was later accompanied by rapid subsidence and the deposition of immature clastic sediments (fig. 6.1c) generally refered to as syn-rift sediments. The rift stage at the margin probably started in the Late Jurassic as along the continental margin in the study area the Late Albian appears to mark the end of the rifting stage and the beginning of a period of regional subsidence.

The Benue trough is an evidence of extension of the rift system into the Niger delta region and the rift element beneath the study area may be seen as part of that framework.

6.3.1.3. Stage 3

This stage involves crustal subsidence and the deposition of sediments which formed a wedge (fig. 6.1c) as part of a sag basin, between the half graben system and the breakup unconformity. The end of rifting is seismically characterised by a breakup unconformity that seals the extensional faults, and with packages of sub-parallel reflectors within the basement as has been elaborately studied in chapters 3 and 4. This unconformity is in places angular and commonly found at the top of the rift sequence and at the base of the transition –early drift sequence. This uncorformity is clearly visible between

the syn-rift fill of the half-graben form rift elements and the post-rift
succession.

The unconformity has cut down into the syn-rift fill and records the
denudation of footwall crests, thus indicating some erosion of the already
thinned crust due to rifting as was described in chapter 3, so it also possible to
include at this juncture that this process of erosion also contributed to the
reduced thickness of the crust as observed in the study.

The beginning of the drift-related sequence may be correlatable with the
time of cessation of rifting, uplift and truncation of rift sediment, contractive
collapse of continental crust and the onset of seafloor spreading; drifting is
therefore as old as the oldest magnetic anomaly (Austin and Uchupi, 1982).
However, this stage has been ascribed to a pre-Mid Aptian age in the study.
There is evidence of a a pre-Mid Aptian syn-rift /post rift succession
preserved within the framework of the NE-SW and WNW-ESE trending half-
graben structure (fig. 6.2). This older sediments are presumed to be Albian to
Palaeogene in age as a Late Aptian to Late Albian age has been given for the
onset of continental separation in the Gulf of Guinea (Gradstein et al., 1995;
Wagner and Pletsch, 1999; Macgregor et al., 2003; Morgan, 2003). However,
the syn-rift sequence of the nearby Ise Formationin in the Benin section of the
Dahomey Trough has been dated as Barriasian-Hauterivian (Morgan, 2004).

Late drift sequences are deposited in the study area during the
development of the ocean and continued to widen by seafloor spreading.
Subsidence in the delta was caused by decaying crustal thermal contraction
and sediment loading integrated with variable sediment supply, local tectonic
activity and cyclic eustatic rises and falls.

The drift related sedimentary wedge constitute the upper Aptian to
Recent marine megasequences as imaged on figure 6.2. The existence of this
wedge preserved in the half-graben rift element is evident from this study
where sections in excess of 1km thick are observed.
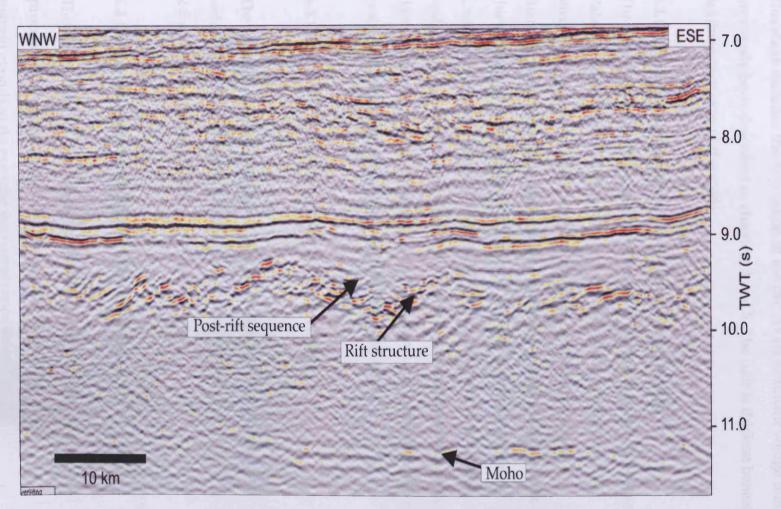
Figure 6.2: A WNW-ESE oriented seismic section showing examples of basement and the deposition of syn-rift and post-rift sediements.

6.3.1.4 Stage 4

This stage includes the deposition of the pre-Akata sediment wedge that has previously been described in chapters 4 and 5. The unit is thickest beneath the northwestern area of the study.

6.3.1.4.1 Marine transgression-Pre Akata sediment wedge

The pre-Akata sediment wedge is believed to represent a Late Cretaceous to Palaeogene section and sits over the pre-Mid Aptian syn-rift/post rift succession preserved in the rift element. The top of this formation is characterised as a major onlap surface, marking the onset of deposition of a thick section of hemipelagic mud above a sediment apron of presumed Upper Cretaceous–Paleogene age (Morgan, 2003). The existence of older sediments underlying the Akata Formation in the study is very evident on the seismic data where sediment in excess of 1 km in thickness are seen preserved in half-graben rift elements and overlain by this large sediment .

6.3.1.5 Stage 5: Palaeocene-Eocene Akata Deposition

The Akata Formation (see fig. 6.3) onlaps the older progradational pre-Akata sediment package described above has elaborately been described in chapters 2-5 and would not be described any further here.

6.4 Cretaceous compression/ reactivation and control of delta sedimentation
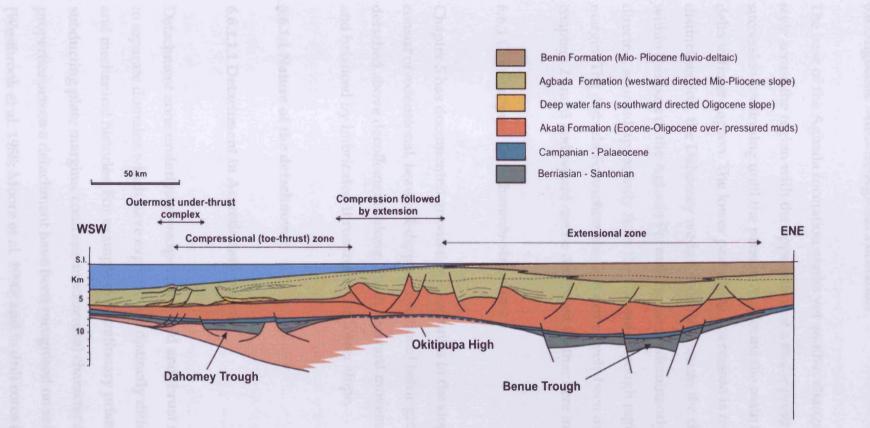
This thesis shows a very strong evidence of compression during the formation process of the margin, however, the general evolutionary models for passive margin evolution do not take into cognizance the effect of post-rift compression as is described in chapter 4. This has not previously been introduced in the study area and is only being recently observed with the

availability of seismic data over the area as a result of increased petroleum exploration.

Other compression –Paleocene/Eocene/Recent

A key hypothesis in the Niger Delta is that the stratigraphic succession and reservoir, seal and source distribution are controlled by the paleo-structural evolution of the delta. Basement architecture in the oceanic crust, related mostly to transform faults, had a strong influence on the early sedimentation in the delta. The Niger Delta (fig. 6.3) began developing in Eocene time, and by Oligocene-Miocene time updip detached extension was driving down dip contraction in a linked structural system; tear faults form part of the linkage where differential movement in the delta occurs. While the early, detached structures are not basement involved, the pre-existing basement features had a strong influence on where subsequent structures and related sub-basins formed. A key example is the Charcot Fracture zone described in chapter 4, which splits the delta into two distinct lobes (Mann et al. 2005) and could also control the structural distribution pattern in the area but this could not be confirmed as it is outside the scope of the present study.

The linked extension and contraction set up an evolving paleo-topography in the basin. This evolving structural deformation (mainly folds and thrusts) was the controlling factor in the stratigraphic succession in the delta, influencing the evolution of the toe of slope, basin floor, slope channels and shelf margin depositional systems. This paleo-topography also influenced source deposition. Knowledge of the timing and distribution of these structurally influenced stratigraphic systems provides important insights into the paleogeography of the basin and into understanding play elements across the delta.

Figure 6.3. A regional scale cross section showing the structural and stratigraphic subdivision of the Niger Delta. In terms of the structure it shows the variations in structural styles from the extensional to the compressional zones. The litho-stratigraphic distributions of the different formations are clearly observed. Note that the topmost Benin Formation disappears downslope. Overpressure in the Akata Formation has rendered the Akata structurally weak and the entire sediment cone has collapsed on intra-Akata detachment faults creating extensional, faulted-diapiric and compressional belt within the region (From Morgan, 2004).

6.6 Oligocene Miocene-Agbada Formation

The base of the Agbada formation marks yet another change in depositional style across the region with the appearance of a major progradational succession continuing until the present and forms the main body of the Niger delta sediment apron. The lower part of this succession is represented by a distinct section, the Dahomey wedge, so called beause the channel complexes within this part of the Agbada Formation are predominantly southwards directed, sourced apparently from the Dahomey trough region of the Nigeria margin. The Agbada Formation also has extensively been described in chapters 2 and 5 and would not be described further here in this chapter.

6.6.1 Gravitational Detachments-structures

Chapter 5 has documented gravitational tectonics in the slope area. The delta consist of extensional, seaward-dipping rotational listric growth faults, detached above decollements along which seaward movement is transferred and balanced by imbricated thrusting in the lower slope.

6.6.1.1 Nature of the detachment

6.6.1.1.1 Detachment in Accretionary prisms

Detachment zone underlying wedge shape fold and thrust systems are known to separate domains which have experienced distinctly different structural and mechanical histories. For example in accretionary prism along actively subducting plate margins, contrasts in structural character and physical properties across a detachment have been recognised on seismic profile (Westbrook et al. 1988; Moore et al. 1990) and in drill cores (Taira et al. 1991).

In the modern detachment zone at the toe of the Northern Barbados accretionary prism, deformation is apparently localised at a single stratigraphic interval characterised by low density relative to the surrounding sediments and abundant radiolarian microfossils (Wallace et al. 2003). The detachment zone is defined on seismic reflection data by a reflector separating the thrust faulted accretionary prism from the less underthrust sedimentary sequence (Wallace et al. 2003). Subtle reflector truncations in the underthrust sequence at the detachment zone may be interpreted as locations where the detachment zone has delocalised (Zhao et al. 1998).

In addition, studies from the Barbados ridge accretionary complex indicate that the detachment zone is heterogeneous and is characterised by localised fluid flow and compartmentalisation (Gieskes et al. 1990; Shipley et al. 1997; Moore et al. 1995; Bangs et al. 1999). The heterogeneity of the zone gives rise to very different seismic responses that have been associated with fluid distribution (Shipley et al. 1994; Bang et al. 1996, 1999).

6.6.1.1.2 Seismic Character of detachment zones in accretionary wedges

Though most interest in detachment have been related to their behaviour as mechanical boundary, detachment zones themselves have complex and enigmatic characteristic that relates to their history as well as their role in accretionary setting. Seismic observations of detachments provide clues as to how they initiate, evolve and respond to hydrologic perturbation.

6.6.1.1.2.1 Seismic character of the detachment

Seismic profiles from the Nankai and Barbados prism portray the detachment as zones of high amplitude, reverse polarity reflections (Bangs et al. 1990; Moore et al. 1990). These reflections have been modelled as zones with low

velocity and/or density (Bangs & Westbrook, 1991; Moore & Shipley, 1993). Lateral variations in reflector amplitude both along and across strike are interpreted as resulting from lateral changes in velocity, density and thickness of the detachment and are surmised to reflect transient pore pressure fluctuation (Bangs & Westbrook, 1991, Moore & Shipley, 1993; Shipley et al. 1994).

6.6.1.1.3 Drill core character of the detachment in accretionary wedges

Information from drilling detachment zone at the Barbados and Nankai margins shows that they are characterised by distinctive structure, geochemistry and physical properties (Taira et al. 1991). They show thick zones of lightly fractures and sheared mudstone. Although it is revealed from seismic that the detachment zones show relatively high porosities, the drill cores suggest reduced sediment porosity in this zone. Also acoustic measurements on discrete samples yielded anomalously high velocities consistent with their reduced porosities (Taira et al. 1991). Detachment zones have higher permeability than the bounding domains, because of the many fractures in the scaly clays comprising these zones (Moore, 1989). High permeability are thought to be associated with anomalously high pore pressure and fluid flow as implied by geochemical and thermal anomalies correlated with the detachment zone (Gieskes et al. 1990; Kastner et al. 1993). Though they have been found to have high bulk porosities from seismic due to intense fracturing and high pore pressures (Bangs et al. 1990; Moore et al. 1990) they have been found to show significantly lower porosities than the sediment encasing them (Taira et al. 1991).

Conclusion

Interaction between upper lithosphere deformation as manifested in the structure and evolution of the Niger delta basin, and the lower lithospheric deformation presumably reflect large-scale regional or global tectonic events. This thesis has reviewed the current state of knowledge regarding these interactions and suggest areas of research which may lead to an improvement in this knowledge.

Chapter Seven: Conclusions

This chapter presents the principal conclusions of this PhD thesis and presents suggestions for future research on the structural evolution of the deepwater west Niger Delta margin. The interpretation of 2D and 3D seismic reflection data complimented with gravity data have been used in this PhD research to investigate the structural evolution of the deepwater west Niger delta passive margin. The investigations undertaken have produced detailed observations and deductions with regards to diverse aspects of the structural evolution of the west Niger delta and generally on the Niger Delta margin. Furthermore insights of the effect of the change in the pole of rotation during the Santonian time have been provided by this research. The results obtained should be of applicability to other passive margin fold and thrust belts and to other sedimentary basins worldwide. The primary conclusions for this PhD research study and the specific conclusions that can be drawn from each of the previous chapters are summarised below.

7.1 General conclusions

This PhD study documents how 3D and 2D seismic data analysis coupled with gravity data can help improve our knowledge of structural and tectonic processes active during the evolution of the deepwater west Niger Delta basin.

The 3D seismic interpretation has proved to be a powerful tool when analysing the structural configuration of basement faults. The availability of a three-dimensional understanding of the interaction of crustal-scale faults has been

critical to evaluating the triggering mechanism of the anomalous basement structures.

7.2. Crustal structure from the interpretation of seismic reflection data

➤ The abnormally thin igneous crust within the study area is one of the most striking results of this study. More than 90% of the study area is below the global thickness of 7.08 km for a normal oceanic crust (White et al. 1992) but within published values for the Atlantic Ocean normal oceanic crust (Rosendahl and Groschel-Becker, 1999). The anomalously thin oceanic crusts away from the major fracture zone (Chain FZ) can be attributed to three main settings; at very slow spreading ridges (White et al. 1984; Minshull et al. 1991), adjacent to non-volcanic continental rifted margins and at fracture zones (White et al. 1992).

➤ 2D and 3D seismic reflection data interpretation of the deepwater west Niger Delta has demonstrated the existence of normal oceanic crust in the area. This is revealed from the thickness map of the crust (Fig 3.9) which shows that the crust here is between 5.0 and 8.3 km.

➤ The Chain Fracture zone earlier interpreted as Continent-Ocean Fracture zone by Davies et al. (2005) is in fact an Ocean-Ocean fracture zone similar to those observed in the North Atlantic (Rabinowitz and LaBrecque, 1979; Muller and Roest, 1992). This study has also shown that there is no significant difference in the crustal thickness across the fracture zone as the crust on opposite side of the transform is made up of about 5-7 km

thick oceanic crust and this is supported by the pervasive tectonic spreading fabric observed on the north across the Chain fracture zone.

➢ Tectonic spreading fabric terminating at the Chain Fracture zone is clearly diagnostic of a normal oceanic crust. Subsurface scoop-like forms of faults terminating at the Chain fracture zone are generally observable at ocean-ocean fracture zones (Searle and Laughton, 1977)

➢ The Moho (horizon M) here acts as a detachment surface for some of the listric intracrustal faults in the study area.

➢ Volcanoes are erupted at the ancient seafloor during the accretion of the crust and the subsequent development of tectonic spreading fabrics.

➢ The development of the anomalous thrust structure here may be related to the change in the pole of rotation during the Santonian.

➢ The crust in the study could be divided into 2 layers based on seismic characteristic of the packages within major regional reflectors.

➢ The Moho reflection in the study area shows a variable reflection pattern, as they are present in some areas and being absent in others. This may be attributable to either variation in lateral composition.

7.3. Thrusting at Oceanic crust as observed from seismic data

➤ Normal faults seen as tectonic spreading fabric due to accretion of the oceanic crust and trend northwest-southeast, and compressional faults with a northeast-southwest orientation that formed later are the two distinct structural styles that have been identified in the basement.

➤ There are two-scales of thrust fault that have been identified, several folds with wavelength of a few kilometres and one much larger structure which is 60 kilometres wide.

➤ In the case of the small-scale thrusts there is evidence of thrust faults cross-cutting the entire oceanic crust, possibly soling-out near to the Moho interpreted as reflection 1 in the study.

➤ The moderate quality of the seismic reflection data over the Charcot Ridge means that the detailed interpretation of this structure is problematic. Our preferred interpretation is that it represents a major crustal scale thrust, which has a thin-skinned, origin, again with the soling-out of the main thrust occurring near the Moho. This would be best described with availability of 3D seismic reflection data over the structure.

➤ The Charcot ridge forms a major structural high that splits the Niger Delta into western and southern lobes. It probably formed due to the thrusting of oceanic crust to the north of the Charcot Fracture zone over crust to the south of it.

➤ The Charcot structure also represents one of the largest oceanic compressional structures ever observed at a passive margin.

➢ Very approximate age dating based upon the long range seismic correlations of others indicates that the compressional phase is of Cretaceous age. It may be equivalent to the Santonian event, and caused by a change in spreading direction during continental drift.

7.4. Multiple detachments

➢ The study has shown that in the deepwater fold and thrust belt of the Niger Delta there is a strong dependence of structural style on the thickness and lithology of the detachment unit.

➢ In Zone A, folds formed in response to ductile deformation of the inherently weak Dahomey wedge, which was susceptible to flow due to the regional overpressure developed at or around the top of the Akata Formation and shown from the greater amount of shortening that could be due to lithologic changes. In Zone B, the folds are more clearly linked to thrust propagation.

➢ The study has shown that two distinct structural patterns are possible within the deepwater west Niger Delta. They are the thrusted detachment folds in Zone A and the thrust propagation folds in Zone B.

➢ The two structural styles can be distinguished on the basis of markedly contrasting displacement-distance plots (Fig 5.13). More symmetrical displacement patterns with a discrete maximum in the mid-ramp position

are found for all the thrusts in Zone A associated with detachment folds, whereas the thrust propagation folds are associated with a downward increasing pattern of displacement towards the detachment.

7.5. Tectonic evolution

Generally, the expectations are that this research will go a long way towards resolving many of the questions expressed or implied herein, and undoubtedly raise a host of new issues to guide future research on the architecture and evolution of this segment of the South Atlantic passive margin.

7.6 Future Research

As could be expected, this research has gone a long way towards resolving some of the questions expressed at the beginning of the research and has undoubtedly raised a host of new issues to guide future research on the structural evolution of the Niger Delta in particular and the architecture and evolution of the south Atlantic passive margin.

The work presented in this thesis opens up new possibilities for the research and understanding of the structural evolution of the deepwater Niger Delta. The first step which should precede any investigation on a specific area is to achieve a good understanding of the fundamental structural framework. Although this thesis has focused on large scale structures, a more detailed and focused research in the area is required. This should include.

1. Collection of detailed biostratigraphic information from future exploration wells in the research area is necessary for a better definition of the age of specific reflectors in the area.

2. Since the data is in time, true velocity information is necessary in order to properly depth convert the seismic sections and the faults.

3. Application of 2D progressive restoration to actually define the sequence of evolution combined with their growth package analysis over the Charcot ridge using 2DMove would also be important.

4. Construction and progressive restoration in 2D and 3D of the contractional fold belt systems (from detailed 2D seismic data and incorporating more 3D seismic data).

5. Further quantitative analysis of the contractional detachment fold systems is necessary to determine their 3D tectonic evolution as well as the mechanisms of detachment folds initiation and growth (fold amplification).

6. Thermal and mechanical numerical modelling of the progressive evolution of the passive margin of the west Niger Delta Basin. This should in particular analyse the effects of differential sediment loading on the isostatic and flexural uplift and subsidence of the passive margin basin.

7. Quantitative hydrocarbon modelling combined with source rock analyses in order to evaluate the hydrocarbon systems and their evolution along this part of the west Niger Delta margin.

8. In addition, this study should be extended to the east/south deepwater Niger Delta and the JDZ (Joint Development Zone) fold and thrust belts to test the model of thrust propagations vs. thrusted detachment folding.

9. Further studies should also be aimed at investigating the role of coupling if any between the basement and later deformation/evolution of the Niger Delta.

References

Adeogba, A.A., McHargue, T.R., Graham, S.A. 2005. Transient fan architecture and depositional controls from near-surface 3-D seismic data, Niger Delta continental slope. *AAPG Bull.*, **89** (5), pp. 627-643.

Ajakaiye, D.E and Bally, A.W. 2002. Some structural styles on reflection profiles from offshore Niger Delta. *Search and Discovery*, **10031**, pp. 1-6.

Ajakaiye, D.E and Bally, A.W. 2002a. Course manual and atlas of structural styles of reflection profiles from Niger Delta. *AAPG Continuing Education Course Note Series* **41**, pp. 1-107.

Allmendinger, R.W. 1998. Inverse and forward numerical modeling of trishear fault-propagation folds. *Tectonics* **17**, pp. 640–656.

Austin, J.A.Jr and Uchupi, E., 1982. Continental-oceanic crustal transition off Southwest Africa. *AAPG Bull.*, **66**, pp. 1328–1347.

Auzende, J.M., Cannat, M., Gente, P., Henriet, J.P., Juteau, T., Karson, J., Lagabrielle, Y., Mevel, C., Tivey, M., 1994. Observations of sections of oceanic crust and mantle cropping out on the southern wall of Kane FZ (N. Atlantic). Terra Nova, **6**, pp. 143-148.

Avbovbo, A.A 1978. Tertiary lithostratigraphy of the Niger Delta. *AAPG Bulletin* **62**(2), pp. 295-306.

Avbovbo, A. A., Ayoola, E. O., and Osahon, G. A., 1986. Depositional and structural styles in Chad Basin of northeast Nigeria. *AAPG Bulletin* **70**(12), pp. 1787-1798.

Babalola, O.O. 1985. Crustal structure and tectonic development of Gulf of Guinea Cul-de-Sac from integrated interpretation of new aeromagnetic and existing geophysical data (abstract). *AAPG Bull.*, **69**, p.235.

Bangs, N and Westbrook, G. K. 1991. Seismic modelling of the décollement zone at the base of Barbados accretionary complex. *Journal of Geophysical Research* **96**, pp. 3853-3866.

Bangs, N. L., Westbrook, G. K., Ladd, J. W and Buhl, P. 1990. Seismic velocities from the Barbados Ridge Complex: Indicators of high pore fluid pressures in an accretionary complex. *Journal of Geophysical Research* **95**, pp. 8767-8782.

Bangs, N. L., Shipley, T. H and Moore, G.F. 1996. Elevated fluid pressure and fault zone dilation inferred from seismic models of the northern Barbados Ridge décollement. *Journal of Geophysical Research* **101**, pp. 627-642.

Bangs, N. L., Shipley, T. H., Moore, J. C and Moore, G. 1999. Fluid accumulations and channeling along the Northern Barbados Ridge décollement thrust. *Journal of Geophysical Research* **104**, p. 20,399-20,414.

Barth, G., Kastens, K.A., Klein, E.M., 1994. The origin of bathymetric highs at ridge transform intersections: A multi-disciplinary case study at the Clipperton Fracture Zone. Marine Geophysical Researches **16**, pp. 1-50.

Bassetto, M., Alkmim, F.F., Szatmari, P and Mohriak, W.U. 2000. The oceanic segment of the southern Brazilian margin: Morpho-Structural domains and their tectonic significance, in *Atlantic rifts and continental margins*, edited by W.U. Mohriak and M. Talwani, *AGU Geophysical Monograph* **115**, pp. 235-259.

Benkhelil, J. Mascle, J and Guiraud, M. 1998. Sedimentary and structural characteristics of the Cretaceous along the Cote D'Ivoire-Ghana transform margin and in the Benue trough: A comparison, in: Mascle. J., Lohmann, G.P., Moullade, M. (Eds.), *Proceedings of the Ocean Drilling Program, Scientific Results* **159**, pp. 93-99.

Bilotti, F.D and Shaw, J.H. 2001. Modelling the compressive toe of the Niger Delta as a critical taper wedge (abs.). *AAPG* Annu. Meeting Program 10, pp. A18-A19.

Bilotti, F.D and Shaw, J.H. 2005. Deepwater Niger Delta fold and thrust belt modelled as a critical-taper wedge: the influence of elevated of elevated basal fluid pressure on structural styles. *AAPG Bulletin* **89**, pp. 1475-1491.

Bilotti, F., Shaw, J.H., Cupich, R.M and Lakings, R.M. 2005. Detachment fold, Niger Delta. In: Seismic Interpretation of Contractional Fault-Related Folds (Ed. J.H. Shaw, C. Connors & J. Suppe), An *AAPG Seismic Atlas, Studies in Geology* **53**, pp.103-104.

Binks, R.M and Fairhead, J.D. 1992. A plate tectonic setting for Mesozoic rifts of West and Central Africa. *Tectonophysics* **213**, pp. 141-151.

Boldreel, L.O and Andersen, M.S. 1993. Late Paleocene to Miocene compression in the Faeroe-Rockall area, Petroleum Geology of Northwest Europe: Proceedings of the 4th conference, pp. 1025-1034

Bonatti, E. 1978. Vertical tectonism in oceanic Fracture zones. *Earth and Planetary Science Letters* **37**, pp. 369-379.

Bonatti, E and Chermak, A. 1981. Formerly emerging crustal blocks in the Equatorial Atlantic. *Tectonophysics* **72**, pp. 165-180.

Bonatti, E and Crane, K. 1982. Oscillatory spreading explanation of anomalously old uplifted crust near oceanic transforms. *Nature* **300**, pp. 343-345.

Bonatti, E., M. Ligi, L. Gasperini, A. Peyve, Y. Raznitsin, and Y.J. Chen (1994), Transform migration and vertical tectonics at the Romanche fracture zone, Equatorial Atlantic, *Journal of Geophysical Research* **99**, pp. 21779-21802.

Bonneville, A and McNutt, M. 1992. Shear strength of the great Pacific fracture zones, *Journal of Geophysical Research* **19**, pp. 2023-2026.

Bosworth, W. 1992. Mesozoic and early Tertiary rift tectonics in east Africa, *Tectonophysics* **209**, pp. 115–137.

Bott, M.H.P. 1982. The interior of the Earth: Its structure, constitution and evolution, 2nd. Ed. Edward Arnold, London. 493 pp.

Brever, J.A and Oliver, J.E. 1980. Seismic reflections studies of deep crustal structures. *Annual Reviews of Earth and Planetary Sciences* **8**, pp. 205-230.

Briggs, S.E., Davies, R.J., Cartwright, J., Morgan, R., (submitted). Seismic evidence for crustal-scale thrusts in oceanic crust offshore Niger delta, Equatorial Africa. *Tectonics.*

Briggs, S.E., Davies, R.J. Cartwright, J and Morgan, R. (in review). Crustal structure of the deepwater west Niger Delta passive margin from the interpretation of seismic reflection data. *Marine and Petroleum Geology*

Briggs, S.E., Davies, R.J., Cartwright, J and Morgan, R. 2006. Multiple detachment levels and their control on fold styles in the compressional

domain of the deepwater west Niger Delta. *Basin Research* **18**, pp. 435-450.

Brown, L.F.Jr. and Fisher, W.L. 1977. Seismic interpretation of depositional systems, in: Payton C.E. (Ed.), Seismic Stratigraphy—applications to hydrocarbon exploration. *AAPG Memoir* **26**, pp. 213-248.

Bruce, C.H. 1973. Pressured shale and related sediment deformation: mechanism for development of regional contemporaneous faults. *AAPG Bulletin* **57**, pp. 878-886.

Bull, J.M. 1990. Structural style of intra-plate deformation, Central Indian Ocean Basin: evidence for the role of fracture zones. *Tectonophysics* **184**, pp. 213-228.

Bull, J.M and Scrutton, R.A. 1990. Fault reactivation in the Central Indian Ocean basin and the rheology of the oceanic lithosphere. *Nature* **344**, pp. 855-858.

Bull, J.M and Scrutton, R.A 1992. Seismic reflection images of intraplate deformation, central Indian Ocean, and their tectonic significant. *Journal of the Geological Society, London* v.**149**, pp. 955-966.

Burke, K. 1972. Longshore Drift, Submarine Canyons and Submarine Fans in development of Niger Delta. *AAPG Bulletin* **56**(10), pp. 1975-1983.

Burke, K. 2001. Origin of the Cameroon Line of Volcano-Capped Swells, *Journal of Geology* **109**, pp. 349-362.

Burke, K.C and Dewey, J.F. 1973. Plumes generated triple junctions: key indicators in applying plate tectonics to old rocks. *J. Geol.* **81**, pp. 406-443.

Burke, K., Dessauvagie, T.F.J and Whiteman, A.J. 1971. Opening of the Gulf of Guinea and geological history of the Benue depression and Niger Delta. *Nature Physical Science* **233**, pp. 51-55.

Burke, K.C and Whiteman, A.J. 1973. Uplift, rifting and the breakup of Africa. In Tarling and Runcorn (Eds): Implications of Continental Drift to the Earth Sciences, pp. 735-755, Academic Press, London.

Byerlee, J. 1993. Model for episodic flow of high-pressure water in fault zone before earthquakes. *Geology* **21**, pp. 303-306.

Castro Jr., A.C.M. 1987. The northeastern Brazil and Gabon Basins: a double rifting system associated with multiple crustal detachment surfaces. *Tectonics* **6**(6), pp. 727-738.

Chapin, M., Shipp, C and Winker, C. 2002. Bonga field, deep water Nigeria: Comparison of near surface, well calibrated submarine channels with reservoir channel sands, paper presented at the AAPG Annual Meeting, Houston, Texas, 10-13 March.

Christensen, N.I and Salisbury, M.H. 1975. Structure and composition of the lower Oceanic crust. *Review of Geophysics* **13**, pp. 57-86.

Clemson, J. 1997. Segmentation of the Namibian passive margin. Unpubublished PhD Thesis, University of London (Imperial College of Science, Technology and Medicine), 347 pp.

Cloos, E. 1961. Bedding slip, wedges and folding in layered sequences. *Société Géologique de Finlande*, Extrait des Comptes Rendus **33**, pp. 106-122.

Cobbold, P.R., Meisling, K and Mount, V.S. 2001. Reactivation of an obliquely rifted margin, Campos and Santos basins, southeastern Brazil, *AAPG Bulletin* **85**, pp. 1925-1944.

Cobbold, P.R., Szatmari, P., Santiago Demercian, L., Coelho, D and Rossello, E. A. 1995. Seismic and experimental evidence for thin-skinned horizontal shortening by convergent radial gliding on evaporites, deep-water Santos Basin, Brazil, *in* M. P. A. Jackson, D. G. Roberts, and S. Snelson, eds., Salt tectonics: a global perspective. *AAPG Memoir* **65**, pp. 305-321.

Cobbold, P.R., Mourgues, R and Boyd, K. 2004. Mechanism of thin-skinned detachment in the Amazon Fan: assessing the importance of fluid overpressure and hydrocarbon generation. *Marine and Petroleum Geology* **21**, pp. 1013-1025.

Cohen, H. A and McClay, K. 1996. Sedimentation and shale tectonics of the northwestern Niger Delta front. *Marine and Petroleum Geology* **13**, pp. 313- 328.

Collier, J.S., Danobeitia, J.J., Canales, J.P., Dalwood, R., Gadd, S., Hayward, N., Henstock, T.J., Krastel, S., Peirce, C., Watts, A. 1997. Evidence for

asymmetric accretion and low-angle, planar faults in slow-spreading oceanic crust. *Geology* **25**(12), pp. 1075-1078.

Connors, C.D., Denson, D.B., Kristiansen, G and Angstadt, D.M. 1998. Compressive anticlines of the mid-outer slope, Central Niger Delta (abs.). *AAPG Bulletin* **82**, p.1903.

Corredor, F., Shaw, J.H and Bilotti, F. 2005a. Structural styles in the deep-water fold and thrust belts of the Niger Delta. *AAPG Bulletin* **89**, pp. 753-780.

Corredor, F., Shaw, J.H and Suppe, J. 2005b. Shear fault-bend fold, deepwater Niger Delta. In: Seismic Interpretation of Contractional Fault-Related Folds (Ed. by J.H. Shaw, C. Connors & J. Suppe), *AAPG Studies in Geology* **53**, pp. 87-95.

Coward, M.P., Purdy, E.G., Ries, A.C and Smith, D.G. 1999. The distribution of petroleum reserves in basins of the South Atlantic margins. In: In: The Oil and Gas habitatats of the South Atlantic (Ed. N.R. Cameron, R.H. Bates & V.S. Clure), *Geological Society Special Publication* **153**, pp. 101-131.

Cramez, C and Jackson, M.P.A. 2000. Superposed deformation straddling the continental-oceanic transition in deep-water Angola. *Marine and Petroleum Geology* **17**, pp. 1095– 1109.

Dailly, G.C. 1976. A possible mechanism relating progradation, growth faulting, clay diapirism and overthrusting in the regressive sequence of sediments. *Bulletin of Canadian Petroleum Geology* **24**, pp. 92-116.

Dailly, P. (2000), Tectonic and stratigraphic development of the Rio Muni Basin, Equatorial Guinea: The role of transform zones in Atlantic Basin evolution, in *Atlantic rifts and continental margins,* edited by W. Mohriak, and M. Talwani, *American Geophysical Union Geophysical Monograph,* **115**, pp. 105–128.

Damuth, J.E 1994. Neogene gravity tectonics and depositional processes on the deep Niger Delta continental margins. *Marine and Petroleum Geology* **11**, pp. 321-346.

Davies, R.J. 2003. Kilometer- scale fluidization structures formed during early burial of a deep-water slope channel on the Niger Delta. *Geology* **31**(11), pp. 949-952.

Davies, R.J., Macleod, C.J., Morgan, R and Briggs, S.E. 2005. Termination of a fossil continent-ocean fracture zone imaged with three-dimensional seismic data: the Chain Fracture Zone, eastern equatorial Atlantic. *Geology* **33**(8), pp. 641-644.

Davis, D.M and Engelder, T. 1985. The role of salt in fold-and-thrust belts. *Tectonophysics* **119**, pp. 67-88.

Davis, G.H., and S.J. Reynolds (Eds.) (1996), *Structural Geology of Rocks and Regions*, 2nd ed., 776 pp., John Wiley & Sons, New York.

Davison, I. 1999. Tectonics and hydrocarbon distribution along the Brazilian South Atlantic margins. In: The Oil and Gas habitatats of the South Atlantic (Ed. N.R. Cameron, R.H. Bates & V.S. Clure), *Geological Society Special Publication* **153**, pp. 133-151.

De Matos, D. 2000. Tectonic evolution of the Equatorial South Atlantic. In: Atlantic Rifts and Continental Margins. (Ed. By W. Mohriak & M. Talwani), American Geophysical Union, Washington, DC. *Geophysical Monograph* **115**, pp. 331-354.

Delteil, J.R., Valery, P., Montadert, L., Fondeur, C., Patrait, P and Mascle, J. 1974. Continental margins in the northern part of the Gulf of Guinea. In: The Geology of Continental Margins (Ed. by C.A. Burk & C.L. Drake), pp. 297-311. Springer Verlag, New York.

Demercian, S., Szatmari, P and Cobbold, P.R. 1993. Style and pattern of salt diapirs due to thin-skinned gravitational gliding, Campos and Santos basins, offshore Brazil. *Tectonophysics* **228**, pp. 393–433.

Deptuck, M.E., Steffens, G.S., Barton, M.D and Pirmez, C. 2003. Architecture and evolution of upper fan channel belts on the Niger Delta slope and in the Arabian Sea. *Marine and Petroleum Geology 20*, pp. 649–676.

Dewey, J.F and Burke, K. 1974. Two plates in Africa during the Cretaceous? *Nature* **249**, pp. 313–316.

Dixon, J.M and Liu, S. 1992. Centrifuge modelling of the propagation of thrust faults. In: *Thrust Tectonics* (Ed. by K.R. McClay), pp.53-69. Chapman and Hall, London,

Doré, A.G and Lundin, E.R. 1996. Cenozoic compressional structures on the NE Atlantic margin: nature, origin and potential significance for hydrocarbon exploration. *Petroleum Geosciences* 2, pp. 299-311.

Doré, A.G., Lundin, E.R., Fichler, C and Olesen, O. 1997. Patterns of basement structure and reactivation along the NE Atlantic margin. *Journal of the Geological Society, London* 154, pp. 85–92.

Doust, H and Omatsola, E. 1990. Niger Delta: Divergent Passive Margin Basins, *AAPG Memoir* 48, pp. 201-238.

Duval, B.C., Cramez, C and Jackson, M.P.A. 1992. Raft tectonics in the Kwanza Basin, Angola: Geological Society of America, 1990 annual meeting symposium on Salt tectonics 9, pp. 389-404.

Eisenstadt, G and De Paor, D.G. 1987. Alternative model of thrust-fault propagation. *Geology* 15, pp. 630-633.

Ellis, M.A and Dunlap, W.J. 1988. Displacement variation along thrust faults: implications for the development of large faults. *Journal of Structural Geology* 10, pp.183-192.

Emery, K.O., Uchupi, E., Phillips, J., Brown, C and Mascle, J. 1975. Continental margins oɟ western Africa: Angola to Sierra Leone. *AAPG Bulletin* 59, pp. 2209-2265.

Erickson, S.G. 1996. Influence of mechanical stratigraphy on folding vs. faulting. *Journal of Structural Geology* 18, pp. 443-450.

Erslev, E.A. 1991. Trishear fault-propagation folding. *Geology* 19, pp. 617-620.

Evamy, B.D., Haremboure, J., Kamerling, P., Knaap, W.A., Malloy, F.A and Rowlands, P.H. 1978. Hydrocarbon habitat of Tertiary Niger Delta. *AAPG Bulletin* 62, pp. 1-39.

Fairhead, J.D. 1988. Mesozoic and Cenozoic plate tectonic reconstructions of the central South Atlantic Ocean: the role of the West and Central African Rift System. *Tectonophysics* 155, pp. 181-191.

Fairhead, J.D., 1988a. Late Mesozoic rifting in Africa, in: Manspeizer, W. (Ed.), Triassic-Jurassic Rifting-Continental Breakup and the origin of the Atlantic Ocean and Passive Margins. (Developments in Geotechnics, 22) Elsevier, Amsterdam, pp. 821-831.

Fairhead, J.D and Binks, R.M. 1991. Differential opening of the Central and South Atlantic Oceans and the opening of the West African rift system. *Tectonophysics* **187**, pp. 191-203.

Fairhead, J.D. and Okereke, C.S. 1987. A regional gravity study of the West African rift system in Nigeria and Cameron and its tectonic interpretation. *Tectonophysics* **143**, pp. 141-159.

Fairhead, J.D and Wilson, B.M. 2005. Plate tectonic processes in the South Atlantic Ocean: do we need deep mantle plumes?, in: Foulger, G.R., Natland, J.H., Presnall, D.C., Anderson, D.L. (Eds.), Plates, plumes and paradigms, *Geological Society of America Special Paper*, 388, Boulder, Colorado, USA: Geological Society of America, 537-553.

Fischer, M.P., Woodward, N.B and Mitchell, M.M. 1992. The kinematics of break-thrust folds. *Journal of Structural Geology* **14**, pp. 451-460.

Fornari, D.J., Gallo, D.G., Edwards, M.H., Madsen, J.A., Perfit, M.R., Shor, A.N., 1989. Structure and topography of the Siqueiros transform fault system: Evidence for the development of intra-transform spreading centres: *Marine Geophysical Researches*, **11**, pp. 263-299.

Frankl, E.J and Cordry E.A. 1967. The Niger Delta Oil Province: Recent Development Onshore and Offshore". 7th World Petroleum Proceedings, Vol. IB: Mexico City, Mexico.195 -209.

Frost, B.R. 1997. A Cretaceous Niger Delta Petroleum System, *in*, Extended Abstracts, AAPG/ABGP Hedberg Research Symposium, Petroleum Systems of the South Atlantic Margin, November 16-19, 1997, Rio de Janeiro, Brazil.

Genik, G.J. 1992. Regional framework, structural and petroleum aspects of rift basins in Niger, Chad, and the Central African Republic (C.A.R.). *Tectonophysics* **213**, pp. 169–185.

Gieskes, J.M., Vrokijk. P and Blanc, G. 1990, Hydrogeochemistry of the northern Barbados accretionary complex transect: Ocean Drilling Program Leg 110: Journal of Geophysical Research 95, pp. 8809–8818.

Gorini, M.A. 1981. The tectonic fabric of the Equatorial Atlantic and adjoining continental margins: Gulf of Guinea to Northeastern Brazil. In: Asmus, H.E. ed. *Estruturas e tectonismo da margem continental brasileira e suas*

implicações nos processos sedimentares e na avaliação do potencial de recursos minerais. Rio de Janeiro, PETROBRÁS, CENPES, DINTEP, pp. 11-116.

Gradstein, F.M., Agterberg, F.P., Ogg, J.G., Hardenbol, J., Van Veen, P., Thierry, J and Huang, Z. 1995. A Triassic, Jurassic and Cretaceous time scale. In: Geochronology, Time Scale and Global Stratigraphic Correlation (Ed. by W.A. Berggren, D.V. Kent, M.P. Aubrey and J. Hardenbol), *Special Publication Society of Econonic Palaeontologists and Mineralogists* **54**, pp. 95-126.

Grando, G. 2005. Growth fold systems in deepwater compressional fold and thrust belts. PhD thesis Royal Holloway University London, 481p.

Grant, N.K. 1971. A compilation of radiometric ages from Nigeria. *Journal of Mining and Geology* **6**, pp. 37-54.

Grant, N.K. 1971b. The south Atlantic, Benue Trough and Gulf of Guinea Cretaceous triple junction. *Bull. Geol. Soc. Am.* **82**, pp. 2295-2298.

Graue K. 2000. Mud volcanoes in deepwater Nigeria. *Marine and Petroleum Geology* **17**, pp. 959–974.

Grelaud, S., Verges, J., Nalpas, T and Karpuz, R. 2003. Impact of multiple detachment levels on deformation of external fold-and-thrust belts. *Geophysical Research Abstract* **5**, p.11003.

Gudmundsson, A. 1995. Stress fields associated with oceanic transform faults. *Earth and Planetary Science Letters* **136**, pp. 603-614.

Guiraud, R and Maurin, J.C., 1992. Early Cretaceous Rifts of Western and Central Africa: an overview. In P.A. Ziegler (Ed). Geodynamics of Rifting, Volume II. Case history studies on Rifts: North and South America, Africa-Arabia. *Tectonophysics* **213**, pp. 153-368.

Guiraud, R and Bellion, Y. 1995. Late Carboniferous to Recent geodynamic evolution of the West Gondwanian, cratonic Tethyan margins, *in* Nairn, A.E.M., Ricou, L.E., Vrielynck, B. and Dercourt, J., eds., The Ocean basins and Margins, vol. 8: The Tethys Ocean: Plenum Press, New York, pp. 101–124.

Guiraud, R and Bosworth, W. 1997. Senonian basin inversion and rejuvenation of rifting in Africa and Arabia: synthesis and implications to plate-scale tectonics. *Tectonophysics* **282**, pp. 39-82.

Guiraud, R., Binks, R.M., Fairhead, J.D and Wilson, M. 1992. Chronology and geodynamic setting of Cretaceous-Cenozoic rifting in West and Central Africa. In: Ziegler, EA. (Ed.), Geodynamics of Rifting, Vol. II. Case History studies on Rifts: North and South America, Africa-Arabia. *Tectonophysics* **21**, pp. 227-234.

Haack, R.C., Sundararaman, P., Diedjomahor, J.O., Xiao, H., Gant, N.J., May, E.D and Kelsch, K. 2000. Niger Delta petroleum systems, Nigeria. In: Petroleum Systems of South Atlantic Margins (Eds. by M.R. Mello & B.J. Katz), *AAPG Memoir* **73**, pp. 213-231.

Haxby, W.F. 1985. Exploring the sea floor from space, *Bulletin of the Society of Independent Professional Earth Scientists* **11**, pp. 19–28.

Heinio, P and Davies, R.J. 2006. Degradation of compressional fold belts: deepwater Niger delta. *AAPG Bulletin* **90**(5), 753-770.

Hills, M.N. 1957. Recent geophysical exploration of the ocean floor. Progr. *Phys. Chem. Earth* **2**, pp. 129-163.

Hooper, R.J., Fitzsimmons, R.J., Grant, N and Vendeville, B.C. 2002. The role of deformation in controlling patterns in the south-central Niger delta, West Africa. *Journal of Structural Geology* **24**, pp. 847-859.

Hospers, J. 1965. Gravity field and Structure of the Niger Delta, Nigeria, West Africa. *Geological Society of America Bulletin* **76**, pp. 407-422.

Hospers, J. 1971. The geology of the Niger delta area, in: Delany, F.M. (Ed.), The Geology of the East Atlantic continental margin, volume 4, Africa ICSU/SCOR working party 31 Symposium Cambridge. Report No. 70/16, *Institute of Geological Science*, London, pp. 124-142.

Houtz, R.E. 1980. Crustal structure of the North Atlantic on the basis of large airgun-sonobuoy data. *Geological Society of America Bulletin* **91**, pp. 406-413.

Hubbert, M.K and Rubey, W.W. 1959. Role of fluid pressure in mechanics of over-thrust faulting, part I and II. *Geological Society of America Bulletin* **70**, pp. 115-205.

Hudec, M.R and Jackson, M.P.A. 2002. Structural segmentation, inversion, and salt tectonics on a passive margin: Evolution of the Inner Kwanza Basin, Angola, *Geologic Society of America Bulletin* **114**, pp. 1222-1244.

Jamison, W.R. 1987. Geometric analysis of fold development in overthrust terranes. *Journal of Structural Geology* 9, pp. 207-219.

Janssen, M.E., Stephenson, R.A and Cloetingh, S. 1995. Temporal and spatial correlations between changes in plate motions and the evolution of rifted basins in Africa, *Geologic Society of America Bulletin* 107, pp. 1317-1332.

JDZ. 2004. Guide to the 2004 JDZ licensing round. URL:www.nigeriasaotomejda.com/PDFs/JDZ%20Brochure.pdf 24 (Accessed 21 January 2005)

Jones, E.J.W. 1987. Fracture Zones in the equatorial Atlantic and the breakup of western Pangea. *Geology* 15, pp. 533-536.

Jubril, M. A., Shaw, H.F and Fallick, A.E. 1998. Stable isotope and geochemical evidence of formation pore fluid evolution during diagenesis of Tertiary sandstones and mudrocks of the Niger Delta, *Journal of African Earth Sciences* 27(3-4), pp. 417-435.

Jubril, M.A and Amajor, L.C. 1991. The Afam Clay Member: a Lower Miocene incised channel in the south-eastern Niger Delta. *Marine and Petroleum Geology* 8, pp. 163-173.

Kastner, M., Elderfield, H., Jenkins, W.J., Gieskes, J.M. and Gamo, T. 1993. Geochemical and isotopic evidence for fluid flow in the Western Nankai subduction zone, Japan. In: Hill, I.A. Taira, A. and Firth, J.V. (Eds.), *Proc. ODP Sci. Results* 131, Ocean Drilling Program, College Station, TX, pp. 423-425.

Keen, M.J., Courtney, R., McClain, J and Purdy, G.M. 1990. Ocean-ridge crustal thickness correlated with paleobathymetry (abstract). *EOS Transactions* 71, 1573.

Klitgord, K.D and Schouten, H. 1986. Plate kinematics of the central Atlantic, *In* Vogt, P.R., and Tucholke, B.E. (Eds.), The Geology of North America (Vol. M): The Western North Atlantic Region. *Geological Society of America*, pp. 351–378.

Knox, G.J and Omatsola, E.M. 1989. Development of the Cenozoic Niger Delta in Terms of the 'Escalator Regression' Model and Impact on Hydrocarbon Distribution. Proceedings KNGMG Symposium 'Coastal

Lowlands, Geology and Geotechnology' (pp. 181-202). Kluwer Academic Publishers, Dordrecht.

Krishna, K.S., Bull, J.M and Scrutton, R.A. 2001. Evidence for multiphase folding of the central Indian Ocean lithosphere. *Geology* 29(8), pp. 715-718.

Krueger, S.W and Grant, N.T. 2006. Evolution of Fault-Related Folds in the Contractional Toe of the Deepwater Niger Delta. AAPG 2006 Annual Convention Houston, USA

Kulke, H. 1995. Nigeria, *In*, Kulke, H., ed., Regional Petroleum Geology of the World. Part II: Africa, America, Australia and Antarctica: Berlin, Gebrüder Borntraeger, pp. 143-172.

Laughton, A.S and Searle, R.C. 1979. Tectonic processes on slow spreading ridges, in: Talwani, M., Harrison, C.G., Hayes, D.E (Eds.), Deep drilling results in the Atlantic Ocean, American Geophysical Union, Washington, pp. 15-32.

Le Pichon, X and Fox, P.J. 1971. Marginal offsets, fracture zones, and the early opening of the North Atlantic. *Journal of Geophysical Research* 76, pp. 6294-6308.

Le Pichon, X and Hayes, D.E. 1971. Marginal offsets, fracture zones and the early opening of the South Atlantic. *Journal of Geophysical Research* 76(26), pp. 6283-6293.

Lehner, P and De Ruiter, P.A.C. 1977. Structural history of the Atlantic margin of Africa. *AAPG Bulletin* **61**, pp. 961-981.

Letouzey, J., Colletta, B., Vially, R and Chermette, J.C. 1995. Evolution of salt related structures in compressional settings, *in* M. P. A. Jackson, D. G. Roberts and S. Snelson, eds., Hedberg international research conference 65, *American Association of Petroleum Geologists*, pp. 41-60.

Lonsdale, P. 1994. Geomorphology and structural segmentation of the crest of the southern (Pacific-Antarctic) East Pacific Rise. *Journal of Geophysical Research* **99** (B3), pp. 4683 – 4702.

Lundin, E. R. 1992. Thin-skinned extensional tectonics on a salt detachment, northern Kwanza basin, Angola. *Marine and Petroleum Geology* **9**, pp. 405–411.

Macdonald, K.C., Fox, P.J., Alexander, R.T., Pockalny, R. A., Gente, P. 1996. Seafloor topography: A faulted or volcanic origin? *Nature* **380**, pp. 125-129.

Macgregor, D.S., Robinson, J and Spear, G. 2003. Play fairways of the Gulf of Guinea transform margin. In: Petroleum Geology of Africa: New Themes and Developing Technologies (Ed. by J.J. Arthur, D.S. Macgregor and N.R. Cameron), *Special Publication of the Geological Society London* **207**, pp. 131-150.

MacLeod, C.J., Escartín, J., Banerji, D., Banks G.J., Gleeson, M., Irving, D.H.B., Lilly, R.M., McCaig, A.M., Niu, Y., Allerton, S., Smith, D.K. 2002. Direct geological evidence for oceanic detachment faulting: the Mid-Atlantic Ridge, 15°45¹N. *Geology* **30**, pp. 879-882.

Malinverno, A and Pockalny, R.A. 1990. Abyssal hill topography as an indicator of episodicity in crustal accretion and deformation. *Earth and Planetary Science Letter* **99**, pp. 154-169.

Maluski, H., Coulon, C., Popoff, M and Baudin, P. 1995. 40Ar/39Ar chronology, petrology and geodynamic setting of Mesozoic to early Cenozoic magmatism from the Benue Trough, Nigeria. *Journal of the Geological Society London* **152**, pp. 311-326.

Marshak, S and Wilkerson, M.S. 2004. Fold-thrust belts - an essay. In: *Earth Structure*, 2nd edn (Ed. by B.A.Van Der Pluijm, and S. Marshak), pp.444-474. Norton Publishers, New York.

Marton, L.G. Tari, G.C and Lehmann, C.T. 2000. Evolution of the Angolan Passive margin, West Africa, with emphasis on post-salt structural styles. In: *Atlantic Rifts and Continental Margins* (Ed. by W. Mohriak and M. Talwani), pp.129-149. *Geophysical Monograph* **115**, American Geophysical Union, Washington, DC.

Mascle, J. 1976. Submarine Niger Delta structural framework. *Journal of Nigeria Minning Geology and Metallurgical Society* **13**, pp. 12-28.

Mascle, J., Blarez, E. and Marinho. M. 1988. The shallow structures of the Guinea and Ivory Coast-Ghana transform margins: their bearing on the Equatorial Atlantic Mesozoic evolution. *Tectonophysics* **155**, pp. 193-209.

Mascle, J., Bornhold, B.D and Renard, V. 1973. Diapiric structures off Niger Delta. *AAPG Bulletin* **57**, pp. 1672-1678.

Masson, D., Cartwright, J.A., Whitmarsh, R., Pinheiro, L. P., Sibuet, J-C. 1994. Compressional reactivation of a passive continental margin. *Journal of the Geological Society of London* **151**, pp. 607-613.

Matos, R.M.D., 2000. Tectonic evolution of the Equatorial South Atlantic. In: Mohriak, W., Talwani, M. (Eds.), Atlantic Rifts and continental margins. *Geophysical Monograph* **115**, pp. 331-354. AGU, Washington, D.C.

McCarthy, J., Mutter, J.C., Morton, J.L., Sleep, N.H., Thompson, G.A. 1988. Relic magma chamber structures preserved within the Mesozoic North Atlantic crust. *GSA Bulletin* **100**, pp. 1423-1436.

McClain, J.S. 1981. On long-term thickening of the oceanic crust. *Geophysical Research Letter* **8**, pp. 1191-1194.

McClain, J.S and Atallah, C.A. 1986. Thickening of the oceanic crust with age. *Geology* **14**, pp. 574-576.

McClay, K.R. 1992. Glossary of thrust tectonics terms, in *Thrust Tectonics* edited by K.R. McClay, pp. 419-433, Chapman and Hall, London.

McClay, K.R. 2004. Thrust tectonics and hydrocarbon systems: introduction. In: Thrust Tectonics and Hydrocarbon Systems (Ed. by K.R. McClay), *AAPG Memoir* **82**, ix-xx.

McClay, K and Bonora, M. 2001. Analogue models of restraining stepovers in strike-slip fault systems, *Bulletin of the American Association of Petroleum Geologists*, **85**, pp. 233 - 260.

McClay, K.R., Dooley, T and Lewis, G. 1998. Analog modeling of progradational delta systems. *Geology* **26**, pp. 771-774.

McClay, K.R., Dooley, T., Ferguson, A and Poblet, J. 2000. Tectonic evolution of the Sanga Sanga Block, Mahakam Delta, Kalimantan, Indonesia. *AAPG Bulletin* **84**, pp. 765-786.

McClay, K., Dooley, T and Zamora, G. 2003. Analogue models of delta systems above ductile substrates, *in* P. Van Rensbergen, R. R. Hillis, A. J. Maltman, and C. K. Morley, eds., Subsurface sediment mobilization. *Geological Society of London Special Publication* **216**, pp. 411-428.

McNaught, M.A and Mitra, G. 1993. A kinematic model for the origin of footwall synclines. *Journal of Structural Geology* **15**, pp. 805-808.

McNeill, L.C., Piper, K.A., Goldfinger, C., Kulm, L.D and Yeats, R.S. 1997. Listric normal faulting on Cascadia continental margin. *Journal of Geophysical Research* **102** (B6), pp. 12123-12138.

Menard, H.W and Atwater, T. 1968. Changes in direction of sea floor spreading. *Nature* **219**, pp. 463-467.

Menard, H.W and Atwater, T. 1969. Origin of fracture zone topography, *Nature* **222**, pp. 1037-1040.

Meyers, J.B and Rosendahl, B. 1991. Seismic reflection character of the Cameroon volcanic line: Evidence for uplifted oceanic crust. *Geology* **19**, pp. 1072-1076.

Meyers, J.B., Rosendahl, B.R and Austin, J.A. 1996a. Deep-penetrating MCS images of the South Gabon Basin: implications for rift tectonics and post breakup salt remobilization. *Basin Research* **8**, pp. 65–84.

Meyers, J.B., Rosendahl, B.R., Groschel-Becker, H., Austin, J.A and Rona, P.A. 1996b. Deep-penetrating MCS imaging of the rift to drift transition, offshore Douala and North Gabon Basins, West Africa. *Marine and Petroleum Geology* **13**, pp. 791– 835.

Minshull, T.A and Hall, B.D. 1997. Geometry of a mid-ocean-ridge normal fault. *Geology* **25**(9), pp. 835-838.

Minshull, T.A., White R.S., Mutter, J.C, Buhl, P., Detrick, R.S., Williams, C.A and Morris, E. 1991. Crustal structure at the Blake Fracture Zone from expending spread profiles. *Journal of Geophysical Research* **96** (B6), pp. 9955-9984.

Mitra, S. 1990. Fault-propagation folds: geometry, kinematic evolution, and hydrocarbon traps. *AAPG Bulletin* **74**, pp. 921-945.

Mitra, S. 2002a. Fold-accommodation faults. *AAPG Bulletin* **86**, pp. 671-693.

Mitra, S. 2002b. Structural models of faulted detachment folds. *AAPG Bulletin* **86**, pp. 1673-1694.

Mohriak, W.U and Rosendahl, B.R. 2003. Transfer zones in the South Atlantic rifted continental margins, in *Intraplate strike –slip deformation belts*, edited by F. Storti, R.E. Holdsworth, and F. Salvini, *Geological Society of London Special Publications* **210**, pp. 211-228.

Mohriak, W. U. et al. 1995. Salt tectonics and structural styles in the deep-water province of the Cabo Frio region, Rio de Janeiro, Brazil, *in* M. P. A. Jackson, R. G. Roberts, and S. Snelson, eds., Salt tectonics: a global perspective. *AAPG Memoir* **65**, pp. 273–304.

Moore, J. C. 1989. Tectonics and hydrogeology of accretionary prisms: role of the décollement zone. *Journal of Structural Geology* **11**, pp. 95-106.

Moore, G.F. and Shipley, T.H. 1993. Character of the décollement in the ODP Leg 131 area, Nankai Trough. In Taira, A., Hill, I.A., Firth, J.V., et al (eds) Proceedings of the Ocean Drilling Program, Scientific Results 131, pp. 73-82.

Moore, J.C., Shipley, T.H., Stoffa, P.L., Karig, D.E., Taira, A., Kuramoto, S., Tokuyama, H. and Suyehiro, K. 1990. Structure of the Nankai Trough accretionary zone from multichannel seismic reflection data. J.Geophys. Research 95, pp. 8753-8765.

Moore, J.C., Shipley, T.H., Goldberg, D., Ogawa, Y., Filice, F., Fisher, A., Jurado, M.J., Moore, G.F., Rabaute, A., Yin, H., Zwart, G., Bruckmann, W., Henry, P., Ashi, J., Blum, P., Meyer, A., Housen, B., Kastner, M., Labaume, P., Laier, T., Leitch, E.C., Maltman, A.J., Peacock, S., Steiger, T.H., Tobin, H.J., Underwood, M.B., Xu, Y. and Zheng, Y. 1995. Abnormal fluid pressures and fault-zone dilation in the Barbados accretionary prism: evidence from logging while drilling. Geology **23**, pp. 605-608.

Morgan, R. 2003. Prospectivity in ultradeep water: the case for petroleum generation and migration within the outer parts of the Niger Delta apron. In: Petroleum Geology of Africa: New Themes and Developing Technologies (Ed. by T.J. Arthur, D.S. MacGregor & N.R. Cameron), *Special Publication of the Geological Society of London* **207**, pp. 151-164.

Morgan, R. 2004. Structural controls on the positioning of submarine channels on the lower slopes of the Niger Delta. In: 3D Seismic Technology: Application to the Exploration of Sedimentary Basins (Ed. by R.J. Davies, J. Cartwright, S.A. Stewart, J.R. Underhill & M. Lappin), *Geological Society London Memoir* **29**, pp. 45-51.

Morgan, W.J. 1971. Convection plumes in the lower mantle. Nature **230**, pp. 42-43.

Morley, C.K. 1988. Out of sequence thrusts. *Tectonics* **7**, pp. 539-561.

Morley, C. K. 2003. Mobile shale related deformation in large deltas developed on passive and active margins, *in* P. Van Rensbergen, R.R. Hillis, A. J. Maltman, and C. K. Morley, eds., Subsurface sediment mobilization, *Special Publication of the Geological Society of London* **216**, pp. 335-357.

Morley, C. K and Guerin, G. 1996. Comparison of gravity-driven deformation styles and behaviour associated with mobile shales and salt: *Tectonics* **15**, pp. 1154-1170.

Morris, E., Detrick, R.S., Minshull, T.A., Mutter, J.C., White, R.S., Su, W., Buhl, P. 1993. Seismic structure of oceanic crust in the western North Atlantic. *Journal of Geophysical Research* **98**, pp. 13879–13903.

Müller, R.D and Roest, W.R. 1992. Fracture zones in the North Atlantic from combined Geosat and Seasat data. *Journal of Geophysical Research* **97**(B3), pp. 3337– 3350.

Muraoka, H and Kamata, H. 1983. Displacement distribution along minor fault traces. *Journal of Structural Geology* **5**, pp. 395-483.

Mutter, J.C and NAT Study Group. 1985. Multichannel Seismic Images of the Oceanic Crust's Internal Structure: Evidence for a Magma Chamber beneath the Mesozoic Mid-Atlantic Ridge. *Geology* **13**, pp. 629-632.

Nürnberg, D and Müller, R.D. 1991. The tectonic evolution of the South Atlantic from Late Jurassic to present. *Tectonophysics* **191**(1-2), pp. 27-53.

Ofoegbu, C.O. 1984. A model for the tectonic evolution of the Benue trough of Nigeria. *International Journal of Earth Sciences* **73**, pp. 1007-1018.

Pardo-Casas, F. and Molnar, P. 1987. Relative motion of the Nazca (Farallón) and South American plates since late Cretaceous time. *Tectonics* **6**, pp. 233–248.

Peel, F.J., Travis, C.J and Hossack, J.R. 1995. Genetic structural provinces and salt tectonics of the Cenozoic onshore US Gulf of Mexico: a preliminary

analysis. In: Salt Tectonics: A Global Perspective (Ed. byM.P.A. Jackson, D.G. Robert & S. Snelson), *AAPG Memoir* **65**, pp. 153-175.

Peive, A.A. 2006. Vertical tectonic movements of the crust in transform fracture zones of the Central Atlantic, *Geotectonics* **40**(1), pp. 25-36.

Petters, S.W. 1984. An ancient submarine canyon in the Oligocene-Miocene of the Western Niger Delta. *Sedimentology* **31**, pp. 805-810.

Petters, S.W and Ekweozor, C.M. 1982. Petroleum geology of the Benue trough and southeastern Chad Basin, Nigeria. *AAPG Bulletin* **66**, pp. 1141-1149.

Pfiffner, O.A. 1985. Displacements along thrust faults. *Eclogae Geologicae Helvetiae* **79**, pp. 313-333.

Pilipenko, A.I. 1994. Tectonic delamination of oceanic crust in deepwater. *Geotectonics* **28**, pp. 44-55.

Pindell, J.L. and Dewey. J. 1982. Permo- Triassic reconstruction of Western Pangea and the evolution of the Gulf of Mexico/Carribean domain. *Tectonics* **1**, pp. 179-217.

Planke, S., Symonds, P., Alvestad, E and Skogseid, J. 2000. Seismic volcanostratigraphy of large volume basaltic extrusive complexes on rifted margins. *Journal of Geophysical Research* **105**(B2), pp. 19335-19351.

Poblet, J and McClay, K. 1996. Geometry and kinematics of single-layer detachment folds. *AAPG Bulletin* **80**, pp. 1085-1109.

Poblet, J., McClay, K., Storti, F and Munoz, J.A. 1997. Geometries of syntectonic sediments associated with single-layer detachment folds, *Journal of Structural Geology* **19**, pp. 369-381.

Pockalny, R.A. 1997. Evidence of transpression along the Clipperton transform: Implications for processes of plate boundary reorganization. *Earth & Planetary Science Letters* **146**, pp. 449-464.

Popoff, M., Ojoh. K.A. and Baudin, Ph. 1989. Opening of the South Atlantic and Mesozoic rifting in the Benue Trough. Geochronique **30** (Special Washington), pp. 64-65 (abstract)

Rabinowitz, P.D and LaBrecque, J. 1979. The Mesozoic South Atlantic Ocean and evolution of its Continental margins. *Journal of Geophysical Research* **84**(B11), pp. 5973-6002.

Radler, M. 2006. Oil production, reserves increase slightly in 2006. *Oil and Gas Journal* **104** (47), (December 18, 2006), pp. 20-21.

Raitt, R.W. 1963. The crustal rocks, in: Hill, M.N. (Ed.), The Sea, Volume 3, Wiley-Interscience, New York, pp. 85-102.

Ramsay, J.G and Huber, M.I. 1987. The technique of modern structural geology, Vol. 2, Fold and Faults. Academic Press, London, 391p.

Reijers, T.J.A., Petters, S.W and Nwajide, C.S. 1997. The Niger Delta Basin. African Basins, *in* Sedimentary basins of the world 3, R.C. Selley, ed., pp. 151-172.

Reston, T. J., Ruoff, O., McBride, J.H., Ranero, C.R and White, R.S. 1996. Detachment and steep normal faulting in Atlantic oceanic crust west of Africa. *Geology* **24**(9), pp. 811-814.

Rich, J.L. 1934. Mechanics of low-angle overthrust faulting as illustrated by Cumberland thrust block, Virginia, Kentucky, Tennessee. *AAPG Bulletin* **18**, pp. 1584-1596.

Roberts, M. 2004. Geologic history and petroleum systems of the Eastern deepwater Niger Delta (Abstract). NAPE and AAPG West Africa Deepwater Regional Conference November 14-18, 2004, Abuja, Nigeria.

Rosendahl, B.R. 1992. Nature of the transition from continental to oceanic crust and the meaning of reflection Moho. *Geology*, **20**, pp. 721-724.

Rosendahl, B.R and Groschel-Becker, H. 1999. Deep seismic structure of the continental margin in the Gulf of Guinea; a summary report, in: Cameron, N.R, Bate, R.H., Clure, V.S. (Eds.), The oil and gas habitats of the South Atlantic. *Geological Society Special Publications* **153**, pp. 75-83.

Rosendahl, B.R., Groschel-Becker, H., Meyers, J.B and Kaczmarick, K. 1991. Deep seismic reflection study of a passive margin, southeastern Gulf of Guinea. *Geology* **19**, pp. 291–295.

Rosendahl, B.R., Meyers, J., Groschel-Becker, H and Scott, D. 1992. Nature of the transition from continental to oceanic crust and the meaning of reflection Moho. *Geology* **20**, pp. 721-724.

Rowan, M.G., Peel, F.J and Vendeville, B.C. 2004. Gravity-driven fold belts on passive margins. In: *Thrust Tectonics and Hydrocarbon Systems* (Ed. K.R. McClay), *AAPG Memoir* **82**, pp. 157-182.

Rowan, M.G., Trudgill, B.D and Fiduk, J.C. 2000. Deep-water salt-cored foldbelts: Lessons from the Mississippi fan and Perdido fold belts, northern Gulf of Mexico, in Atlantic rifts and continental margins: American Geophysical Union *Geophysical Monograph* **115**, pp. 173–191.

Sage, F., Basile, C., Mascle, J., Pontoise, B and Whitmarsh, R.B. 2000. Crustal structure of the continent-ocean transition off the Cote d`Ivoire-Ghana transform margin: implication for thermal exchange across the palaeo-transform boundary. *Geophysical Journal International* **143**, pp. 662-678.

Sandwell, D.T and Smith, W.H.F. 1997. Marine gravity anomaly from Geosat and ERS-1 satellite altimetry. *Journal of Geophysical Research* **102**, pp. 10039-10050.

Saugy, I and Eyer, A. 2003. fifty years of exploration in the Niger Delta (west Africa), *in* M. T. Halbouty, ed., Giant oil and gas fields of the decade 1990-1999. *AAPG Memoir* **78**, pp. 211-226.

Schreurs, G. 1994. Experiments on strike-slip faulting and block rotation. *Geology* **22**, pp. 567-570.

Searle, R.C. 1979. Side-scan sonar studies of North Atlantic fracture. *Journal of the Geological Society London*, **136**, pp. 283-292.

Searle, R.C. 1983. Multiple, closely spaced transform faults in fast-slipping fracture zones. *Geology* **11**, pp. 607-610.

Searle, R.C and Laughton, A.S. 1977. Sonar studies of the Mid-Atlantic ridge and Kurchatov fracture zone. *Journal of Geophysical Research* **82**(33), pp. 5313-5328.

Searle, R.C., Francis, T.J.G., Hilde, T.W.C., Somers, M.L., Revie, J., Jacobs, C.L., Saunders, M.R., Barrow, B.J and Bicknell, S.V. 1981. 'Gloria' Side-Scan Sonar in the east Pacific. *EOS Transaction* **62**, pp. 121-122.

Shaw, J.H., Novoa, E and Connors, C.D. 2004. Structural controls on growth stratigraphy in contraction fault-related folds. In: *Thrust tectonics and hydrocarbon systems* (Ed. K.R. McClay). *AAPG Memoir* **82**, pp. 400-412.

Shipley, T.H., Moore, G.F., Bangs, N.L., Moore, J.C. and Stoffa, P.L. 1994. Seismically inferred dilatancy distribution, northern Barbados Ridge décollement: implications for fluid migration and fault strength. *Geology* **22**, pp. 411-414.

Shipley, T., Moore, G. F. , Tobin, H. J., Moore, J. C., Ogawa, Y., Blum, P., Ashi, J., Brueckmann, W., Filice, F., Fisher, A.T., Goldberg, D., Henry, P., Housen, B., Jurado, M.-J., Kastner, M., Labaume, P., Laier, T., Leitch, E.C., Maltman, A.J., Meyer, A., Peacock, S., 1997. Synthesis of the Barbados detachment seismic reflection response from drilling-based geophysical observations and physical properties, Proc., Ocean Drilling Project., Sci. Results, vol. **156**, pp. 293-302.

Shirley, K. 2002. Agbami a 20-Mile long thrust-faulted anticline. *Explorer*, February, 2002, pp.11.

Shor, G.G. Jr., Menard, H.W and Raitt, R.S. 1970. Structure of the Pacific Basin, in: The Sea, vol. 4, Part II, Maxwell, A.E. (Ed.), 3-27, Wiley-Interscience, New York.

Short, K.C and Stauble, A.J. 1967. Outline of Geology of Niger Delta. *AAPG Bulletin* **51**, pp. 761-779.

Sibson, R.H. 1981. Fluid flow accompanying faulting: Field evidence and models. In: *Earthquake prediction, an international review* (Ed. by D.W. Simpson and R.G Richards), American Geophysical Union Maurice Ewing Series 4, pp. 593-603.

Spathopoulos, F. 1996. An insight on salt tectonics in the Angola Basin, South Atlantic, in D. J. Blundel, G. I. Alsop, and J. Davison, eds., Salt tectonics: *Geological Society (London) Special Publication* **100**, pp. 153–174.

Sonder, L.J., Pockalny, R.A., 1999. Anomalously rotated abyssal hills along active transforms: Distributed deformation of oceanic lithosphere. *Geology* 27, pp. 1003-1006.

Stacher, P. 1995. Present understanding of the Niger Delta hydrocarbon habitat, *in*, Oti, M.N., and Postma, G., eds., *Geology of Deltas*: Rotterdam, A.A. Balkema, pp. 257-267.

Stewart, S.A. 1996. Influence of detachment layer thickness on style of thin-skinned shortening. *Journal of Structural Geology* **18**, pp. 1271-1274.

Stone, D.S. 1995. Structure and kinematic genesis of the Quealy wrench duplex: transpressional reactivation of the Precambrian Cheyenne belt in the Laramie basin, Wyoming, *AAPG Bulletin* **79**, pp. 1349–1376.

Suppe, J. 1985. *Principles of Structural Geology*. Prentice-Hall, Englewood Cliffs, New Jersey.

Suppe, J and Medwedeff, D.A. 1984. Fault-propagation fold: *Geological Society of America Annual Meeting Program with Abstract* **16**, p.670.

Suppe, J and Medwedeff, D.A. 1990. Geometry and kinematics of fault-propagation folding. *Eclogae Geologicae Helvetiae* **83**, pp. 409-454.

Sykes, L.R. 1978. Intraplate seismicity, reactivation of pre-existing zones of weakness, alkaline magmatism, and other tectonism postdating continental fragmentation. *Rev. Geophys. Space Phys.* **16**(4), pp. 621-688.

Sykes, L.R and Sbar, M.L. 1974. Focal mechanism solution of intraplate earthquakes and stresses in the lithosphere, in *Geodynamics of Iceland and the North Atlantic area*, edited by L. Kristjansson, pp. 207-224, D. Reidel, Hingham, Massachusetts

Sylvester, A.G. 1988. Strike-slip faults. *Geological Society of America Bulletin* **100**, 1666-1703.

Taira, A. et al. 1991. Proceedings of the Ocean Drilling Program, Initial Reports, 131, Ocean Drill. Program, College, College Station, Texas

Trudgill, B.D., et al. 1995a. The structural geometry and evolution of the salt-related Perdido fold belt, Alaminos Canyon, northwestern deep Gulf of Mexico, *in* C. J. Travis, B. C. Vendeville, H. Harrison, F. J. Peel, M. R. Hudec, and B. F. Perkins, eds., Salt, sediment and hydrocarbons: Gulf Coast Section of the SEPM Foundation 16th Annual Research Conference, GCSSEPM Foundation, pp. 275–284.

Trudgill, B.D., Rowan, M.G., Fiduk, J.C., Weimer, P., Gale, P.E., Korn, B.E. Phair, R.L., Gafford, W.T., Roberts, G.R and Dobbs, S.W. 1999. The Perdido fold belt, northwestern deep Gulf of Mexico; Part 1, Structural

geometry, evolution and regional implications: *AAPG Bulletin* **83**, pp. 88-113.

Uchupi, E., 1989. The tectonic style of the Atlantic Mesozoic rift system. *Journal of African Earth Sciences* **8**(2-4), pp. 143-164.

Urien, C.M. and Zambrano, J.J. 1973. The geology of the basins of the Argentine continental margin and Malvinas Plateau, In: A.E.M. Naim and F.G. Stehli (Editors), The Ocean Basins and Its Margins. Vol. 1, The South Atlantic, Plenum, New York, pp. 135-169.

Van Rensbergen, P and Morley, C.K. 2003. Re-evaluation of mobile shale occurrences on seismic sections of the Champion and Baram deltas, offshore Brunei. In: Van Rensbergen, P., Hillis, R.R., Maltman, A.J., Morley, C.K. (Eds.), Subsurface Sediment Mobilization. *Geological Society of London Special Publication* **216**, pp. 395–409.

Vazquez-Meneses, M.E and McClay, K. 2003. Gravity Tectonics in Western Gulf of Mexico. AAPG International Conference Abstract, Barcelona, Spain, September 21-24, 2003.

Wallace, W.K and Homza, T.X. 2004. Detachment folds versus fault-propagation folds and their truncation by thrust faults. In: *Thrust tectonics and hydrocarbon systems* (Ed. by K.R. McClay), *AAPG Memoir* **82**, pp. 324-355.

Wallace, G., Moore, J.C. and Dileonardo, C.G. 2003. Controls on localization and densification of a modern décollement: Northern Barbados accretionary prism. Geol. Soc. Am. Bulletin 115, pp. 288-297.

Wagner, T., and T. Pletsch, (1999), Tectono-sedimentary controls on Cretaceous black shale deposition along the opening of the Equatorial Atlantic Gateway (ODP Leg 159), in *The oil and gas habitats of the South Atlantic*, edited by N.R. Cameron, R.H. Bate and V.S.Clure, *Geological Society London Special Publication* **153**, pp. 241–265.

Walsh, J.J and Watterson, J. 1987. Distributions of cumulative displacement and seismic slip on a single normal fault surface. *Journal of Structural Geology* **9**, pp. 1039-1046.

Watterson, J. 1986. Fault dimensions, displacement, and growth. *Pure and Applied Geophysics* **124**, pp. 365–373.

Weber, K. J. 1971. Sedimentological aspects of oilfields in the Niger Delta. *Géologie Mijnb.* **50**(3), pp. 559-576.

Weber, K.J and Daukoru, E.M. 1975. Petroleum geology of the Niger Delta. Proceeding of the 9thWorld. Petroleum Congress, Tokyo, Japan, pp. 209-221.

Weimer, P and Buffler, R.T. 1992. Structural geology and evolution of the Mississippi Fan fold belt, deep Gulf of Mexico. *AAPG Bulletin* **76**, pp. 225-251.

Westbrook, G.K., Ladd, J.W., Buhl, P., Bangs, N. and Tiley, G.J. 1988. Cross section of an accretionary wedge: Barbados Ridge complex. *Geology* **16**, pp. 631-635.

White, R.S., Detrick, R.S., Sinha, M.C and Cormier, M.H., 1984. Anomalous seismic crustal structure of oceanic fracture zones. *Geophysical Journal of the Royal Astronomical Society* **79**, pp. 779-798.

White, R.S., McKenzie, D and O'nions, R.K. 1992. Oceanic crustal thickness from seismic measurements and rare element inversions. *Journal of Geophysical Research* **97**, pp. 19683-19715.

White, R.S., Detrick, R.S., Mutter, J.C., Buhl, P., Minshull, T.A and Morris, E. 1990. New seismic images of oceanic crustal structure. *Geology* **18**, pp. 462-465.

White, R.S., McBride, J.H., Henstock, T.J and Hobbs, R.W. 1994. Internal structure of a spreading segment of Mesozoic oceanic crust. *Geology* **22**, 597-600.

Whiteman, A.J. 1982. Nigeria: Its Petroleum Geology, Resources and Potential, Vol. I. Graham& Trotman, London, 394p.

Whitmarsh, R.B and Laughton, A.S. 1975. The fault pattern of a slow-spreading ridge near a fracture zone. *Nature* **258**, pp. 509-510.

Whitmarsh, R.B., Manatschal, G and Minshull, T.A. 2001. Evolution of magma-poor continental margins from rifting to seafloor spreading. *Nature* **413**, pp. 150-154.

Wiedmann, J and Neugebauer, J. 1978. Lower Cretaceous ammonites from the South Atlantic Leg 40 (DSDP), their stratigraphic value and sedimentologic parameter. In: H.M. Bolly, W.B.F. Ryan et al. (Editors),

Intial Reports of the Deep Sea Drilling Project, Suppl. 38-41. U.S.
Government Printing Office, Washington, D.C., pp. 709-721.

Wilkins, S.J and Gross, M.R. 2002. Normal fault growth in layered rocks at
Split Mountain, Utah: influence of mechanical stratigraphy on dip
linkage, fault restriction and fault scaling. *Journal of Structural Geology*
24(9), pp. 1413-1429.

Williams, G and Chapman, T. 1983. Strains developed in the hanging walls of
thrusts due to their slip/propagation rate: a dislocation model. *Journal of
Structural Geology* **5**(6), pp. 563-571.

Wilson, J.T. 1965. Evidence from oceanic islands suggesting movement in the
earth. *Phil. Trans. R. Soc. Lond.* **258**, pp. 145-167.

Wilson, J.T. 1973. Mantle plumes and plate motions. *Tectonophysics* **19**, pp.
149-164.

Wilson, M. 1993. Plate-moving mechanisms: constraints and controversies,
Journal of Geological Society, London, **150** (5), pp. 923-926.

Wilson, R.C.L. 1975. Atlantic opening and Mesozoic Continental margin
basins of Iberia. *Earth and Planetary Science Letter* **25**, pp. 33-43.

Wilson, R.C.L and Williams, C.A. 1979. Oceanic transform structures and the
development of Atlantic continental margin sedimentary basins – a
review. *Journal of the Geological Society London,* **136**, pp. 311-320.

Wilson, P.G., Turner, J.P and Westbrook, G.K. 2003. Structural architecture of
the ocean-continent boundary at an oblique transform margin through
deep-imaging seismic interpretation and gravity modelling: Equatorial
Guinea, West Africa. *Tectonophysics* **374**(1-2), pp. 19-40.

Wollard, G.P. 1975. The inter-relationships of crustal and upper mantle parameter
values in the Pacific. *Review of Geophysics* **13**, pp. 87-137.

Wu, S and Bally, A.W. 2000. Slope Tectonics-comparisons and contrasts of
structural styles of salt and shale tectonics of the Northern Gulf of
Mexico with shale tectonics of offshore Nigeria in Gulf of Guinea. In:
Atlantic Rifts and continental margins (Ed. by W. Mohriak and M. Talwani)
Geophysical Monograph **115**, pp. 151-172.

Wu, S., Vail, P.R and Cramez, C. 1990. Allochthonous salt, structure and

stratigraphy of the north-eastern Gulf of Mexico; Part 1, Stratigraphy. *Marine and Petroleum Geology* **7**(4), pp. 318-333.

Yilmaz, O., 2001. Seismic Data Analysis: Processing, Inversion and Analysis of Seismic Data (2Vol). Society of Exploration Geophysicists, Tulsa.

Zhao, Z., Moores, G.F and Shipley, T.H. 1998. Deformation and dewatering of the subducting plate beneath the lower slope of the northern Barbados accretionary prism. *Journal of Geophysical Research* **103**, pp. 30431-30449.

Multiple detachment levels and their control on fold styles in the compressional domain of the deepwater west Niger Delta

Sepribo E. Briggs,* Richard J. Davies,† Joe A. Cartwright* and Richard Morgan‡

*3DLab, School of Earth, Ocean & Planetary Sciences, Cardiff University, Cardiff, UK
†CeREES, Department of Earth Sciences, University of Durham, Science Labs, Durham, UK
‡Veritas DGC Limited, Crompton Way, West Sussex, UK

ABSTRACT

We interpret recently acquired two-dimensional (2D) and 3D seismic data from the contractional domain of the Tertiary deepwater west Niger Delta, which is an area of current hydrocarbon exploration and development to show that during its gravitational collapse, multiple detachments were active. Detachments are located within (1) what we herein refer to as the 'Dahomey unit', (2) the transition between the Agbada and Akata formations (Top Akata) and (3) the Akata formation. Seismic interpretation and quantitative measurements of fault displacements show that the utilisation of different detachments results in contrasting styles of thrust propagation and fold growth. Two geographical zones are defined. In zone A (NW sector of the study area), the stratigraphically shallowest Dahomey detachment is dominant and is associated with *thrust truncated folds*. In zone B (SE sector of the study area), a stratigraphically lower detachment approximately at the Agbada–Akata formation boundary is associated with *thrust propagation folds*. A third detachment, within the Akata formation, is locally developed and is also associated with *thrust propagation folds*. The different deformational histories are probably related to the mechanical stratigraphy and the pore-pressure characteristics of the succession.

INTRODUCTION

Deformation caused by gravity tectonics is common to many deepwater passive margins (Bruce, 1973; Dailly, 1976; Evamy *et al.*, 1978; Doust & Omatsola, 1990; Marton *et al.*, 2000). As petroleum exploration becomes increasingly focused on these deepwater settings, insights into the evolution of the contractional deformation structures that are located in the toe regions of the gravity tectonic system and their suitability as hydrocarbon traps have become important. The deepwater west Niger Delta region (Fig. 1a) is predominantly a compressional structural domain that has recently become the focus of significant oil and gas exploration activity. However, there is currently no documentation of the variability of the fold styles across the area and their structural evolution. This has been due to the historical lack of extensive two-dimensional (2D) and 3D seismic reflection data and well bore calibration of the stratigraphy. Earlier studies were based largely on a few widely spaced reconnaissance seismic lines (Burke, 1972; Delteil *et al.*, 1974; Emery *et al.*, 1975; Mascle, 1976; Lehner & De Ruiter, 1977; Damuth, 1994) and focused

Correspondence: Sepribo E. Briggs, 3DLab, School of Earth, Ocean & Planetary Sciences, Cardiff University, Main Building, Park Place, CF10 3YE, Cardiff, UK. E-mail: briggss1@Cardiff.ac.uk

upon the mapping of fracture zones and other basement structures, whereas recent publications (Ajakaiye & Bally, 2002a, b; Shaw *et al.*, 2004; Bilotti & Shaw, 2005; Corredor *et al.*, 2005a, b) have focused on studying the gravitational structures (Fig. 1b). Specifically, Corredor *et al.* (2005a) have carried out structural reconstructions of the progressive development of the fold and thrust belts, describing the style of thrusting and associated folding. They drew links between detachment level and structural style but did not focus on the deepwater west Niger Delta.

Thrust-related folds can evolve in many ways (e.g. McClay, 2004). These can be distinguished based upon (a) the shape of the thrust that underlies the fold and the relationship between folding and the kinematics of the thrust tip or (b) whether they have formed above a thrust with no ramp; a lower flat and ramp; or a lower flat, ramp and upper flat. They can also be differentiated kinematically depending on whether they have formed from a fixed tip a propagating tip, or from a thrust that continues beyond the fold (Wallace & Homza, 2004).

The seismic data used in this study were acquired over what are herein termed the (a) inner (proximal) fold and thrust belt, (b) detachment (inter thrust) fold belt and (c) outer (distal) fold and thrust belt of the deepwater west Niger Delta (Fig. 1a). This work complements that of Corredor *et al.* (2005a), who carried out structural reconstructions in 2D over selected cross sections across the
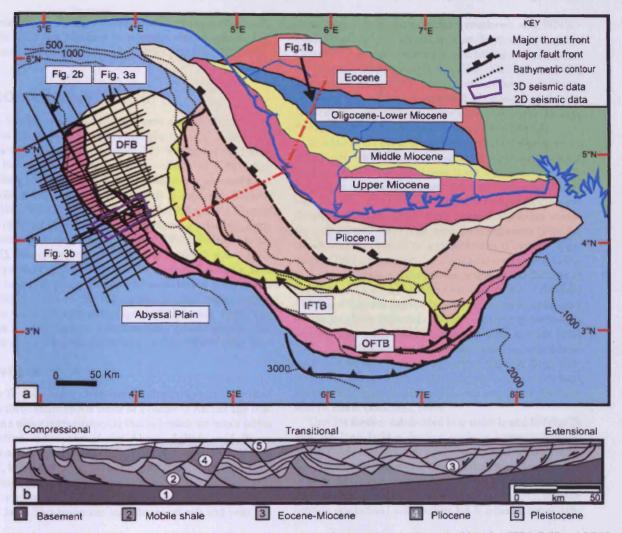
Fig. 1. (a) Map of the Niger Delta showing the different structural domains (modified after Damuth, 1994). Note IFTB, DFB and OFTB are equivalent to the inner fold and thrust belt, detachment fold belt and outer fold and thrust belt, respectively. (b) Regional dip line extending across the onshore into the deepwater west Niger delta. Modified after Haack *et al.* (2000). Vertical exaggeration = 2.0.

delta. The aim of this paper is to document regional variations in thrust and fold styles and relate these to the stratigraphic characteristics of different detachment levels.

PREVIOUS RESEARCH ON DETACHMENT ZONES

The structural styles of deepwater fold and thrust belts are influenced by a number of parameters including the original mechanical stratigraphy (Erickson, 1996) and the fluid pressure distribution (Ramsay & Huber, 1987). The strength and thickness of the competent layer being deformed control the wavelength, amplitude and asymmetry of thrust-related fold structures (Erickson, 1996). As such, they control the location of a thrust or fold within a multilayered stratigraphic package.

Pore fluid pressure plays a key role in the development of deepwater fold and thrust belts particularly where there

are no evaporitic sediments capable of localising a detachment surface. According to the Mohr–Coulomb failure theory, an increase in pore pressure will reduce the effective normal stress, thereby lowering shear strength. The occurrence of excess fluid pressure helps to account for the phenomenon of weak faults in general (Sibson, 1981; Byerlee, 1993) and this mechanical principle can also be applied to the localisation of detachment surfaces in thrust domains (Hubbert & Rubey, 1959). Previous work on fold belts such as that of the Western Gulf of Mexico (Peel *et al.*, 1995) and the Niger Delta (Doust & Omatsola, 1990; Morley & Guerin, 1996; Wu & Bally, 2000) considered detachment to occur on overpressured shales. Where multiple overpressured levels exist in passive margin deepwater settings, multiple detachment levels are not uncommon. Some compressional belts have developed above multiple detachment levels composed of either shale (Rowan *et al.*, 2004), rock salt or other evaporites

(Grelaud *et al.*, 2003) or a combination of these (Peel *et al.*, 1995). This has resulted in complex thrust-related fold geometries (Davis & Engelder, 1985; Cobbold *et al.*, 1995).

GEOLOGICAL SETTING

The Niger Delta is one of the largest modern deltas in the world (Doust & Omatsola, 1990; Hooper *et al.*, 2002). It is situated at the southern end of NE–SW folded rift basin, the Benue trough which formed during the Cretaceous opening of the South Atlantic, when the equatorial parts of Africa and South America began to separate (Burke *et al.*, 1971; Whiteman, 1982; Fairhead & Binks, 1991). During the opening of the Equatorial Atlantic in the late Early Cretaceous (Nürnberg & Müller, 1991; Maluski *et al.*, 1995), the trough became filled progressively with Albian and younger post-rift deposits. By the Late Eocene, a delta had begun to prograde over the continental margin following the end of the Palaeocene marine transgression when the Imo Shales were deposited (Damuth, 1994). The delta now consists of a sedimentary prism some 12 km thick with a subaerial extent of about 75 000 km^2 (Fig. 1a).

Stratigraphy

The Tertiary Niger Delta can be stratigraphically divided into three diachronous units of Eocene to Recent age that form a major regressive cycle that is broken up into a series of offlap cycles named the Akata, Agbada and Benin formations (Short & Stauble, 1967; Avbovbo, 1978; Evamy *et al.*, 1978; Whiteman, 1982; Knox & Omatsola, 1989; Doust & Omatsola, 1990). The delta prograded over both oceanic and continental basement (Davies *et al.*, 2005; Figs 2a, b and 3a, b). This basement includes a syn-rift and post-rift

succession that fills a northeast–southwest and WNW–ESE trending rift structure that formed during the Cretaceous, probably during Aptian rifting of the Equatorial Atlantic (Gradstein *et al.*, 1995; De Matos, 2000; Macgregor *et al.*, 2003). An unconformity (mid-Aptian break-up unconformity) separates the syn-rift and post-rift sediment fill. Above this lies a low-reflectivity package thought to be of Late Cretaceous to Palaeocene age.

In addition to the previously described subdivisions, we informally defined two major seismic–stratigraphic packages (units 1 and 2) based upon contrasting seismic amplitude, seismic facies and deformational characteristics. Unit 2 is about 3–4 km thick and comprises a low-reflectivity package, which lacks internal reflection except for a single mid-level high-amplitude reflection (Fig. 3b), which may be related to a detachment (Corredor *et al.*, 2005a). This unit onlaps the older Late Cretaceous to Palaeocene succession, is of marine origin and at the base of the delta, corresponds to the Akata formation of Avbovbo (1978) and Knox & Omatsola (1989). It is mainly composed of marine shales believed to be the source rock for hydrocarbons and some locally developed sand and silt beds. This unit exhibits anomalously low P-wave seismic velocities ($\sim$2000 m s^{-1}) that may reflect regional fluid overpressures (Bilotti & Shaw, 2001). It provides a detachment horizon for large growth faults, located up dip of the study area (Knox & Omatsola, 1989).

Unit 1 is further subdivided into units 1a and 1b (Figs 2b and 3a). Unit 1a is a distinct package between 300 and 600 m thick, consisting of semi-continuous to continuous low-amplitude reflections that are deformed into a series of folds that are clearly evident in the NW of the deepwater region (Figs 2b and 3a). It thins southwards until it is below seismic resolution ($\sim$20 m; Fig. 3b). It is herein termed the
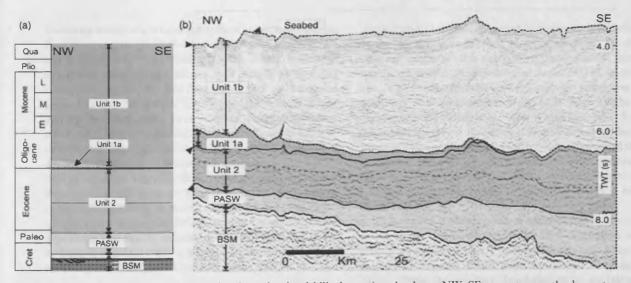
Fig. 2. (a) Chronostratigraphic diagram showing the regional variability in stratigraphy along a NW–SE transect across the deepwater west Niger Delta. (b) Two-dimensional seismic line showing the abrupt change in stratigraphy between units 1a, 1b and 2. Note that BSM, PASW, units 2, 1a and 1b correspond to the basement (Ajakaiye & Bally, 2002a, b), pre-Akata sediment wedge (see Morgan, 2003, 2004), Akata formation (Avbovbo, 1978; Knox & Omatsola, 1989), Dahomey wedge (Morgan, 2003, 2004) and Agbada Formation (Short & Stauble, 1967; Avbovbo, 1978), respectively.
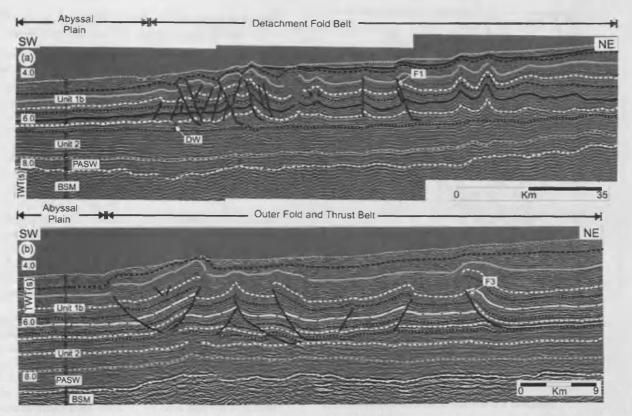
Fig. 3. Interpreted seismic lines from (a) the two-dimensional (2D) dataset, (b) the 3D dataset, showing the major stratigraphic subdivisions of the deepwater west Niger delta. The major reflectors defined in this section are the top of the basement, the pre-Akata sediment wedge, unit 2 corresponding to the Akata formation, unit la, which is the Dahomey detachment unit and unit lb, which defines the Agbada Formation. Note the sinusoidal geometry of the Dahomey unit that thins towards the SW direction here and in the SE direction in Fig. 2 but becomes relatively thicker towards the NE. The compressional faults tip out from the thick units marked DW. Older inactive fold features are observed buried without any seafloor expression. The mid–Akata detachment level is clearly defined on the 3D dataset with thrusts propagating from it and showing situations of shale welding. Note the very strong and low-frequency reflector defining the top of the crust and below which no coherent reflections exist.

Dahomey wedge and is believed to have been sourced from the Dahomey trough of the onshore Guinea basin in the north of this study area (Morgan 2003, 2004). Unit lb is about 3 km thick below a water depth of over 4000 m and corresponds to the Agbada Formation that has been described by Short & Stauble (1967) from the Agbada-2 well and by Avbovbo (1978). It consists of alternating sandstones and shales deposited by channelised turbidites, debrites and hemipelagites (e.g. Davies, 2003; Deptuck et al., 2003). The sands constitute the main reservoirs in this part of the delta. Sand to shale ratio generally decreases downwards as the formation passes gradually into the Akata formation. The age of this formation is Eocene to Pleistocene (Short & Stauble, 1967; Doust & Omatsola, 1990). The Benin Formation, as described from the Elele-1 well by Short & Stauble (1967), is not encountered in the deep-water region of the Niger Delta (Morgan, 2003).

Structure

The Niger Delta tectonic province is a typical example of a linked regional gravity tectonic system where horizontal translation of the post rift cover is driven by gravitational failure of the margin. This is accommodated by thin-skinned tectonics with extensional, intermediate transitional and downdip compressional domains (Fig. 1b) above one or more detachment levels. Extension occurs on the shelf and is accommodated by growth faults (Weber & Daukoru, 1975; Evamy et al., 1978; Whiteman, 1982; Knox & Omatsola, 1989). A transitional domain is located basinwards of this and is characterised by shale diapirs and their associated inter-diapir depocentres. The compressional domain is sited beneath the lower continental slope and rise, and is characterised by thrust faults and their associated folds.

Thin-skinned compressional deformation is manifest as regularly spaced thrust faults and associated with mainly asymmetric folds. The thrust faults have a regular spacing of between 2 and 5 km and occasionally up to 10 km. These thrusts have developed in an overall seaward-propagating sequence with some out-of-sequence thrusting caused by the reactivation of older in-sequence thrust by the development of new thrust faults through a deformed thrust sheet (Morley, 1988).

The region has been subdivided into three structural domains (Connors *et al.*, 1998; Corredor *et al.*, 2005a)

(a) *Inner fold and thrust belt* (Fig. 1a), characterised by a higher structural dip with an average distance between imbricated thrust sheets of between 1 and 2 km and with the formation of occasional piggy-back basins (Corredor *et al.*, 2005a). The dataset does not extend over this domain.

(b) *Detachment fold belt* (Fig. 1a), characterised by large areas of minor deformation from thrust- or shale-induced folding (thrusting and folding due to shale swelling), with along-transport thrust sheet dimensions ranging from 2 to 5 km (Fig. 3a).

(c) *Outer fold and thrust belt* (Fig. 1a), comprised of local depocentres and both basinward and hinterland verging thrusts. This domain is situated further downdip, with channelised turbidite sands trapped in broad-wavelength anticlines above incipient thrust propagation zones (Fig. 3b).

We divided the study area into two zones; A and B (Fig. 4), according to structural styles. Zone A is in the detachment fold belt located in the NW of the delta and is characterised by the presence of a group of open folds with asymmetric to symmetric geometry, and with minor thrust faults on the steeper limbs. Further to the SE, and along structural strike from zone A, we have defined a second set of thrust faults that are coupled with strongly asymmetric to symmetric, tighter folds, which we have been grouped into zone B. We argue below that the distinctly different structural styles within the compressional domains may be due to detachment zones that underlie the wedge-shaped fold and thrust systems.

DATA AND METHODOLOGY

Zone B is partially covered by 1970 km^2 of high-quality 3D seismic data acquired in 1999 over water depths of between 1500 and 4000 m and a 1998 vintage of 2D seismic data that has a combined length of 5230 km. Zone A is, however, only covered by 2D seismic data. These data have a dip and strike line spacing of 4 and 10 km, respectively, with a data record interval of 12 s and a 6 km cable length with an airgun source. These data were processed using a Kirchhoff bent ray pre-stack time migration. The 3D dataset has a 6 km offset length and a 12-s record interval. Its processing sequence is similar to that of the 2D data. The datasets are displayed with a reverse polarity (European convention) so that an increase in acoustic impedance is represented by a trough and is black on the seismic data in all figures presented here. The data are displayed in seconds two-way-travel time (TWT). The vertical and lateral resolutions are estimated to be between 10 and 20 m at the top of unit 1 and 100 m at the base of unit 2. Stacking velocities obtained from Morgan (2003) were used to depth convert the seismic data (see Yilmaz, 2001). The overall seismic data quality is considered to be good within the Tertiary
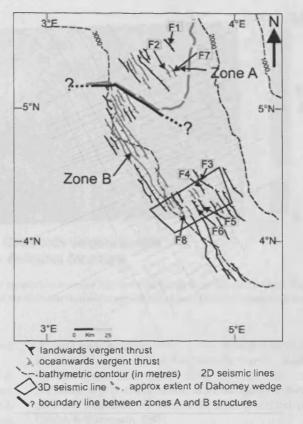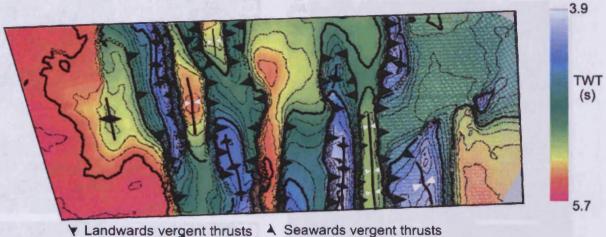
Fig. 4. Location map of the study area showing the two-dimensional (2D) and 3D seismic database, the approximate demarcation of zones A and B and the location of faults F1–F8 described in this study. It also shows the approximate extent of the Dahomey wedge.

section; seismic noise is, however, noted in the dataset, occasionally due to poor migration of seismic energy in areas where there are abrupt lateral velocity changes i.e. in the footwall regions beneath the major thrust planes.

Regional mapping was undertaken to subdivide the seismic-stratigraphy into units 1a, 1b and 2 (Figs 2b and 3a, b). We then mapped high-amplitude continuous reflections to further subdivide the stratigraphy. These reflections have provided a basis for time stratigraphic interpretation throughout the study area because of the ease with which they can be correlated. This stratigraphic framework was then used as the basis for measuring fault offsets. The high continuity of the mapped reflections was invaluable in aiding correlation across thrust faults within the 3D survey area in particular, because the lateral tips of the thrusts were found to tie beyond the limits of the survey area. Further constraints on the correlation between footwalls and hangingwalls were obtained by linking the regional 2D data to the 3D seismic data.

To analyse the faults, we adopted the 'displacement–distance' method developed by Muraoka & Kamata (1983) and Williams & Chapman (1983). This graphical method provides a primary visual representation of the displacement distribution along the fault trace and provides im-

▼ Landwards vergent thrusts   ▲ Seawards vergent thrusts
＼ Synclinal structures   ⤨ Anticlinal Structure

Fig. 5. Time structural map of Miocene (10.3 Ma) showing the parallelism between fold axes and the strike of the thrust faults. The figure is dominated by a dip–slip regime. The measurements of the fault displacements were made on profiles that are generally parallel to the likely transport direction.

portant constraints for the growth history of the thrust (Watterson, 1986; Ellis & Dunlap, 1988).

Depth-converted sections were constructed for each fault analysed. For thrust faults in zone A, the faults were mapped using the widely spaced regional 2D seismic grid, and specific profiles were selected for depth conversion on the grounds that they were most orthogonal to the strike of the thrust faults. It was assumed that because in the better-constrained distal parts of the region, fold axes were mapped parallel to the strike of the thrust faults, the likely motion vector on the thrust faults was orthogonal to fault strike. Hence, the seismic profiles selected are likely to be in or close to the transport direction. This interpretation accords well with what is known of the regional kinematics of the gravity tectonic system as a whole (e.g. Bilotti & Shaw, 2005). For thrust faults in zone B, we selected profiles based on mapping of the thrusts and associated folds using the dense line spacing of the 3D seismic survey (Fig. 5). The parallelism observed on structure maps of the 3D survey area between fold axes and strike of thrust faults again strongly argues for a dominantly dip–slip regime, and hence we selected profiles that were considered parallel to the likely transport direction.

The displacement (D) values were measured directly from the depth–converted; true-scale sections using 2DMove structural restoration software that allows for depth-converted seismic profiles to be displayed at any scale.
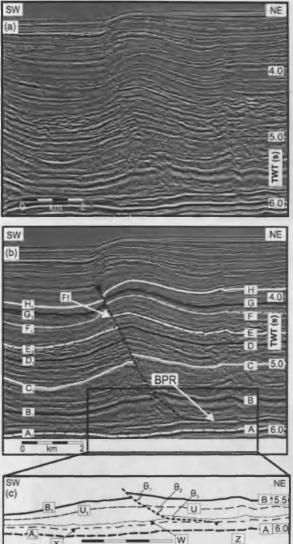
Displacement values were plotted graphically against the distance (X) measured along the thrust fault plane from the upper fault tip to the midpoint position between footwall and hangingwall cutoffs for each specific marker horizon. Displacement values were only recorded for those markers where there was a high confidence in the accuracy of the cross-fault correlation. This method ensured that distortions due to fault plane listricity were not introduced into the graphical display, thus preserving the value of the

displacement gradients that can be derived directly from the plots. This approach differs from that used in displacement analysis of extensional faults, where it is more conventional to plot displacement or throw against a distance ordinate measured by projection onto a vertical plane (Walsh & Watterson, 1987).

OBSERVATIONS

In this section, we use representative 2D (Figs 6 and 7) and 3D (Figs 8 and 9) seismic lines to illustrate the structural interpretation, pertinent features of the structural geology of the deepwater region and to demonstrate the location of the detachment levels. The displacement distribution of individual thrusts is presented and discussed as a guide to reconstructing the structural evolution.

Fault interpretation and detachment level

The thrust faults in the study area are generally observed to be oceanward verging and striking in a NW–SE direction, but some are landward-verging and out of sequence (Morley, 1988). In general, the thrust planes are listric (concave upwards), steepening upwards to a more planar geometry in the upper parts of the fault planes (Figs 6–9). The listric geometry of these thrust faults and the generally asymptotic relationship of the thrust planes with the regional stratigraphy at their base are strongly indicative of the presence of a detachment surface (McNeill *et al.*, 1997). The upper tips are well defined by the shallowest resolvable offset of seismic markers, although loss of signal coherence in shallow reflections around the upper tips sometimes obscures its precise location (Figs 8 and 9). Individual fault planes range in dip from sub-horizontal, close to the inferred detachment level to approximately 40° close to the upper tip. The steepest, more planar sections of the

Fig. 6. Uninterpreted (a) and interpreted (b) representative seismic section from zone A showing a typical fault (F1) detaching within the Dahomey wedge and (c) an enlarged section of the sole segment where the fault plane reflection terminates within a bedding parallel layer marked as BPR.

Fig. 7. Uninterpreted (a) and interpreted (b) representative seismic section from zone A showing a typical fault (F2) detaching in the Dahomey wedge.

thrusts were observed to be generally steeper for faults in zone A in comparison with those in zone B. Depth conversion showed that the listric geometry is not simply due to an increase in seismic velocity with depth (Fig. 8e).

Fault planes were interpreted based on the following criteria: (a) abrupt offset of steeply dipping stratal reflections, (b) tracking of fault plane reflections, (c) juxtaposition across the fault plane reflection of dissimilar units and (d) a deterioration in the data resolution beneath the faults as a result of the juxtaposition of faster velocity rocks in the footwall juxtaposed laterally against slower velocity rocks in the hanging wall.

The majority of the thrust faults could be traced from a detachment level at depth upwards to close to the seafloor

(e.g. Figs 6a, 7a, 8a and 9a). The detailed geometry of seismic reflections at the sole of the thrusts is critical for the determination of the detachment levels in zones A and B. The quality of the seismic data generally allows the detachment level to be delineated within a vertical resolution limit of less than 25 m thickness (Figs 6–9), and hence contrasting detachment levels observed from faults in zones A and B can be resolved with confidence. The detachment level is defined based on tracing the discordance between reflections in footwall and hangingwall to a position where there is no longer any visible discordance (see Fig. 6c). In the following sections, we examine examples of faults in zones A and B in more detail to illustrate the interpretational approach adopted to identify detachment levels.

Faults in zone A

We illustrate our general approach with reference to a representative example of a fault from zone A (Fig. 6). All
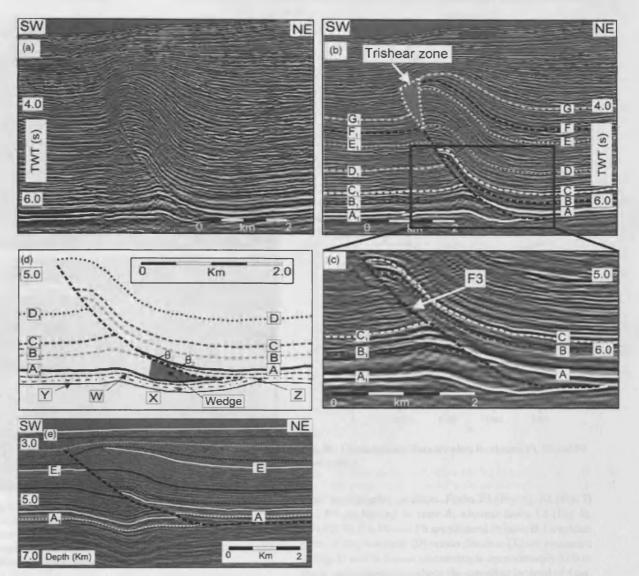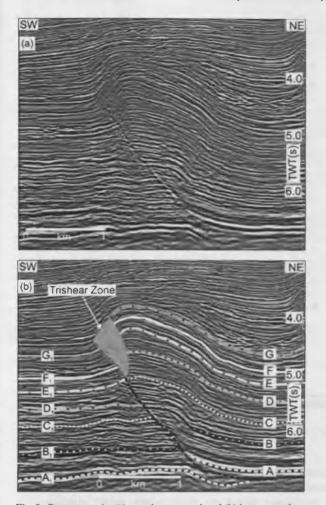
Fig. 8. Representative (a) uninterpreted and (b) interpreted seismic section from zone B showing fault F3. Note how the thrust ramps up, forming a thrust wedge. Also observed is the amount of displacement between the footwall and hanging walls. The upper tip is invisible within a trishear zone. (c) A section of the sole segment defining the exact position of the detachment layer. (d) Line drawing of the sole segment describing the relationship between the reflections. (e) A depth-converted seismic section showing fault F3 from which actual displacement measurements were made.

angular relationships were measured from true-scale depth-converted profiles. We note that the fault plane exhibits an acute cutoff for reflection B but not for reflection A. Reflection B has a greater cut-off angle with the fault (approximately 28–30° – labelled θ_1 in Fig. 6c), than reflection U (approximately 18–20° – labelled θ_2 in Fig. 6c) and reflection W (approximately 12–15° – labelled θ_3 in Fig. 6c). These values are based on depth-converted sections. Similar relationships are identified elsewhere (Fig. 7). The fault then shallows in dip asymptotically so that the discordance between hangingwall and footwall stratal reflections diminishes to the point where the units are concordant, which, in this case, is coincident with reflection X (Fig. 6c). This is where we pinpoint the junction between

the thrust fault and the strata-parallel detachment, which is labelled Z in Fig. 6c, and is the basis for our method of identifying the detachment level. We find that the detachment is often marked by a reflection that has variable and often high amplitude. Similar relationships are identified for most of the faults that we examined (e.g. Fig. 7).

Faults in zone B

In the fault displayed in Fig. 8, reflections A and B both exhibit acute cutoffs. We observed footwall cutoffs at reflection W, but none for reflections W and X (Fig. 8). Again, reflection A has a greater cut-off angle (approximately 20–25° – labelled θ_1 in Fig. 8d) and this reduces downwards

Fig. 9. Representative (a) non-interpreted and (b) interpreted seismic section from zone B showing fault F4. Note how the thrust ramps up, forming a thrust wedge on the top Akata formation defined by A–A. The upper tip of the thrust is invisible within the trishear zone.

to approximately 12–15° (marked labelled θ_2) in Fig. 8d. It is also evident that the point where the thrust is interpreted to become layer parallel with stratal reflections (i.e. the point at which it becomes a detachment) defines the apex of a wedge-shaped element (Fig. 8d). Similar geometries have been described by Cloos (1961) and Mitra (2002b). Similar wedge elements are observed at the base of the footwall in Fig. 9. In marked contrast, there are no comparable 'wedges' of this type associated with faults in zone A. Also, it is observed that the upper tips of the faults in zone B are characterised by upward-widening triangular region of markedly reduced amplitude (Figs 8 and 9). These low-amplitude regions bear a striking resemblance to a tip-related shear zone called the trishear zone identified in many outcropping thrusts (Erslev, 1991).

Displacement–distance characteristics

Displacement measurements for eight faults (F1, F2, F3, F4, F5, F6, F7 and F8; located in Fig. 4) were plotted against
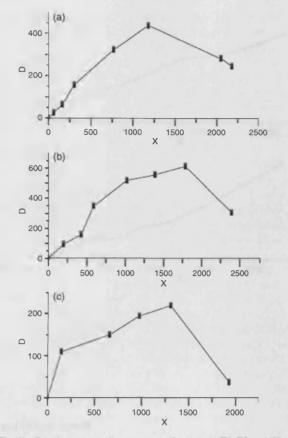
Fig. 10. Displacement–distance plots for thrusts F1, F2 and F7 from zone A.

their stratigraphic position. Faults F1 (Fig. 6), F2 (Fig. 7) and F7 are located in zone A, whereas faults F3 (Fig. 8), F4 (Fig. 9), F5, F6 and F8 are situated in zone B. Graphical plots of displacement (D) versus distance (X) are presented in Figs 10 and 11. Errors amounting to aprroximately 10% in these measurements include the sampling interval of 4 ms, the errors in positioning due to uncertainty in the migration velocities and interpretational errors.

Zone A

All the thrust faults in zone A characterised by displacement–distance plots that show an increase in displacement from the upper tip, to a position approximately midway down the main thrust ramp, where the displacement is a maximum, and from which point to the detachment position, show a clear decrease in displacement values. Three examples of this type of pattern are presented in Fig. 10. In the case of fault F1, for example (Fig. 10a), the displacement maximum recorded at the mid-ramp position is 438 m and decreases to 247 m at the deepest horizon before the detachment. This reduction in displacement downwards is too large to be within the error range, and thus appears to be a genuine feature of this example. Similar patterns of asymmetrically peaked displacement–distance patterns can be seen for faults F2 and F3 (Fig. 10b
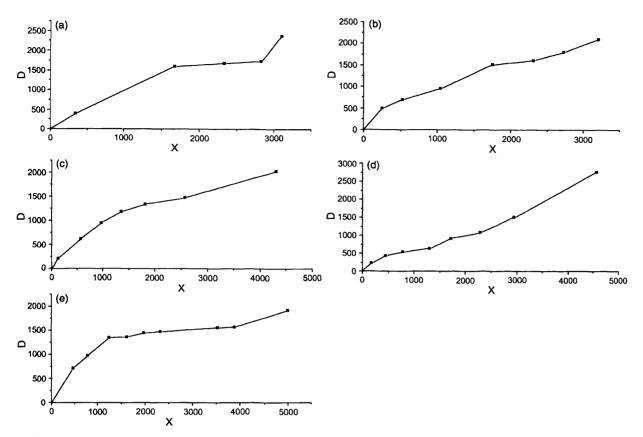
Fig. 11. Displacement–distance plots for thrusts F3, F4, F5, F6 and F8 from zone B.

and c), where there are even more pronounced downward decreases in displacement values from the maximum position. These observations are highly significant in the context of overall kinematic analysis (Williams & Chapman, 1983) in that the displacement clearly decreases as the detachment is approached.

Zone B

In contrast to the thrust faults in zone A, those in zone B are characterised by displacement–distance plots that show an increase in displacement from the upper tip downwards to the last measurable horizon offset close to the detachment position. Five representative examples of displacement–distance plots for zone B faults are presented in Fig. 11. The general increase in displacement values downwards from the upper tips can either be quite linear with a constant displacement gradient (e.g. upper part of Fig. 11a), or more step-like (Fig. 11b), or bipartite, with a larger upper gradient, and a smaller deeper gradient (Fig. 11b and c). The displacement gradients are similar to those reported for normal faults, and range from 0.2 to over 3.0. The larger values are almost certainly indicative of stratigraphic thinning in the region of the upper tip, rather than the result of ductile strain associated with fault propagation. The deepest values in all cases were measured quite close to the detachment, so the progressive increase in displacement as the detachment is approached stands in marked

contrast to the reduction in displacement observed at the same position for zone A faults. This contrast in displacement characteristics is universal for the faults in the two zones, respectively, and is considered further below with a view to explaining the difference in behaviour.

DISCUSSION

Multiple detachments

One of the most important observations made from the seismic interpretation is that the thrust planes are seen to detach into two separate levels in the deepwater region of the west Niger Delta. A third (mid-Akata) detachment has also been identified but has only local significance in zone B. These detachments are interpreted to be located within spatially extensive and mechanically weak units, based on long-range correlations of the stratal units containing the regional detachment levels. Over 95% of the combined fold-thrust structures mapped on the regional 2D and 3D seismic data detach into either of these two levels. These two detachments are informally termed the Dahomey and Top Akata detachments. The Dahomey detachment (within the Dahomey 'wedge') is a zone rather than a narrowly defined level, with a thickness of between 100 and 120 m. It is characterised by parallel internal reflections with some bedding parallel slip producing minor deformation and allowing the definition of the detachment interval.

This thick detachment 'zone' is conceivably due to the presence of a specifically weak lithology, such as a condensed interval with high organic content, or due to specific clay mineralogy (e.g. smectite rich). In contrast to the Dahomey detachment, the Top Akata detachment shows no buckle-type minor deformation. It has a thickness of between 40 and 70 m.

Displacement patterns

The displacement–distance profile exhibited by faults in zone A (Fig. 10) have been shown to be characterised by a distinct peak in displacement value some distance above the detachment. It is not possible to constrain whether the displacement continues to diminish along the flat portion of the detachment, possibly even to a lower tip zone, as has been suggested for some thrust faults (Pfiffner, 1985; Eisenstadt & De Paor, 1987). What is clear, however, is that the peak value occurs approximately midway up the post-detachment stratigraphy, relative to the overburden present at the onset of thrusting. The displacement–distance plots of these faults thus bear some resemblance to the 'C'-type plots described from small normal faults by Muraoka & Kamata (1983) and for thrust faults by Williams & Chapman (1983).

The 'C' type of displacement–distance plot implies that the thrust fault loses displacement both updip and downdip from a point near the centre of the thrust, with considerable displacement gradients in both directions (and presumably, therefore, laterally too). Small variations in the profile are attributed to lithological effects such as bed-pervasive ductile thickening within weaker shale layers. The relative smoothness of the profile could be interpreted to indicate an essentially uniform lithology throughout the section consistent with the deepwater depositional setting. The recognition of displacement gradients implies that the wall rocks must be strained in order to accommodate the displacement variation (Walsh & Watterson, 1987), which raises interesting questions about discrimination between thinning due to wallrock strain versus thinning due to syn-kinematic changes in accommodation space.

Previous studies have linked the recognition of a 'C'-type displacement pattern to a specific propagation and growth model, in which the site of initiation of the fault coincides with the locus of maximum displacement on the fault (Walsh & Watterson, 1987). More recently, this concept has been challenged in cases where strong rheological contrasts in the faulted succession have been shown to skew the position of maximum displacement away from the initial locus of propagation (Wilkins & Gross, 2002). In some previous models for thrust nucleation, analysis of this type of displacement pattern has been equated with initial propagation in the ramp region of a ramp-flat thrust structure, with both updip and downdip propagation as strain accumulates (Pfiffner, 1985; Eisenstadt & De Paor, 1987), and we follow their interpretation in suggesting that the 'C'-type patterns we observe are prob-

able indicators of a localised nucleation site above the detachment, with later propagation of the thrust downwards into the detachment. This propagation sequence is thought by some workers to be characteristic of faulted detachment folds (Mitra, 2002b), alternatively referred to as thrust-truncated folds (Wallace & Homza, 2004). This interpretation is similar to that proposed for a thrust and fold in the inter thrust sub-domain of the eastern part of the deepwater Niger delta, which was termed a 'thrust-faulted detachment-fold anticline' (Shirley, 2002).

In marked contrast, faults in zone B (Figs 8 and 9) show a steadily increasing pattern of displacement with distance from the upper tip to the last measurable point close to the detachment level (Fig. 11). As with faults in zone A, the distribution of displacement on the flat portion of the detachment is unknown. Because the displacement values are unconstrained along the detachment, we cannot infer anything about nucleation and propagation other than to link the distinctive displacement gradients across the entire post-detachment stratigraphic section to thrust propagation in the transport direction. As noted earlier, the folds in zone B are seen to be more open than folds in zone A, which could possibly be linked to the differences in displacement patterns on the thrust faults associated with the folds in the two areas, and the relative partitioning of contractional strain between the thrusts and the folds. The parts of the displacement–distance plot with 0 slope may be indicative of fault segments that have propagated with little associated wall strain (Muraoka & Kamata, 1983; Suppe & Medwedeff, 1984, 1990).

In summary, it can be concluded that there are substantial differences between the thrusts in the two zones, both in their displacement patterns and in their relationship with associated folds. Before addressing the key question of why there are differences between these two zones, we first present a model for thrusting and folding in zones A and B based on our kinematic observations linked to those of previous workers.

Descriptive model for thrust propagation and fold-style development

Zone A

In this zone, the dominant structural fold type is the thrusted detachment fold, which we suggest resulted from buckling of a stratified succession, and that initially bent without rupture, leading to the formation of an open anticline and syncline pair. It is proposed that the fold then tightened and became more asymmetric as deformation progressed. When the fold could no longer accommodate the strain by folding, ruptures localised and linked on the steeper limb, producing a thrust that broke through the forelimb of the fold and finally connected to a mobile detachment layer within the Dahomey unit. These types of structure have been called break-thrust folds (Dixon & Liu, 1992; Fischer *et al.*, 1992), thrusted detachment folds (Mitra, 2002b) or thrust-truncated folds (Wallace & Homza, 2004), and have been described mainly from

kinematic models. The term fold-accommodation fault (Mitra, 2002a) would not be appropriate as these type of faults do not connect to a major detachment, which these structures do. This is critically supported by several examples of thrust faults on the limbs of detachment folds that are at an early stage in their development (Fig. 12), in which the thrust has not propagated downwards to connect with the detachment. The presence of this buckled bed with lack of a thrust during shortening may be modified by later truncations of a fault (Jamison, 1987; Mitra, 1990; McNaught & Mitra, 1993). The difference is also shown by the variation in nucleation pattern and the stratigraphic position of the detachment.

Zone B

In zone B, we suggest that in contrast to zone A, the fault propagation folds developed coevally with thrusting and consumed slip at the tips of blind thrusts (Suppe & Medwedeff, 1984; Suppe, 1985; Marshak & Wilkerson, 2004). As the thrust tip migrated, strata are folded in front of it and are eventually breached by the thrust. The upward decrease in displacement observed on the displacement-distance plots is quite typical of a thrust-propagation fold but is not really diagnostic of this class of structure (Mitra, 2002b; Wallace & Homza, 2004). Here, the folds develop in front of the upper tip of the developing thrust as the ramp propagates up section (see Mitra, 1990, 2002b).

Controls on detachment level

The detachment layer in zone A, which is the unit referred to as the Dahomey 'wedge', is over 100 m thick beneath the entire main structures in the area, and is clearly a mechanically weak unit that relates in some way to its lithology. In contrast, in zone B, the detachment level is defined across a much thinner interval corresponding to the Top Akata. This detachment level may be due to the presence of overpressure build-up as revealed from a velocity drop (Morgan, 2003) and shown by the high amplitude and reverse polarity reflections (Figs 8 and 9). Wells drilled in nearby areas have proved this to be the case (large pressure ramp at the Top Akata). So overpressure is the likely mechanism for the Top Akata detachment level.

Stewart (1996) argued that detachment layer thickness played a critical role in the style of shortening in contractional settings. He showed that if a detachment occurred within a thick layer, significant fold amplification could be expected before thrusting. If the detachment layer is thin, shortening quickly leads to thrust nucleation and thrust propagation folds could be expected thereafter.

Combining the mapped distribution of detachment folds of zone A with the regional distribution of the Dahomey wedge detachment 'layer' (Fig. 4), it can be seen that the zone of detachment folds coincides exactly with the mapped extent of the Dahomey wedge. Adopting the argument advanced by Stewart (1996) on the influence of detachment layer thickness, we can therefore simply
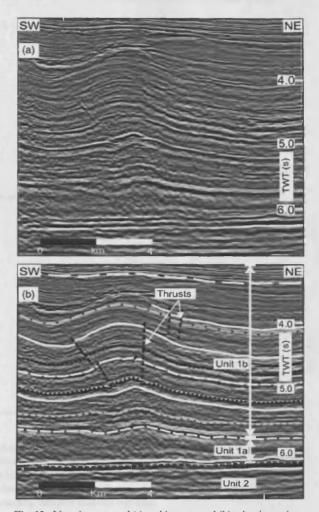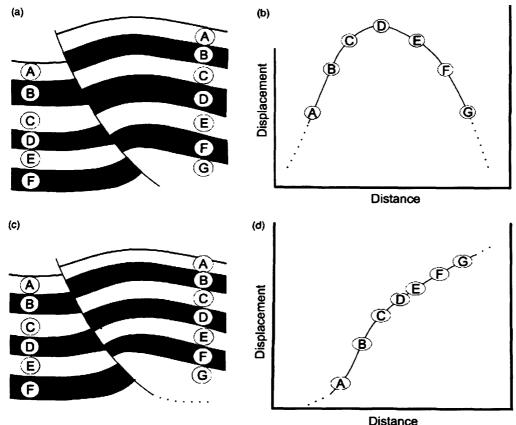

Fig. 12. Non-interpreted (a) and interpreted (b) seismic section showing early stage of development in a faulted detachment fold. Fault and deformation zones form on steeply dipping rotated segments on both limbs, resulting in pop-up-like structures.

propose that the main factor controlling the development of two distinct structural styles in the deepwater fold belt is the presence or absence of a thick detachment layer. Where present, detachment folds develop, with differing degrees of associated thrusting out of the limbs. Where absent, instead, the shortening slope sediments detach at the Top Akata pressure ramp, which forms a discrete and thin detachment level, above which the nucleation of early thrusts is encouraged, which evolve into the distinctive high strain, thrust propagation folds.

By analogy with the results of numerical and analogue modelling of the factors affecting fold style such as differences in competency and stratigraphic thickness between the upper Dahomey detachment and the underlying Akata detachment units have probably affected the style of folding we have observed. The Dahomey unit is relatively incompetent, and thus is able to move into the cores of the developing anticlines from the adjacent synclinal hinge. We suggest that this incompetent unit allowed the growth of the fold by flexural slip while maintaining parallel folding,

(a)

(b)

(c)

(d)

Displacement

Distance

Displacement

Distance

Fig. 13. Model showing thrust-related fold types and their associated displacement–distance profiles. (a) Thrust-related fold type with apparent nucleation point at the centre of the fault. (b) Idealised displacement–distance pattern from a 'C-type' fault (after Muraoka & Kamata, 1983). (c) Thrust-related fold type showing nucleation point at the base of the fault. (d) Idealised displacement–distance pattern from a type II fault. Note here that the nucleation point corresponds to a detachment level. Displacement values are projected from a perpendicular down to a horizontal line from the midpoint between the hanging wall and footwall cut-offs.

bed length and thickness. The deformation from the top Akata unit may primarily be due to internal ductile strain or flexural slip as indicated by thickness changes across fold limbs and widely spaced bed parallel slip surfaces.

IMPLICATIONS

Understanding the evolution of structures in the deep-water west Niger delta is necessary in order to avoid the improper assessment of not only the trap geometry, location, shape, size, depth and vertical extent but also the reservoir, seal, source and migration. We find that fault propagation folds generally form tighter anticlines than thrusted detachment folds and as such would have different type and size of trap. This may be supported by the fact that most of the world class discoveries are located within zone A where the thrusted detachment folds are the dominant structure with low relief and high area as compared with zone B, which is dominated by thrust propagation folds that have higher relief but with smaller area.

The interpretation of these different structures will have contrasting implications for the presence and geometry of

the fault type whether they impede the migration of fluid or result in compartmentalisation of the reservoirs. The structures are likely to control hydrocarbon migration in that in the zone A area, there may be no fault-linking source to trap and reservoir, whereas elsewhere (zone B) there generally would be a link. Therefore, we propose that the risk of a trap not being on a migration pathway is higher in zone A structures. This is particularly true for the early developmental stages of thrusted detachment folds, where a through-going fault linking trap to source has not fully developed.

CONCLUSIONS

Our study has shown that in the deepwater fold and thrust belt of the Niger Delta, there is a strong dependence of structural style on the thickness and lithology of the detachment unit. In zone A, folds formed in response to ductile deformation of the inherently weak Dahomey wedge, which was susceptible to flow due to the regional overpressure developed at or around the top of the Akata formation and shown from the greater amount of shorten-

ing that could be due to lithologic changes. In zone B, the folds are more clearly linked to thrust propagation.

This study has shown that two distinct structural patterns are possible within the deepwater west Niger Delta. They are the thrusted detachment folds in zone A and the thrust propagation folds in zone B. The two structural styles can be distinguished on the basis of markedly contrasting displacement–distance plots (Fig. 13). More symmetrical displacement patterns with a discrete maximum in the mid-ramp position are found for all the thrusts in zone A associated with detachment folds, whereas the thrust propagation folds are associated with a downward-increasing pattern of displacement towards the detachment.

ACKNOWLEDGEMENTS

REFERENCES

AJAKAIYE, D.E. & BALLY, A.W. (2002a) Course manual and atlas of structural styles of reflection profiles from Niger Delta. *AAPG Continuing Educ. Course Note Ser.*, 41, 1–107.

AJAKAIYE, D.E. & BALLY, A.W. (2002b) Some structural styles on reflection profiles from offshore Niger Delta. *Search Discov.*, 10031, 1–6.

AVBOVBO, A.A. (1978) Tertiary lithostratigraphy of the Niger Delta. *AAPG Bull.*, 62(2), 295–306.

BILOTTI, F.D. & SHAW, J.H. (2001) Modeling the compressive toe of the Niger Delta as a critical taper wedge (abs.). *AAPG Annu. Meeting Program*, 10, A18–A19.

BILOTTI, F.D. & SHAW, J.H. (2005) Deepwater Niger Delta fold and thrust belt modelled as a critical-taper wedge: the influence of elevated of elevated basal fluid pressure on structural styles. *AAPG Bull.*, 89, 1475–1491.

BRUCE, C.H. (1973) Pressured shale and related sediment deformation: mechanism for development of regional contemporaneous faults. *AAPG Bull.*, 57, 878–886.

BURKE, K.C.B. (1972) Longshore drift, submarine canyons, and submarine fans. *AAPG Bull.*, 56, 1975–1983.

BURKE, K., DESSAUVAGIE, T.F.J. & WHITEMAN, A.J. (1971) Opening of the Gulf of Guinea and geological history of the Benue depression and Niger Delta. *Nat. Phys. Sci.*, 233, 51–55.

BYERLEE, J. (1993) Model for episodic flow of high-pressure water in fault zone before earthquakes. *Geology*, 21, 303–306.

CLOOS, E. (1961) Bedding slips, wedges and folding in layered sequences. *Société Géologique de Finlande, Extrait des Comptes Rendus*, 33, 106–122.

COBBOLD, P.R., SZATMARI, P., DEMERCIAN, L.S., COELHO, D. & ROSSELLO, E.A. (1995) Seismic and experimental evidence for thin-skinned horizontal shortening by convergent radial gliding on evaporites, deepwater Santos Basin, Brazil. In: *Salt Tectonics: A Global Perspective* (Ed. by M.P.A. Jackson, D.G. Robert & S. Snelson), *AAPG Mem.*, 65, 305–321.

CONNORS, C.D., DENSON, D.B., KRISTIANSEN, G. & ANGSTADT, D.M. (1998) Compressive anticlines of the mid-outer slope, central Niger Delta (abs.). *AAPG Bull.*, 82, 1903.

CORREDOR, F., SHAW, J.H. & BILOTTI, F. (2005a) Structural styles in the deep-water fold and thrust belts of the Niger Delta. *AAPG Bull.*, 89, 753–780.

CORREDOR, F., SHAW, J.H. & SUPPE, J. (2005b) Shear fault-bend fold, deepwater Niger Delta. In: *Seismic Interpretation of Contractional Fault-Related Folds* (Ed. by J.H. Shaw, C. Connors & J. Suppe), *AAPG Stud. Geol.*, 53, 87–95.

DAILLY, G.C. (1976) A possible mechanism relating progradation, growth faulting, clay diapirism and overthrusting in the regressive sequence of sediments. *Bull. Canadian Petrol. Geol.*, 24, 92–116.

DAMUTH, J.E. (1994) Neogene gravity tectonics and depositional processes on the deep Niger Delta continental margins. *Mar. Petrol. Geol.*, 11, 321–346.

DAVIES, R.J. (2003) Kilometer-scale fluidization structures formed during early burial of a deep-water slope channel on the Niger Delta. *Geology*, 31(11), 949–952.

DAVIES, R.J., MACLEOD, C.J., MORGAN, R. & BRIGGS, S.E. (2005) Termination of a fossil continent-ocean fracture zone imaged with three-dimensional seismic data: the Chain Fracture Zone, eastern equatorial Atlantic. *Geology*, 33(8), 641–644.

DAVIS, D.M. & ENGELDER, T. (1985) The role of salt in fold-and-thrust belts. *Tectonophysics*, 119, 67–88.

DE MATOS, D. (2000) Tectonic evolution of the Equatorial South Atlantic. In: *Atlantic Rifts and Continental Margins. Geophysical Monograph 115* (Ed. by W. Mohriak & M. Talwani), pp. 331–354. American Geophysical Union, Washington, DC.

DELTEIL, J.R., VALERY, P., MONTADERT, L., FONDEUR, C., PATRAIT, P. & MASCLE, J. (1974) Continental margins in the northern part of the Gulf of Guinea. In: *The Geology of Continental Margins* (Ed. by C.A. Burk & C.L. Drake), pp. 297–311. Springer Verlag, New York.

DEPTUCK, M.E., STEFFEN, G.S., BARTON, M. & PIRMEZ, C. (2003) Architecture and evolution of upper fan channel-belts on the Niger Delta slope and in the Arabian Sea. *Mar. Petrol. Geol.*, 20(6–8), 649–676.

DIXON, J.M. & LIU, S. (1992) Centrifuge modelling of the propagation of thrust faults. In: *Thrust Tectonics* (Ed. by K.R. McClay), pp. 53–69. Chapman & Hall, London.

DOUST, H. & OMATSOLA, E. (1990) Niger Delta. In: *Divergent/Passive Margins* (Ed. by J.D. Edwards & P.A. Santogrossi), *AAPG Mem.*, 48, 201–238.

EISENSTADT, G. & DE PAOR, D.G. (1987) Alternative model of thrust-fault propagation. *Geology*, 15, 630–633.

ELLIS, M.A. & DUNLAP, W.J. (1988) Displacement variation along thrust faults: implications for the development of large faults. *J. Struct. Geol.*, 10, 183–192.

EMERY, K.O., UCHUPI, E., PHILLIPS, J., BROWN, C. & MASCLE, J. (1975) Continental margins off western Africa: Angola to Sierra Leone. *AAPG Bull.*, 59, 2209–2265.

ERICKSON, S.G. (1996) Influence of mechanical stratigraphy on folding vs. faulting. *J. Struct. Geol.*, 18, 443–450.

ERSLEV, E.A. (1991) Trishear fault-propagation folding. *Geology*, 19, 617–620.

EVAMY, B.D., HAREMBOURE, J., KAMERLING, P., KNAAP, W.A., MALLOY, F.A. & ROWLANDS, P.H. (1978) Hydrocarbon habitat of Tertiary Niger Delta. *AAPG Bull.*, 62, 1–39.

FAIRHEAD, J.D. & BINKS, R.M. (1991) Differential opening of the Central and South Atlantic oceans and the opening of the West African rift system. *Tectonophysics*, 187, 191–203.

FISCHER, M.P., WOODWARD, N.B. & MITCHELL, M.M. (1992) The kinematics of break-thrust folds. *J. Struct. Geol.*, 14, 451–460.

GRADSTEIN, F.M., AGTERBERG, F.P., OGG, J.G., HARDENBOL, J., VAN VEEN, P., THIERRY, J. & HUANG, Z. (1995) A Triassic, Jurassic and Cretaceous time scale. In: *Geochronology, Time Scale and Global Stratigraphic Correlation* (Ed. by W.A. Berggren, D.V. Kent, M.P. Aubrey & J. Hardenbol), *Spec. Publ. Soc. Econ. Palaeontologists and Mineralogists*, 54, 95–126.

GRELAUD, S., VERGES, J., NALPAS, T. & KARPUZ, R. (2003) Impact of multiple detachment levels on deformation of external fold-and-thrust belts. *Geophys. Res. Abstr.*, 5, 11003.

HAACK, R.C., SUNDARARAMAN, P., DIEDJOMAHOR, J.O., XIAO, H., GANT, N.J., MAY, E.D. & KELSCH, K. (2000) Niger Delta petroleum systems, Nigeria. In: *Petroleum Systems of South Atlantic Margins* (Eds. by M.R. Mello & B.J. Katz), *AAPG Mem.*, 73, 213–231.

HOOPER, R.J., FITZSIMMONS, R.J., GRANT, N. & VENDEVILLE, B.C. (2002) The role of deformation in controlling depositional patterns in the south-central Niger Delta, West Africa. *J. Struct. Geol.*, 24, 847–859.

HUBBERT, M.K. & RUBEY, W.W. (1959) Role of fluid pressure in mechanics of over-thrust faulting, part I and II. *Geol. Soc. Am. Bull.*, 70, 115–205.

JAMISON, W.R. (1987) Geometric analysis of fold development in overthrust terranes. *J. Struct. Geol.*, 9, 207–219.

KNOX, G.J. & OMATSOLA, E.M. (1989) Development of the Cenozoic Niger Delta in Terms of the 'Escalator Regression' Model and Impact on Hydrocarbon Distribution. *Proceedings KNGMG Symposium 'Coastal Lowlands, Geology and Geotechnology'* (pp. 181–202). Kluwer Academic Publishers, Dordrecht.

LEHNER, P. & DE RUITER, P.A.C. (1977) Structural history of the Atlantic margin of Africa. *AAPG Bull.*, 61, 961–981.

MACGREGOR, D.S., ROBINSON, J. & SPEAR, G. (2003) Play fairways of the Gulf of Guinea transform margin. In: *Petroleum Geology of Africa: New Themes and Developing Technologies* (Ed. by J.J. Arthur, D.S. Macgregor & N.R. Cameron), *Spec. Publ. Geol. Soc. Lond.*, 207, 131–150.

MALUSKI, H., COULON, C., POPOFF, M. & BAUDIN, P. (1995) ^{40}Ar/^{39}Ar chronology, petrology and geodynamic setting of Mesozoic to early Cenozoic magmatism from the Benue Trough, Nigeria. *J. Geol. Soc.*, 152, 311–326.

MARSHAK, S. & WILKERSON, M.S. (2004) Fold-thrust belts – an essay. In: *Earth Structure*, 2nd edn, Ed. by B.A. Van Der Pluijm & S. Marshak), pp. 444–474. Norton Publishers, New York.

MARTON, L.G., TARI, G.C. & LEHMANN, C.T. (2000) Evolution of the Angolan Passive margin, West Africa, with emphasis on post-salt structural styles. In: *Atlantic Rifts and Continental Margins. Geophysical Monograph 115* (Ed. by W. Mohriak & M. Talwani), pp. 129–149. American Geophysical Union, Washington, DC.

MASCLE, J. (1976) Submarine Niger Delta structural framework. *J. Nigeria Min. Geol. Metal. Soc.*, 13, 12–28.

MCCLAY, K.R. (2004) Thrust tectonics and hydrocarbon systems: introduction. In: *Thrust Tectonics and Hydrocarbon Systems* (Ed. by K.R. McClay), *AAPG Mem.*, 82, ix–xx.

MCNAUGHT, M.A. & MITRA, G. (1993) A kinematic model for the origin of footwall synclines. *J. Struct. Geol.*, 15, 805–808.

MCNEILL, L.C., PIPER, K.A., GOLDFINGER, C., KULM, L.D. & YEATS, R.S. (1997) Listric normal faulting on Cascadia continental margin. *J. Geophys. Res.*, 102(B6), 12123–12138.

MITRA, S. (1990) Fault-propagation folds: geometry, kinematic evolution, and hydrocarbon traps. *AAPG Bull.*, 74, 921–945.

MITRA, S. (2002a) Fold-accommodation faults. *AAPG Bull.*, 86, 671–693.

MITRA, S. (2002b) Structural models of faulted detachment folds. *AAPG Bull.*, 86, 1673–1694.

MORGAN, R. (2003) Prospectivity in ultradeep water: the case for petroleum generation and migration within the outer parts of the Niger Delta apron. In: *Petroleum Geology of Africa: New Themes and Developing Technologies* (Ed. by T.J. Arthur, D.S. MacGregor & N.R. Cameron), *Spec. Publ. Geol. Soc. Lond.*, 207, 151–164.

MORGAN, R. (2004) Structural controls on the positioning of submarine channels on the lower slopes of the Niger Delta. In: *3D Seismic Technology: Application to the Exploration of Sedimentary Basins* (Ed. by R.J. Davies, J. Cartwright, S.A. Stewart, J.R. Underhill & M. Lappin), *Geol. Soc. London, Mem.*, 29, 45–51.

MORLEY, C.K. (1988) Out of sequence thrusts. *Tectonics*, 7, 539–561.

MORLEY, C. & GUERIN, G. (1996) Comparison of gravity-driven deformation styles and behaviour associated with mobile shales and salt. *Tectonics*, 15, 1154–1170.

MURAOKA, H. & KAMATA, H. (1983) Displacement distribution along minor fault traces. *J. Struct. Geol.*, 5, 395–483.

NÜRNBERG, D. & MÜLLER, R.D. (1991) The tectonic evolution of the South Atlantic from late Jurassic to present. *Tectonophysics*, 187, 27–53.

PEEL, F.J., TRAVIS, C.J. & HOSSACK, J.R. (1995) Genetic structural provinces and salt tectonics of the Cenozoic offshore US Gulf of Mexico: a preliminary analysis. In: *Salt Tectonics: A Global Perspective* (Ed. by M.P.A. Jackson, D.G. Robert & S. Snelson), *AAPG Mem.*, 65, 153–175.

PFIFFNER, O.A. (1985) Displacements along thrust faults. *Eclogae Geol. Helv.*, 79, 313–333.

RAMSAY, J.G. & HUBER, M.I. (1987) *The Technique of Modern Structural Geology, Vol. 2, Fold and Faults.* Academy Press, London.

ROWAN, M.G., PEEL, F.J. & VENDEVILLE, B.C. (2004) Gravity-driven fold belts on passive margins. In: *Thrust Tectonics and Hydrocarbon Systems* (Ed. by K.R. McClay), *AAPG Mem.*, 82, 157–182.

SHAW, J.H., NOVOA, E. & CONNORS, C.D. (2004) Structural controls on growth stratigraphy in contraction fault-related folds. In: *Thrust Tectonics and Hydrocarbon Systems* (Ed. by K.R. McClay), *AAPG Mem.*, 82, 400–412.

SHIRLEY, K. (2002) Agbami a 20-Mile long thrust-faulted anticline. *Explorer*, February 2002, p. 11.

SHORT, K.C. & STAUBLE, A.J. (1967) Outline of Geology of Niger Delta. *AAPG Bull.*, 51, 761–779.

SIBSON, R.H. (1981) Fluid flow accompanying faulting: field evidence and models. In: *Earthquake Prediction, an International Review* (Ed. by D.W. Simpson & R.G. Richards), *Am. Geophys. Union Maurice Ewing Ser.*, 4, 593–603.

STEWART, S.A. (1996) Influence of detachment layer thickness on style of thin-skinned shortening. *J. Struct. Geol.*, 18, 1271–1274.

SUPPE, J. (1985) *Principles of Structural Geology.* Prentice-Hall, Englewood Cliffs, NJ.

SUPPE, J. & MEDWEDEFF, D.A. (1984) Fault-propagation fold: Geol. Soc. Am. 1984 Ann. Mtg. Program with Abs., 16, p. 670.

SUPPE, J. & MEDWEDEFF, D.A. (1990) Geometry and kinematics of fault-propagation folding. *Eclogae Geol. Helv*, 83, 409–454.

WALLACE, W.K. & HOMZA, T.X. (2004) Detachment folds versus fault-propagation folds and their truncation by thrust faults. In: *Thrust Tectonics and Hydrocarbon Systems* (Ed. by K.R. McClay), *AAPG Mem.*, 82, 324–355.

WALSH, J.J. & WATTERSON, J. (1987) Distributions of cumulative displacement and seismic slip on a single normal fault surface. *J. Struct. Geol.*, 9, 1039–1046.

WATTERSON, J. (1986) Fault dimensions, displacement, and growth. *Pure Appl. Geophys.*, 124, 365–373.

WEBER, K.J. & DAUKORU, E.M. (1975) Petroleum geology of the Niger Delta. *Proc. 9th. World. Petrol. Cong. Tokyo, Jpn*, 2, 209–221.

WHITEMAN, A.J. (1982) *Nigeria: Its Petroleum Geology, Resources and Potential, Vol I.* Graham & Trotman, London.

WILKINS, S.J. & GROSS, M.R. (2002) Normal fault growth in layered rocks at Split Mountain, Utah: influence of mechanical stratigraphy on dip linkage, fault restriction and fault scaling. *J. Struct. Geol.*, 24(9), 1413–1429.

WILLIAMS, G. & CHAPMAN, T. (1983) Strains developed in the hanging walls of thrusts due to their slip/propagation rate: a dislocation model. *J. Struct. Geol.*, 5(6), 563–571.

WU, S. & BALLY, A.W. (2000) Slope Tectonics-comparisons and contrasts of structural styles of salt and shale tectonics of the Northern Gulf of Mexico with shale tectonics of offshore Nigeria in Gulf of Guinea. In: *Atlantic Rifts and Continental Margins* (Ed. by W. Mohriak & M. Talwani), *Geophys. Monogr.*, 115, 151–172.

YILMAZ, O. (2001) *Seismic Data Analysis: Processing, Inversion and Analysis of Seismic Data (2 Vol).* Society of Exploration Geophysicists, Tulsa.

450